MODELING OF MHD FLOW THROUGH POROUS AND NON-POROUS BOUNDARIES

by

PRADEEP KUMAR
(2009RMA104)
Mathematics Department

Submitted

in fulfillment of the requirements of the degree of Doctor of Philosophy

to the

MALAVIYA NATIONAL INSTITUTE OF TECHNOLOGY JAIPUR

January 2016

Certificate

This is to certify that Mr. Pradeep Kumar has worked under my supervision for the award of the degree of Doctor of Philosophy in Mathematics on the topic entitled "MODELING OF MHD FLOW THROUGH POROUS AND NON-POROUS BOUNDARIES". To the best of my knowledge, the findings contained in this thesis are original and have not been submitted to any University/Institute, in part or full, for the award of any degree.

(Dr. Santosh Chaudhary)
Supervisor

Declaration

I hereby declare that the thesis entitled "MODELING OF MHD FLOW THROUGH POROUS AND NON-POROUS BOUNDARIES" is my own work conducted under the supervision of Dr. Santosh Chaudhary, Assistant Professor, Department of Mathematics, Malaviya National Institute of Technology Jaipur, Rajasthan, India.

I firmly declare that the presented work does not contain any part of any work that has been submitted for the award of any degree either in this University or in any other University/Institute without proper citation.

(Pradeep Kumar)
2009RMA104

Acknowledgements

It is my great pleasure to convey my deepest gratitude and reverence to my esteemed mentor and supervisor Dr. Santosh Chaudhary, Assistant Professor, Department of Mathematics, Malaviya National Institute of Technology Jaipur for her patience, regular encouragement and thoughtful guidance during my research. Her constant support and inspiring suggestions have been precious for me during the preparation of this thesis.

I would like to express my sincere thanks to Head Department of Mathematics, Departmental Research Evaluation Committee (DREC) members and other faculties of the Mathematics Department, Malaviya National Institute of Technology Jaipur for their continuous appreciation.

My greatest gratitude goes to Director of Malaviya National Institute of Technology, Jaipur for providing financial and necessary support to me during the research work.

I am highly indebted to my parents and all other family members for their enormous support and cooperation towards the completion of this thesis.

Last but not least, I am very grateful to all those persons who have rendered their support directly or indirectly for the fulfilment of this endeavour.

(Pradeep Kumar)

Abstract

The thesis mainly deals with the study of the effects of magnetic field on momentum and heat transfer in a porous stretching surface; a flat plate and porous substrate; over a permeable surface; over an exponentially stretching surface; a shrinking surface etc. of electrically conducting, viscous, incompressible fluid. The magnetic Reynolds number, which determines the diffusion of magnetic field along the streamline, is assumed to be small so that the induced magnetic field may be neglected. In most of the cases Ohm's law is assumed to hold and the fluid properties including the electrical conductivity are considered as constant. The flow is considered steady except in the last chapter where we consider unsteady flow. The similar solutions of momentum and energy equations have been obtained in all chapters by suitable transformations of dependent and independent variables. The linear or non-linear partial differential equations, with two point boundary conditions, have been solved by converting the initial value problems using numerical method suggested by Collatz (1966) and then integrated numerically by Runge-Kutta-Nystron scheme by using MATLAB programming.

Contents

List of Figures

List of Tables

Chapter 1

Introduction

Magnetofluiddynamics (MFD) is the study of the flow of an electrically conducting fluid in the presence of a magnetic field. The title Magnetohydrodynamics (MHD) or Hydromagnetics is selected when the fluid is incompressible, such as liquid mercury, and its other properties like viscosity, thermal conductivity and electrical conductivity are regarded as constants. When compressible fluids are used, such as an ionized gas, where its other physical properties are variable, specially temperature dependent the term Magnetogasdynamics (MGD) is used. Since an ionized gas is often called a plasma, one uses the word Plasma dynamics in place of MFD or MGD. However, it may be pointed out that in MFD the continuum approach is generally taken and the fluid is regarded as a continuous media. The other approach is the particle study followed in Plasma Physics.

In 1832, Faraday gave the law of Magnetic Induction, which states that when a charged particle moves in a magnetic field, it experiences a force normal to the plane of the magnetic field and the motion of the particles. Meanwhile, Ritchie, a contemporary of Faraday, discovered that when mutually perpendicular electric and magnetic fields were applied to a conducting fluid, it pumped the fluid in a direction perpendicular to both the fields. Hence it was concluded that the motion of the conducting fluid across the magnetic field generates electric currents, which changes the magnetic field, and the action of the magnetic field on these currents gives rise to

mechanical forces which resist the fluid motion. This force is called Loretz's force $\vec{F}$ which is a body force acting on the fluid and is written as-

$$\vec{F} = \vec{J} \times \vec{B} \tag{1.1}$$

where $\vec{J}$ is the current density vector and $\vec{B}$ is the magnetic induction vector. This discovery opened a new era in science known as MFD.

The principle of MHD power generator is also based on Faraday's law. He suggested that electricity is generated by the motion of a conductor through a magnetic field. In MHD power generators the internal energy of the electrically conducting fluid is converted into electrical energy when it moves through a magnetic field. The practical applications of Faraday's ideas came with Smith and Slepian's (1917) invention, of an instrument for measurements of Ship's speed, and with Williams's (1930) MFD flow meter, which was based on the principle that the induced voltage is proportional to the flow rate. The fundamental work in this area was done by Hartmann (1937) and Hartmann and Lazarus (1937), who studied channel flow of mercury.

MFD has its importance in many natural phenomena and engineering problems. However, its basic importance lies in considering the 'Cosmic' problems, by which we mean the problems of Geophysics and Astrophysics. These are the problems of the earth's interior, the sun, the stars or interstellar space. It is useful in Astrophysics because much of the universe is filled with charged particles and permitted by magnetic fields. So the continuum assumption becomes applicable whereas Geophysicists use it in the interactions of conducting fluids and magnetic fields which

are present in and around heavenly bodies. It is only recently Magnetofluiddynamics attracted the attention of aerodynamicists, mechanical engineers and applied mathematicians because of the interaction of two classical disciplines viz., electromagnetism and fluid dynamics. MFD principles are used by engineers in the design of heat exchangers, pumps, flow meters and submarines; in solving space vehicle propulsion; in designing communications and radar systems; in making power generators; and in developing confinement schemes for controlled fusion. It is also applicable in radio wave propagation in ionosphere, space communication systems, diagnostic techniques, solar flares, geomagnetic storms, and plasma jets.

Theoretically, in ordinary fluid dynamics (OFD) or the dynamics of real fluids (Newtonian and isotropic), the fundamental equations are the Navier-Stokes equation with no dissipation of energy in a spherically symmetrical expansion or compression, so there is only one coefficient of viscosity. But in MFD, the fundamental equations are the electromagnetic and fluid dynamic equations, which are modified to take account of the interaction between the motion of the conducting fluid and the magnetic field or we can say that MFD equations are coupled equations of fluid dynamics with electromagnetic equations.

While deriving the complete equations of MFD, we can follow either of the two approaches, macroscopic or microscopic. In the macroscopic or gasdynamic approach, one modifies the well-known conservation equations of classical fluid dynamics by incorporating into them suitable momentum and energy terms, obtained from Maxwell's equations and Ohm's law. On the other hand, in the microscopic or

gas kinetic treatment, one combines Boltzmann's equation with electromagnetic terms to obtain the fundamental equation of MFD.

For the purpose of most engineering problems, the macroscopic approach is more adequate, and can be applied to situations involving gross electrical conduction, wave propagation, instability, slow motion, boundary layer and turbulence. In the present thesis we use the macroscopic approach.

As stated already, the subject of MFD or MHD comes when electromagnetic phenomenon is combined with fluid dynamics phenomenon. The former are generally expressed by the Maxwell's equations which are linear in form, and the latter are expressed, at least as far as momentum is concerned, by the Navier-Stokes equations which are non-linear in character. It may therefore be concluded that following realities have to be accepted-

(i) Since no general solution exists for the Navier-Stokes equations, no general solution can be expected for the MFD equations.

(ii) The Maxwell's equations introduced the additional boundary conditions which have to be determined and satisfied.

(iii) Because of the occurrence of magnetic and/or electric fields, the external force term in the Navier-Stokes equation may not be treated as constant.

1.1 Fundamental Equations of Magnetofluiddynamics

In the study of MFD, we wish to find out, in addition to the determination of electromagnetic field variables, the velocity distributions as well as the state variables

of the fluid over the whole space for all time. There are, therefore, twenty two unknowns viz., sixteen electromagnetic field variables $\vec{E}$, $\vec{B}$, $\vec{D}$, $\vec{H}$, $\vec{J}$ and ρ_e; the three components of velocity vector $\vec{v}$, and the state variables viz., the temperature T, the pressure p and the density ρ of the fluid. These unknowns are obtained from the following twenty two equations [Bansal (1994)]-

I. Electromagnetic Field Equations

(i) Current Continuity Equation

$$div\,\vec{J} = -\frac{\partial \rho_e}{\partial t} \qquad (\textit{Conservation of charge}) \qquad (1.2)$$

where $\vec{J}$ is the current density vector and ρ_e the charge density.

(ii) Maxwell's Equations

$$Curl\,\vec{E} = -\frac{\partial \vec{B}}{\partial t} \qquad (\textit{Faraday's law}) \qquad (1.3)$$

$$Curl\,\vec{H} = \vec{J} + \frac{\partial \vec{D}}{\partial t} \qquad (\textit{Ampere's law}) \qquad (1.4)$$

$$div\,\vec{D} = \rho_e \qquad (\textit{Gauss' law}) \qquad (1.5)$$

$$div\,\vec{B} = 0 \qquad (\textit{Magnetic field continuity}) \qquad (1.6)$$

where $\vec{E}$ is the electrical field vector, $\vec{B}$ the magnetic field vector, $\vec{H}$ the magnetic intensity vector and $\vec{D}$ the displacement vector in an isotropic medium.

It may be noted that the divergence equations (1.5) and (1.6) follow from the curl equations (1.3) and (1.4) and therefore act as constraints or as initial conditions on the electromagnetic field and cannot be regarded as independent equations.

(iii) Constitutive Equations

$$\vec{D} = \varepsilon \vec{E} \tag{1.7}$$

$$\vec{B} = \mu_e \vec{H} \tag{1.8}$$

where ε is the electrical permittivity or dielectric constant of the medium and μ_e is the magnetic permeability of the medium, which in the present case is an electrically conducting fluid.

Ordinarily, we may assume that both ε and μ_e are constants for a given isotropic material. For anisotropic matter we should consider both ε and μ_e as tensor quantities and in that case neither $\vec{D}$ and $\vec{E}$ are parallel to each other nor $\vec{B}$ and $\vec{H}$. In the study of Magnetofluiddynamics we assume that both ε and μ_e are constants and it is sufficient to take their values in vacuum (free space) as a first approximation.

(iv) Generalized Ohm's Law

$$\vec{J} = \sigma_e \left(\vec{E} + \vec{v} \times \vec{B} \right) + \rho_e \vec{v} \tag{1.9}$$

where σ_e is the electrical conductivity of the fluid.

II. Fluiddynamic Field Equations

(i) Equation of State

Variables that depend only upon the thermodynamic system are called variables of state and these are the pressure p, the density ρ and the temperature T. The equation of state of a perfect gas is

$$p = \rho RT \tag{1.10}$$

where R is the gas constant.

When the fluid is incompressible the equation of state is simply

$$\rho = constant \tag{1.11}$$

(ii) Equation of Continuity - Conservation of Mass

This equation expresses that the rate of generation of mass within a given volume is entirely due to the net inflow of mass through the surface enclosing the given volume. Therefore the equation of continuity is

$$\frac{D\rho}{Dt} + \rho\, div\, \vec{v} = 0 \tag{1.12}$$

where $\frac{D}{Dt} \equiv \frac{\partial}{\partial t} + \left(\vec{v}.\nabla \right)$ is the material derivative.

In the case of steady compressible flow the equation of continuity reduces to

$$div\left(\rho \vec{v} \right) = 0 \tag{1.13}$$

and for incompressible flow we have

$$div\,\vec{v} = 0 \tag{1.14}$$

(iii) Equations of Motion - Conservation of Momentum

The equations of motion are derived from Newton's second law of motion, which states that-

$$Rate\,of\ change\,of\ linear\,momentum = Total\ \ force$$

Therefore the equations of motion are-

$$\rho\frac{D\vec{v}}{Dt} = \rho\vec{F^{(ex)}} + \rho_e\vec{E} + \left(\vec{J}\times\vec{B}\right) - grad\ p + div\,\vec{\tau} \tag{1.15}$$

where $\vec{F^{(ex)}}$ is the external force and $\vec{\tau}$ is the tangential stress, given by

$$\vec{\tau} = \tau_{ij} = 2\mu e_{ij} - \frac{2}{3}\mu e_{kk}\,\delta_{ij} \tag{1.16}$$

where μ is the coefficient of viscosity, $e_{ij} = \frac{1}{2}\left(\frac{\partial v_i}{\partial x_j} + \frac{\partial v_j}{\partial x_i}\right)$ the rate of strain tensor and $\delta_{ij} = \begin{cases} 1 & if\ \ i = j \\ 0 & if\ \ i \neq j \end{cases}$ the Kronecker tensor.

(iv) Equation of Energy - Conservation of Energy

The equation of energy is obtained by the conservation of energy which states that the difference in the rate of supply of energy and the rate at which the energy goes out

must be equal to the net rate of increase of energy. Thus the following general equation of energy is obtained-

$$\rho \frac{D\left(C_p T\right)}{Dt} = \frac{Dp}{Dt} + \frac{\partial Q}{\partial t} + div\left(\kappa\, grad\, T\right) + \frac{J^2}{\sigma_e} + \phi \tag{1.17}$$

where C_p is the specific heat at constant pressure, Q the quantity of heat added per unit mass of the gas, κ the thermal conductivity and $\phi = div\left(\bar{\tau}.\vec{v}\right) - \vec{v}.div\left(\bar{\tau}\right)$ the heat generated due to frictional forces and is known as '**dissipation function**'.

1.2 Physical Importance of Non-dimensional Parameters

Dimensionless parameter plays an important role in fluid mechanics because they give an idea about the terms which are dominant in the governing equations, so that only those terms are retained to find an appropriate solution to the equations. In order to bring out the essential features of the flow problems, it is desirable to find some important dimensionless parameters which characterize the flow problem. They are very useful in the analysis of experimental results and are determined either by inspection analysis or by dimensional analysis. In the inspection analysis we reduce the fundamental equations to a non-dimensional form and obtain the non-dimensional parameters from the resulting equations. In dimensional analysis we form non-dimensional parameters from the physical quantities occurring in the problem, even when the knowledge of the governing equations is missing. Both methods give the same results.

(i) Reynolds Number

The Reynolds number Re is defined as the ratio of inertial forces $\frac{\rho U^2}{L}$ to viscous forces $\frac{\mu U}{L^2}$, i.e.

$$\mathrm{Re} = \frac{\rho U^2 / L}{\mu U / L^2} = \frac{UL}{\upsilon}$$

where, ρ, U, L, μ and υ are some characteristic values of the density, velocity, length, viscosity and kinematic viscosity of the fluid respectively. It is a parameter for viscosity, for if Re is small the viscous forces will be predominant and the effect of viscosity will be felt in the whole flow field. On the other hand if Re is large the inertial forces will be predominant and in such a case the effect of the viscosity can be considered to be confined in a thin layer, known as velocity boundary layer, adjacent to a solid boundary. However, if Re is very large the flow ceases to be laminar and becomes turbulent.

(ii) Magnetic Reynolds Number

The magnetic Reynolds number Re_σ is defined as ratio of fluid flux UL to magnetic diffusivity $\upsilon_H = \frac{1}{\sigma_e \mu_e}$, i.e.

$$\mathrm{Re}_\sigma = \frac{UL}{\upsilon_H} = UL\sigma_e\mu_e$$

where, U, L, σ_e and μ_e are some characteristic values of the velocity, length, electrical conductivity and magnetic permeability of the fluid respectively. This

number has a similar form as ordinary Reynolds number Re, with the kinematic viscosity υ replaced by magnetic diffusivity υ_H, thus it is called magnetic Reynolds number. However, the physical significance of Re and Re_σ differs very much. Ordinary Reynolds number Re is interpreted as the ratio of inertial force to the viscous force which is a dynamic consideration whereas the magnetic Reynolds number Re_σ will be interpreted on how the magnetic field is affected by the fluid motion, which is a kinematic consideration.

(iii) Magnetic Pressure Number

The magnetic pressure number Re_H is defined as the ratio of magnetic pressure $\frac{\mu_e H^2}{2}$ to dynamic pressure $\frac{\rho U^2}{2}$, i.e.

$$\mathrm{Re}_H = \frac{\mu_e H^2/2}{\rho U^2/2} = \frac{\mu_e H^2}{\rho U^2}$$

where μ_e, H, ρ and U are some characteristic values of the magnetic permeability, magnetic intensity, density and velocity of the fluid respectively. It is a measure of the effect of the magnetic field on the fluid motion. Only when Re_H is of the order of unity or larger the fluid will be influenced noticeably by the magnetic field otherwise when $\mathrm{Re}_H << 1$ the magnetic effects on the fluid flow may be disregarded.

(iv) Magnetic Parameter

The magnetic parameter Re_m is defined as the square root of ratio of magnetic force $\sigma_e \mu_e^2 U H^2$ to inertial force $\frac{\rho U^2}{L}$, i.e.

$$\mathrm{Re}_m = \sqrt{\frac{\sigma_e \mu_e^2 U H^2}{\rho U^2 / L}} = \mu_e H \sqrt{\frac{\sigma_e L}{\rho U}} = \sqrt{\mathrm{Re}_H \, \mathrm{Re}_\sigma}$$

where σ_e, μ_e, U, H, ρ, L, Re_H and Re_σ are some characteristic values of the electrical conductivity, magnetic permeability, velocity, magnetic intensity, density, length, magnetic pressure number and magnetic Reynolds number of the fluid respectively. The magnetic parameter Re_m gives an idea of the importance of magnetic force relative to the inertial force.

(v) Prandtl Number

The Prandtl number Pr is defined as the ratio of the kinematic viscosity $\upsilon = \frac{\mu}{\rho}$ to the thermal diffusivity $\alpha = \frac{\kappa}{\rho C_p}$ of the fluid, i.e.

$$\mathrm{Pr} = \frac{\upsilon}{\alpha} = \frac{\mu / \rho}{\kappa / \rho C_p} = \frac{\mu C_p}{\kappa}$$

where μ, ρ, κ and C_p are some characteristic values of the viscosity, density, thermal conductivity and specific heat at constant pressure of the fluid respectively. It is a measure of the relative importance of heat conduction and viscosity of the fluid. The Prandtl number, like the viscosity and thermal conductivity, is a material property and it thus varies from fluid to fluid. For air $\mathrm{Pr} = 0.7$ (approx.) and for water at 60^0 F, $\mathrm{Pr} = 7.0$ (approx.). For liquid metals the Prandtl number is very small, e.g. for mercury $\mathrm{Pr} = 0.044$, but for highly viscous fluids it may be very large, e.g. for glycerine $\mathrm{Pr} = 7250$.

(vi) Eckert Number

The Eckert number Ec is defined as the ratio of the kinetic energy ρU^2 to the thermal energy $\rho C_p T$, i.e.

$$Ec = \frac{\rho U^2}{\rho C_p T} = \frac{U^2}{C_p T}$$

where, ρ, U, C_p and T are some characteristic values of the density, velocity, specific heat at constant pressure and temperature of the fluid respectively. In compressible fluids it determines the relative rise in temperature of the fluid due to adiabatic compression. It can also be retained in incompressible flow, if the frictional heat is to be considered, but the interpretation with reference to adiabatic compression will no longer be true.

(vii) Local Skin Friction Coefficient

The dimensionless shearing stress on the surface of a body, due to a fluid motion, is known as local skin-friction coefficient C_f and is defined as-

$$C_f = \frac{\tau_w}{\rho U^2/2} = \frac{\mu\left(\frac{\partial u}{\partial y}\right)_{y=0}}{\rho U^2/2}$$

where $\tau_w = \mu\left(\frac{\partial u}{\partial y}\right)_{y=0}$, μ, $\frac{\partial u}{\partial y}$, ρ and U are some characteristic values of the local shearing stress on the surface of the body, viscosity, velocity gradient, density and velocity of the fluid respectively.

(viii) Nusselt Number - Dimensionless Coefficient of Heat Transfer

The dimensionless coefficient of heat transfer at the surface, Nusselt number Nu is defined as the ratio of temperature gradient at the wall $L\left(\frac{\partial T}{\partial y}\right)_{y=0}$ to overall temperature difference $T_w - T_\infty$, i.e.

$$Nu = -\frac{L\left(\frac{\partial T}{\partial y}\right)_{y=0}}{\left(T_w - T_\infty\right)}$$

where L, T, and $T_w - T_\infty$ are some characteristic values of the length, temperature and difference between the temperature of the wall and that of the fluid respectively.

1.3 Boundary Layer Flow

The boundary layer flow is one of the most interesting class of problems of viscous flow in fluid dynamics. The formulation of the boundary layer theory paved the way for understanding the phenomenon related to fluid friction at large Reynolds numbers. Boundary layer phenomenon occurs when the influence of a physical quantity is restricted to small regions near confining boundaries. This phenomenon occurs, when the non-dimensional diffusion parameters viz. the Reynolds number or magnetic Reynolds number are large. The boundary layers are then the velocity and thermal or magnetic boundary layers and each thickness of the boundary layer is inversely proportional to the square root of the associated diffusion number.

Prandtl (1904) introduced the concept of boundary layer in OFD. He made a hypothesis that for fluids with small viscosity (small momentum diffusivity $\upsilon = \mu/\rho$) the flow about a solid body can be divided into two regions-

(i) A very thin layer in the neighborhood of the body, known as the velocity boundary layer or viscous boundary layer.

(ii) The region outside this layer where the viscous effects may be considered as negligible and the fluid is regarded as inviscid.

With the aid of this hypothesis, he simplified the Navier-Stokes equations to a mathematically tractable form, which are called the **boundary layer equations**, and thus succeeded in giving a physically penetrating explanation to the importance of viscosity in assessment of frictional drag and flow separation.

In fluids flowing past heated or cooled bodies the transfer of heat takes place by conduction and convection (heat radiation is negligible unless the temperature is very high). Thus in a similar manner, when the thermal conductivity of the fluid is small (small thermal diffusivity $\alpha = \kappa/\rho C_p$) the heat transport due to conduction is comparable to that due to convection only across a thin layer near the surface of the body. This means that temperature field which spreads from body extends, essentially, over a narrow zone in the immediate vicinity of its surface, known as the **thermal boundary layer**, whereas the fluid at a large distance from the surface is not materially affected by the heated body. This leads to the simplification of the energy equation. In the books by Pai (1956), Rosenhead (1963), Evans (1968), Schlichting

(1968), Rehberg et al. (1998), Oleinik and Samokhin (1999), Sobey (2000), Bansal (2004), Date (2005) and White (2006), the details may be found.

The MHD boundary layers, may be classified into two types by considering the limiting cases of large and small electrical conductivity-

(i) When the **electrical conductivity of the fluid is large** (small magnetic diffusivity $\upsilon_H = 1/\sigma_e \mu_e$, i.e. large magnetic Reynolds number) the diffusion of the magnetic field takes place in a narrow zone, called the magnetic boundary layer, and is ordinarily of the same size as the viscous and thermal boundary layers. In this case it is the axial component of the externally applied magnetic field which differentiates the MHD equations from OFD equations and the MHD boundary layer equations, for incompressible flow, for velocity and magnetic field must be solved simultaneously and thereafter the solution of the energy equation may be obtained for the temperature field.

(ii) When the **electrical conductivity of the fluid is small** (magnetic Reynolds number is small), the thickness of the magnetic boundary layer is very large. In this case the flow direction component of the magnetic interaction and the corresponding Joule heating is only a function of the transverse magnetic field and the local velocity in the flow direction. Changes in the transverse magnetic field component and pressure across the boundary layer are negligible. The induced magnetic field is neglected in comparison of the applied magnetic field, which is taken in the transverse direction.

It was probably Rossow (1958) who first studied the boundary layer flow of an incompressible electrically conducting fluid, in the presence of transverse magnetic field past a flat plate. He studied both the cases- for the magnetic field fixed to the plate and fixed to the fluid. Similar solutions of the same have been studied by Lykoudis (1958), Bush (1958, 1960), Wilcox (1962), Gribben (1965, 1967), Ramamoorthy (1965, 1968), Nath (1971, 1973), Bansal (1979, 1981), Bansal and Jat (1984, 1985, 1986, 1988), Bansal et al. (1987, 1988, 1989) and Jat and Chaudhary (2007, 2008, 2009, 2010) for the hydromagnetic compressible and incompressible, steady and unsteady, boundary layer flows about flat plates, and wedges assuming that the magnetic forces, generally, act only on the boundary layer. Some aspects of the magnetohydrodynamic boundary layers may be found in books of Pai (1962), Cambel (1963), Jeffrey (1966), Ferraro and Plumpton (1966), Cabannes (1970), Cramer and Pai (1973), Bansal (1994) and Gerbeau et al. (2006).

The significance of unsteady boundary layer lies in the fact that practically all flows which occurs are, in a sense, unsteady. One of the independent variable of unsteady flow is time. In making the flow unsteady one or more of the following circumstances may prevail-either the time which has elapsed following the initiation of motion is not large (initial value problem) or there are fluctuations in the main stream velocity (Periodic motion problem) or boundary layer is unstable (instability problem). The unsteady boundary layer flow problems have been studied by several authors including Sano (1977), Gorla (1981), Wang (1990), Nazar et al. (2004) and Jat and Chaudhary (2009).

1.4 Fluid Flow through a Porous Medium

Porous medium is a material consisting of a solid matrix (a body composed of a persistent solid part) with an interconnected void. We suppose that the solid matrix is either rigid (the usual situation) or it undergoes small deformation. One or more fluids can flow through the voids due to their interconnections these flow can be-

(i) Single-phase flow- the voids are saturated by single flow or

(ii) Two-phase flow- a liquid and a gas share the void space.

With respect to shape and size the distribution of pores in a natural porous medium is irregular. Common examples of natural porous media are beach sand, sandstone, limestone, rye bread, wood, and the human lung. On the pore scale (the microscopic scale) the flow quantities (velocity, pressure, etc.) will be clearly irregular. But when the quantities of interest are measured over areas consisting of many pores, and such space-averaged (macroscopic) quantities change in a regular manner with respect to space and time, and hence are amenable to theoretical treatment. The details are found in the books written by Muskat (1937), Bear and Bachmat (1990), Kaviany (1995), Crolet and Hatri (1998), Bejan et al. (2004), Nield and Bejan (2006) and George and William (2008).

1.5 Darcy's Law- Permeability

Henry Darcy's (1856) investigations into the hydrology of the water supply of Dijon and his experiments on steady-state unidirectional flow in a uniform medium revealed a proportionality between flow rate and the applied pressure difference, i.e.

$$u = -\frac{K}{\mu}\frac{\partial P}{\partial x} \tag{1.18}$$

where $\frac{\partial P}{\partial x}$ is the pressure gradient in the flow direction and μ is the dynamic viscosity of the fluid. The coefficient K is called specific permeability or intrinsic permeability of the medium and in case of single phase flow it is abbreviate to permeability. Its dimensions are (length)^2 and is independent of the nature of the fluid but is dependent on the geometry of the medium. It should be noted that here P denotes an intrinsic quantity. Darcy's law and its extensions have been studied by Scheidegger (1974), Bear (1972) and Nield and Bejan (2006).

1.6 Stagnation Point Flows

Stagnation point is a point (on a surface of object) where the velocity is zero in the potential flow (i.e., the flow of an ideal fluid). The flow in the surrounding of a stagnation point is called stagnation point flow. Stagnation points exist at the surface of objects in the flow field, where the fluid is brought to rest by the object. The Bernoulli equation shows that the static pressure is highest when the velocity is zero and hence static pressure is at its maximum value at stagnation points. This static pressure is called the stagnation pressure.

Hiemenz (1911) was the first one to introduce the two-dimensional stagnation flow which is also known as the Hiemenz flow. He presented the idea that the Navier-Stokes equations governing the flow can be transformed to an ordinary differential equation of third order by means of a similarity transformation and gave an exact

solution to the governing equations. The idea of stagnation point flow was implemented to stretching or shrinking sheet with forced convection, mixed convection involving heat transfer and chemical reaction. The study of stagnation point flow for various aspects have been done by Hayday and Bowlus (1967), Ghoshal and Ghoshal (1970), Howarth (1975), Gorla (1979), Nikaien and Peddieson (1988), Gorla et al. (1993) and Jat and Chaudhary (2007, 2008, 2010).

1.7 Radiation Heat Transfer

Thermal radiation, commonly known as radiation heat transfer, is proportional to the difference of the individual absolute temperatures of the bodies, each raised to the fourth power. Thus it is evident that the importance of radiation becomes intensified at high absolute temperature levels. Consequently, radiation contributes substantially in combustion application such as fire, furnaces, IC engines, in nuclear reactions such as in the sun or in nuclear explosions and so on.

Thermal radiation is an electromagnetic phenomenon and is transferred by electromagnetic waves, photons, which may travel a long distance without interacting with a medium. Thus thermal radiation is of great importance in vacuum and space applications. Some common examples are heat leakage through the evacuated walls of a thermos flask, or the heat dissipations from the filament of a vacuum tube, engine cooling, furnaces, boilers and solar radiation. Radiation is used to reject waste heat from a power plant operating in space. Cess (1961, 1966), Viskanta and Grosh (1962), Hossain and Takhar (1996), Hossain et al. (1998), Chamkha et al. (2001), Ganesan

and Loganathan (2002), Molla and Hossain (2007), Jat and Chaudhry (2010) and Ali et al. (2011) have studied radiation heat transfer in different aspects.

1.8 Present Investigations

The subject matter of the thesis has been divided into seven chapters, the details of which are as follows-

Chapter 1 deals with the introduction of the subject, recent investigations and the description of the problems investigated in the present thesis.

In **Chapter 2** a general analysis has been developed to study the two-dimensional, laminar flow of a viscous, incompressible, electrically conducting fluid near a stagnation point of a stretching sheet through a porous medium with heat generation in the presence of a magnetic field. The governing boundary layer equations transformed to ordinary differential equations by using suitable similarity variables. The solutions of momentum and energy equations have been obtained independently by a perturbation technique for a small magnetic parameter. The effects of the various parameters such as magnetic parameter, porosity parameter, stretching parameter, Prandtl number, Eckert number and heat generation coefficient for velocity and temperature distributions along with local skin friction coefficient and local Nusselt number have been studied in detail through graphical and numerical representations.

Chapter 3 deals with the study of the flow and heat transfer for an electrically conducting fluid with a porous substrate and a flat plate under the influence of magnetic field is considered. The magnetic field is assumed to be uniform and also

along normal to the surface. The momentum and energy equations are transformed to ordinary differential equations by using suitable similarity transformation and are solved by standard techniques. But the energy equation is solved by considering two boundary layers, one in the porous substrate and the other above the porous substrate. Numerical results are presented through graphs with various values of magnetic parameter for both velocity and thermal boundary layers along with Nusselt number and for various values of Prandtl number and Eckert number in thermal boundary layer.

In **Chapter 4** we have studied the steady two-dimensional, laminar flow of a viscous, incompressible, electrically conducting fluid near a stagnation point with heat transfer over a permeable surface in the presence of a uniform magnetic field. Taking suitable similarity variables, the governing boundary layer equations are transformed to ordinary differential equations and solved numerically by Shooting method. The effects of suction parameter, magnetic parameter, Prandtl number and Eckert number are studied on velocity and temperature distributions along with local skin friction coefficient and local Nusselt number.

Chapter 5 is devoted to the radiation effects on steady two-dimensional laminar boundary layer flow of an incompressible, viscous, electrically conducting fluid over an exponential stretching sheet in the presence of the uniform transverse magnetic field is studied by using Rosseland approximation. The governing boundary layer equations transform to ordinary differential equations by using suitable similarity transformation and are solved numerically by a perturbation technique for a small magnetic parameter. The effects of various parameters such as magnetic parameter,

radiation parameter, Prandtl number and Eckert number for velocity and temperature distributions along with local skin friction coefficient and surface heat transfer have been discussed in detail through graphical and numerical representations.

In **Chapter 6** we have considered the two-dimensional laminar boundary layer flow of a viscous, incompressible, electrically conducting fluid near a stagnation point past a shrinking sheet with slip in the presence of a magnetic field. The governing boundary layer equations are transformed to ordinary differential equations by taking suitable similarity variables and solved numerically by Shooting method. The effects of velocity ratio parameter, slip parameter, magnetic parameter, Prandtl number and Eckert number are studied on the velocity and temperature distributions along with local skin friction coefficient and surface heat transfer.

Chapter 7 is the last chapter which deals with the unsteady two-dimensional, laminar flow of a viscous, incompressible, electrically conducting fluid towards a shrinking surface in the presence of a uniform transverse magnetic field. Taking suitable similarity variables, the governing boundary layer equations are transformed to ordinary differential equations and solved numerically by a perturbation technique for a small magnetic parameter. The effects of various parameters such as unsteadiness parameter, velocity parameter, magnetic parameter, Prandtl number and Eckert number for velocity and temperature distributions along with local skin friction coefficient and local Nusselt number have been discussed in detail through graphical and numerical representations.

Chapter 2

Magnetohydrodynamic Stagnation Point Flow Past a Porous Stretching Surface with Heat Generation

2.1 Introduction

Flow of an incompressible viscous fluid over a stretching surface has important applications in the industry such as the extrusion of polymer in a melt-spinning process, the aerodynamic extrusion of plastic sheets, manufacturing plastic films, artificial fibers etc. Further glass blowing, continuous casting of metals and spinning of fibers involve the flow due to a stretching surface. Crane (1970) probably was first who studied the flow at a stretching sheet and produced a similarity solution in closed analytical form for the steady two-dimensional problem. Gupta and Gupta (1977), Dutta et al. (1985), Chiam (1994), Mahapatra and Gupta (2002), Andersson (2002), Elbashbeshy and Bazid (2003), Miklavcic and Wang (2006) and Jat and Chaudhary (2007) studied the heat transfer to steady the two-dimensional stagnation point flow over a stretching surface taking into account different aspects of the problem.

Recently, boundary layer flow through porous media is a subject of great interest due to its various applications such as oil recovery, composite manufacturing process, filtration processes, paper and textile coating, geothermal engineering. Its engineering and geophysical applications are flow of groundwater, geothermal energy utilization, insulation of buildings, energy storage, recovery and chemical reactor engineering. Attia (2007), Jat and Chaudhary (2009, 2010), Pal and Hiremath (2010),

Bhattacharyya and Layek (2011), Rosali et al. (2011), Singh and Pathak (2012), Mukhopadhyay and Layek (2012) and Ram et al. (2013) studied the boundary layer flow near the stagnation point of a stretching sheet through porous and non-porous boundaries under different physical situations. Very, recently Mahapatra and Nandy (2013) analyzed a stability of dual solutions in stagnation point flow and heat transfer over a porous shrinking sheet with thermal radiation.

In the present chapter, steady two-dimensional stagnation point flow has been investigated in a porous medium with heat generation of an electrically conducting fluid over a stretching surface in the presence of magnetic field. The results of velocity and temperature distribution, skin friction and surface heat transfer for different parameters such as the magnetic parameter, the porosity parameter, the stretching parameter, the Prandtl number, the Eckert number and the heat generation coefficient were obtained.

2.2 Formulation of the Problem

Consider the steady two-dimensional stagnation point flow $(u, v, 0)$ in a porous medium with heat generation of a viscous incompressible electrically conducting fluid near a stagnation point at a surface placed in the plane $y = 0$ of a Cartesian coordinates system with the $x-$axis along the surface, such that the surface is stretched in its own plane with velocity proportional to the distance from the stagnation point in the presence of an externally applied normal magnetic field of constant strength $(0, H_0, 0)$. The stretching surface has velocity u_w and temperature

T_w, while the velocity of the flow external to the boundary layer is u_e and temperature T_∞. The system of boundary layer equations (refer to Fig. 2.1) is given by-

$$\frac{\partial u}{\partial x}+\frac{\partial v}{\partial y}=0 \tag{2.1}$$

$$u\frac{\partial u}{\partial x}+v\frac{\partial u}{\partial y}=u_e\frac{du_e}{dx}+\upsilon\frac{\partial^2 u}{\partial y^2}+\frac{\upsilon}{K}\left(u_e-u\right)-\frac{\sigma_e\,\mu_e^2\,H_0^2\,u}{\rho} \tag{2.2}$$

$$\rho C_p\left(u\frac{\partial T}{\partial x}+v\frac{\partial T}{\partial y}\right)=\kappa\frac{\partial^2 T}{\partial y^2}+Q\left(T-T_\infty\right)+\mu\left(\frac{\partial u}{\partial y}\right)^2+\sigma_e\,\mu_e^2\,H_0^2\,u^2 \tag{2.3}$$

where υ is the kinematic viscosity, K the Darcy permeability, σ_e the electrical conductivity, μ_e the magnetic permeability, ρ the density, C_p the specific heat at constant pressure, κ the thermal conductivity, Q the volumetric rate of heat generation and μ the coefficient of viscosity of the fluid under consideration. The other symbols have their usual meanings.

The boundary conditions are-

$$\begin{aligned} &y=0:\ u=u_w=cx,\ v=0;\ \ T=T_w\\ &y=\infty:\ u=u_e=ax;\ \ T=T_\infty \end{aligned} \tag{2.4}$$

where c is a proportionality constant of the velocity of the stretching sheet and a is a constant proportional to the free stream velocity far away from the stretching sheet.

2.3 Analysis

The continuity equation (2.1) is identically satisfied by stream function $\psi(x,y)$, defined as

$$u = \frac{\partial \psi}{\partial y}, \qquad v = -\frac{\partial \psi}{\partial x} \tag{2.5}$$

For the solution of the momentum and the energy equations (2.2) and (2.3), the following dimensionless variables are defined-

$$\psi(x,y) = \sqrt{c\upsilon}\, x\, f(\eta) \tag{2.6}$$

$$\eta = \sqrt{\frac{c}{\upsilon}}\, y \tag{2.7}$$

$$\theta(\eta) = \frac{T - T_\infty}{T_w - T_\infty} \tag{2.8}$$

Equations (2.5) to (2.8), transform equations (2.2) and (2.3) into

$$f''' + f\, f'' - f'^2 - \mathrm{Re}_m^2\, f' - M\,(f' - C) + C^2 = 0 \tag{2.9}$$

$$\theta'' + \mathrm{Pr}\, f\, \theta' + \mathrm{Pr}\, B\, \theta + \mathrm{Pr}\, Ec\, f''^2 + \mathrm{Pr}\, Ec\, \mathrm{Re}_m^2\, f'^2 = 0 \tag{2.10}$$

where the prime (') denotes differentiation with respect to η, $\mathrm{Re}_m = \mu_e H_0 \sqrt{\frac{\sigma_e}{\rho c}}$ the magnetic parameter, $M = \frac{\upsilon}{K c}$ the porosity parameter, $C = \frac{a}{c}$ the stretching

parameter, $\Pr = \dfrac{\mu C_p}{\kappa}$ the Prandtl number, $B = \dfrac{Q}{c\rho C_p}$ the heat generation coefficient and $Ec = \dfrac{u_w^2}{C_p\left(T_w - T_\infty\right)}$ the Eckert number.

The corresponding boundary conditions are-

$$\begin{aligned} &\eta = 0: \quad f = 0,\ f' = 1; \quad \theta = 1 \\ &\eta = \infty: \quad f' = C; \quad \theta = 0 \end{aligned} \tag{2.11}$$

It may be noted that Chiam (1994) assumed $\mathrm{Re}_m = M = 0$ and $a = c$ without any justification and derived the solution of the equation (2.9), satisfying the equation (2.11), as $f(\eta) = \eta$ leading to $u = ax$, $v = -ay$. From this he inferred that no boundary layer is formed near the stretching surface.

For numerical solution of the equations (2.9) and (2.10), we apply a perturbation technique as-

$$f(\eta) = \sum_{i=0}^{\infty} \left(\mathrm{Re}_m^2\right)^i f_i(\eta) \tag{2.12}$$

$$\theta(\eta) = \sum_{j=0}^{\infty} \left(\mathrm{Re}_m^2\right)^j \theta_j(\eta) \tag{2.13}$$

Substituting equations (2.12) and (2.13) and its derivatives in equations (2.9) and (2.10) and then equating the coefficients of like powers of Re_m^2, we get the following set of differential equations-

$$f_0''' + f_0 f_0'' - f_0'^2 - M\left(f_0' - C\right) + C^2 = 0 \tag{2.14}$$

$$\theta_0'' + \Pr f_0 \theta_0' + \Pr B \theta_0 = -\Pr Ec f_0''^2 \tag{2.15}$$

$$f_1''' + f_0 f_1'' - \left(M + 2f_0'\right) f_1' + f_0'' f_1 = f_0' \tag{2.16}$$

$$\theta_1'' + \Pr f_0 \theta_1' + \Pr B \theta_1 = -\Pr f_1 \theta_0' - \Pr Ec\left(2 f_0'' f_1'' + f_0'^2\right) \tag{2.17}$$

$$f_2''' + f_0 f_2'' - \left(M + 2f_0'\right) f_2' + f_0'' f_2 = -f_1 f_1'' + \left(f_1' + 1\right) f_1' \tag{2.18}$$

$$\theta_2'' + \Pr f_0 \theta_2' + \Pr B \theta_2 = -\Pr\left(f_1 \theta_1' + f_2 \theta_0'\right) - \Pr Ec\left(2 f_0'' f_2'' + f_1''^2 + 2 f_0' f_1'\right) \tag{2.19}$$

with the boundary conditions-

$$\begin{aligned} &\eta = 0: \;\; f_i = 0,\; f_0' = 1,\; f_j' = 0; \;\; \theta_0 = 1,\; \theta_j = 0 \\ &\eta = \infty: \;\; f_0' = C,\; f_j' = 0; \;\; \theta_i = 0 \qquad\qquad i \geq 0,\; j > 0 \end{aligned} \tag{2.20}$$

The equation (2.14) is obtained by Attia (2007) for the non-magnetic case and the remaining equations are linear ordinary differential equations and have been solved numerically by standard techniques. The velocity and temperature distributions for various values of the parameters are shown in Fig. 2.2 and Fig. 2.3 to 2.5 respectively.

2.4 Skin Friction and Surface Heat Transfer

The physical quantities of interest, the local skin friction coefficient C_f and the local Nusselt number Nu i.e. surface heat transfer are given by-

$$C_f = \frac{\tau_w}{\rho u_w^2/2} = \frac{\mu\left(\frac{\partial u}{\partial y}\right)_{y=0}}{\rho u_w^2/2} \tag{2.21}$$

and

$$Nu = -\frac{x\left(\frac{\partial T}{\partial y}\right)_{y=0}}{\left(T_w - T_\infty\right)} \tag{2.22}$$

which, in the present case, can be expressed in the following forms

$$C_f = \frac{2}{\sqrt{\mathrm{Re}}} f''(0)$$

$$= \frac{2}{\sqrt{\mathrm{Re}}} \sum_{i=0}^{\infty} \left(\mathrm{Re}_m^2\right)^i f_i''(0) \tag{2.23}$$

and

$$Nu = -\sqrt{\mathrm{Re}}\,\theta'(0)$$

$$= -\sqrt{\mathrm{Re}} \sum_{j=0}^{\infty} \left(\mathrm{Re}_m^2\right)^j \theta_j'(0) \tag{2.24}$$

where $\mathrm{Re} = \frac{u_w x}{\upsilon}$ is the local Reynolds number.

Numerical values of the functions $f''(0)$ and $\theta'(0)$, which are proportional to local skin friction and local heat transfer rate at the surface, respectively for various values of the parameters are presented in Table 2.1.

2.5 Results and Discussion

The Figure 2.2 shows the variation of velocity distribution against η for various values of the parameters, namely, the magnetic parameter Re_m, the porosity parameter M and the stretching parameter C. It may be observed that the velocity increases as the stretching parameter C increases, whereas it decreases as the magnetic parameter Re_m increases for a fixed η. Also, it can be seen that the velocity increases as the porosity parameter M decreases for $C<1$ and when $C>1$, the opposite phenomenon occurs.

The Figures 2.3 to 2.5 show the variation of the temperature distribution against η for various values of the parameters, namely, the magnetic parameter Re_m, the porosity parameter M, the stretching parameter C, the Prandtl number Pr, the Eckert number Ec and the heat generation coefficient B. From these figures it may be observed that the temperature distribution increases with the increasing value of the magnetic parameter Re_m. It is also seen that for fixed Prandtl number Pr, temperature distribution decreases with increasing value of the stretching parameter C and same phenomenon occurs for the Eckert number Ec. In Fig. 2.3 it is seen that temperature distribution increases with the increasing value of the porosity parameter M for $C<1$ and when $C>1$, the opposite phenomenon occurs. In Fig. 2.4, it is observed that the temperature distribution decreases with the increasing value of the Prandtl number Pr.

In Table 2.1 the numerical values of the functions $-f''(0)$ and $-\theta'(0)$ for various values of the magnetic parameter Re_m, the porosity parameter M, the stretching parameter C, the Prandtl number Pr and the Eckert number Ec with the heat generation coefficient $B = 0.1$ are given. It may be observed from the table that the boundary values of $f''(0)$ and $\theta'(0)$ for the non-magnetic flow are same as those obtained by Attia (2007). Further it may be observed from the table that for $C < 1$, the value of $-f''(0)$ increases with the increasing values of the porosity parameter M and the magnetic parameter Re_m and when $C > 1$ same phenomenon occurs for the magnetic parameter Re_m while opposite phenomenon occurs for the porosity parameter M. It may also be observed that when the stretching parameter C increases, the value of $-f''(0)$ decreases. Moreover for the fixed value of the Prandtl number Pr, value of the function $-\theta'(0)$ decreases with the increasing values of the porosity parameter M, the Eckert number Ec and the magnetic parameter Re_m when $C < 1$ while the opposite phenomenon occurs for the porosity parameter M when $C > 1$. Again the function $-\theta'(0)$ increases with the increase of the Prandtl Number Pr and the stretching parameter C for the fixed value of the porosity parameter M. Also, when the stretching parameter C increases, the value of $-\theta'(0)$ increases.

2.6 Conclusions

In this chapter, the two-dimensional stagnation point flow in a porous medium with heat generation of an electrically conducting fluid over a stretching surface in the

presence of magnetic field has been studied. Similarity equations are derived and solved numerically. It is found that the velocity boundary layer thickness increases with the increasing value of the stretching parameter and decreases with the increasing value of the magnetic parameter. It is further concluded that velocity boundary layer thickness increases with the increasing value of the porosity parameter when the stretching parameter is greater than one while it decreases when the stretching parameter is less than one, but the reverse phenomenon occurs for the thermal boundary layer thickness. Further the thermal boundary layer thickness decreases with the increasing value of the Prandtl number and the Eckert number but for fixed Prandtl number the thermal boundary layer thickness decreases with the increasing value of the stretching parameter. From the results it can be concluded that skin friction and Nusselt number varies in reverse phenomenon as compared to velocity boundary layer thickness and thermal boundary layer thickness respectively with different parameters.

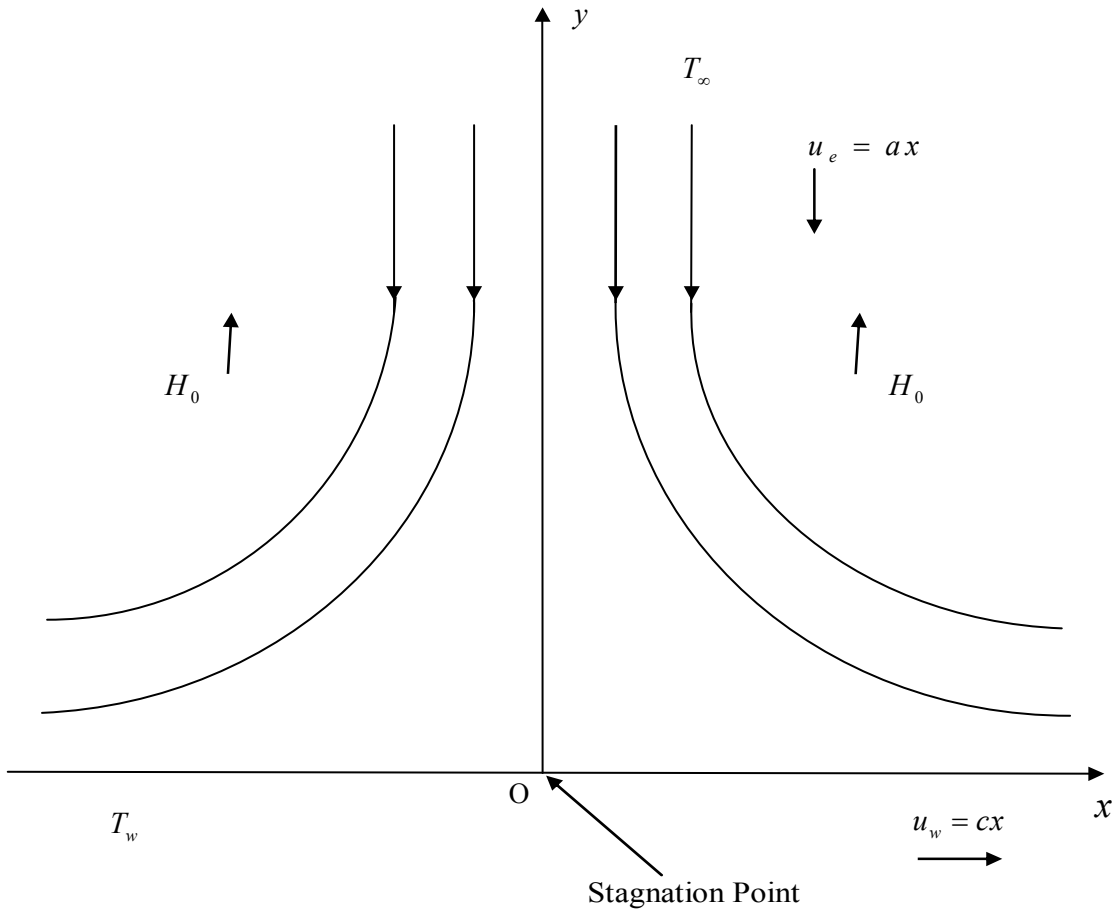

Fig. 2.1 Physical model and coordinate system.

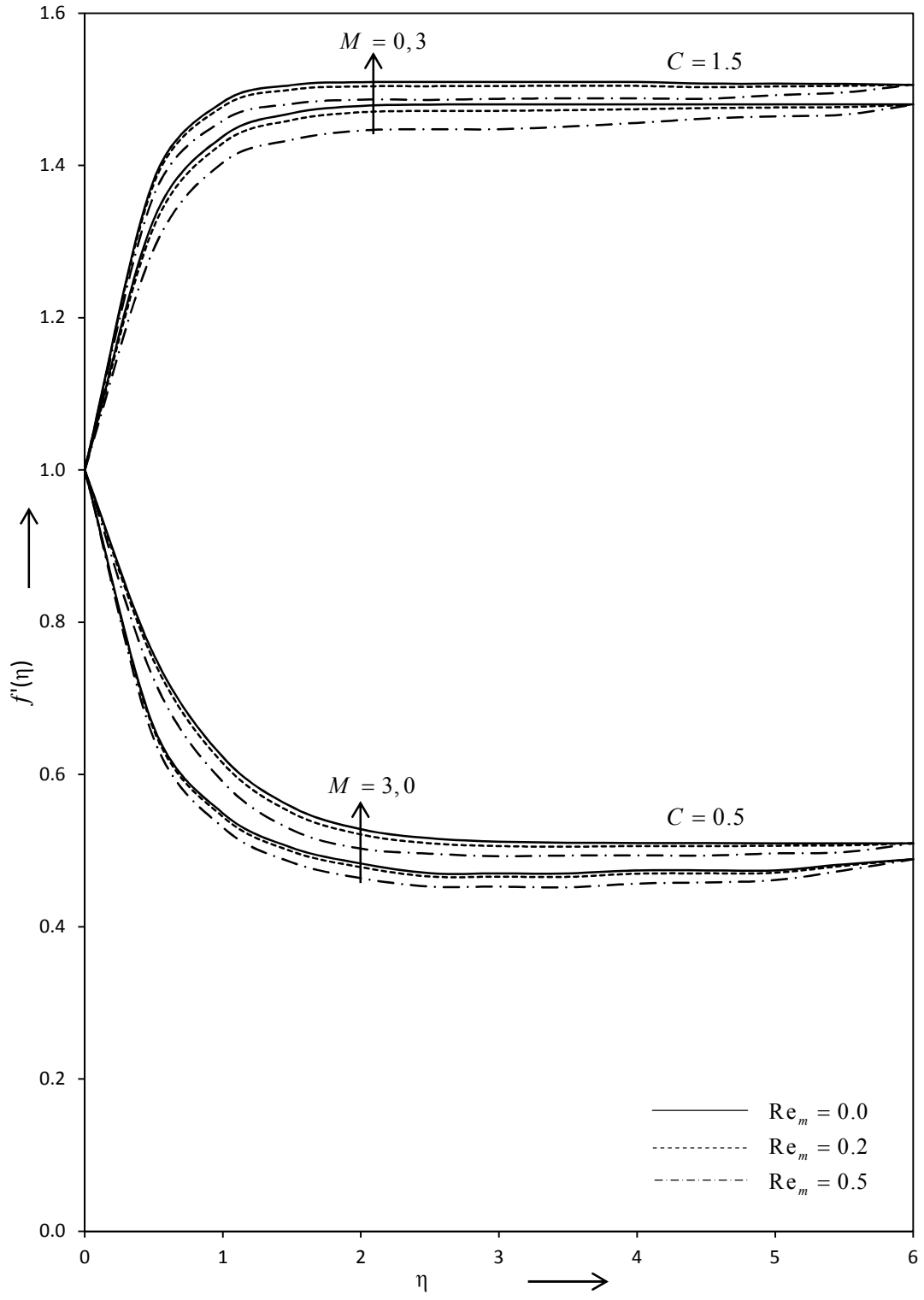

Fig. 2.2 Velocity distribution against η for various values of Re_m, M and C.

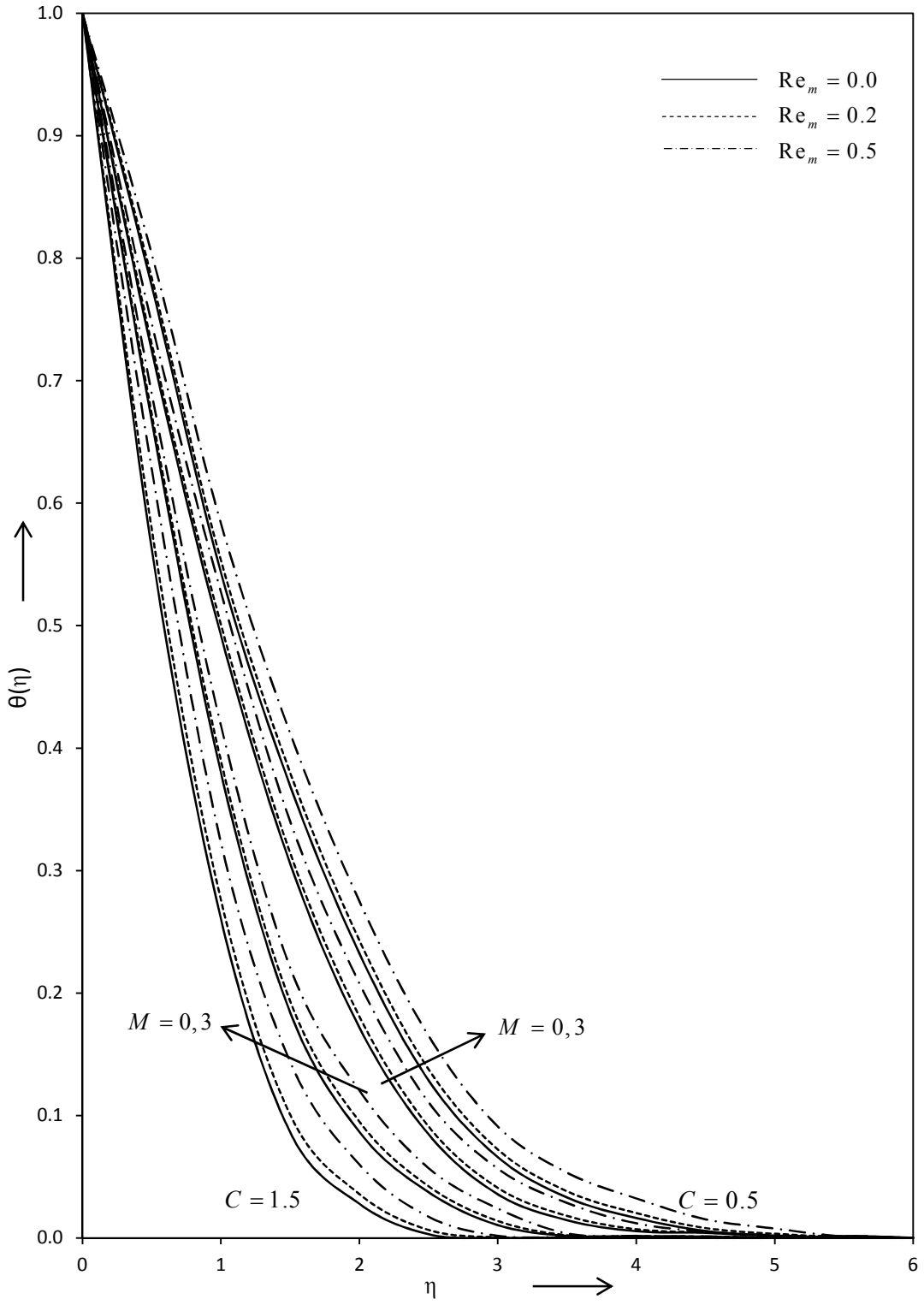

Fig. 2.3 Temperature distribution against η for various values of Re_m, M and C with $\mathrm{Pr} = 0.7$, $Ec = 0.0$ and $B = 0.1$.

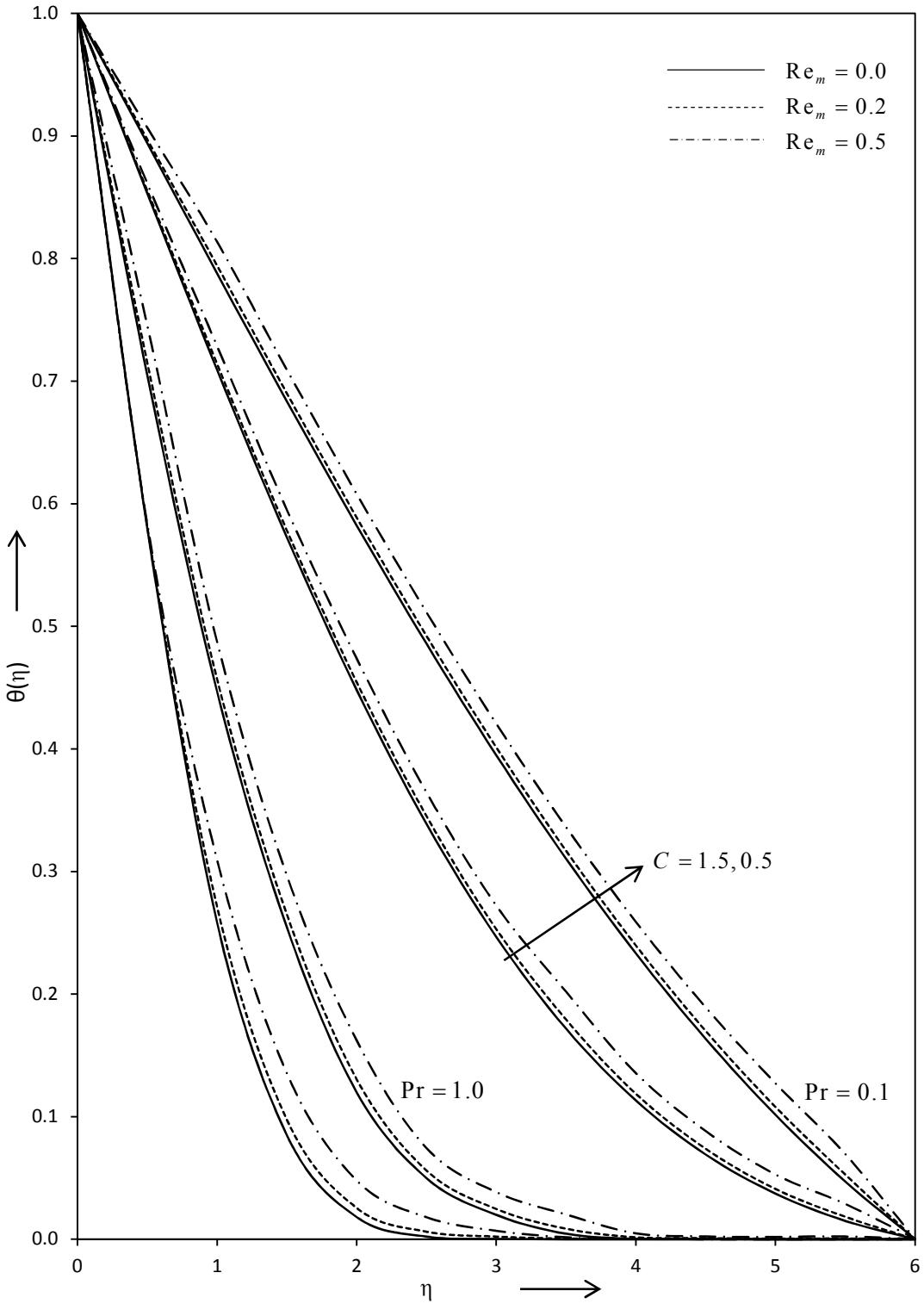

Fig. 2.4 Temperature distribution against η for various values of Re_m, C and Pr with $M = 3$, $Ec = 0.0$ and $B = 0.1$.

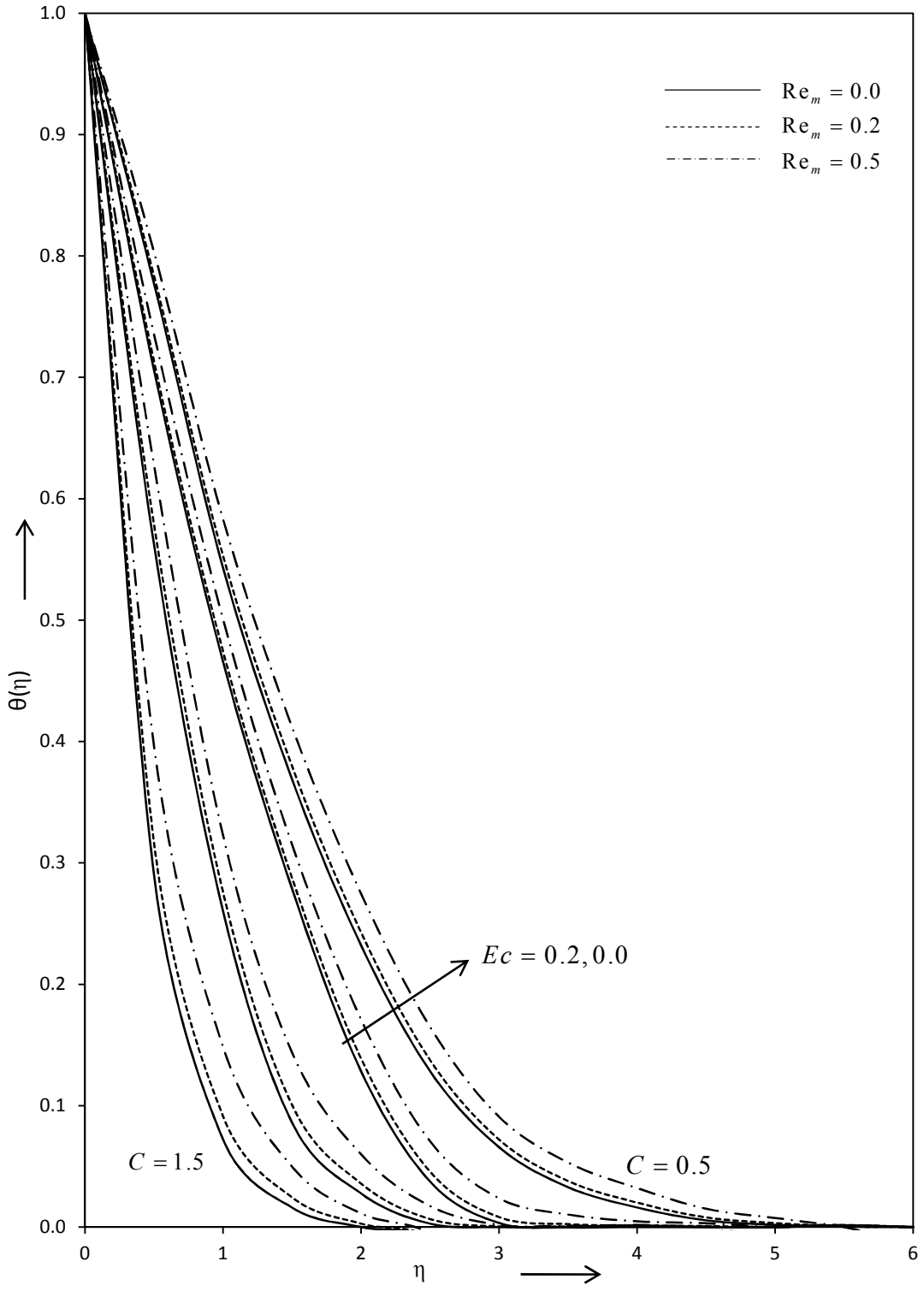

Fig. 2.5 Temperature distribution against η for various values of Re_m, C and Ec with $M = 3$, $\mathrm{Pr} = 0.7$ and $B = 0.1$.

Table 2.1 Numerical values of $-f''(0)$ and $-\theta'(0)$ for various values of Re_m, M, C, Pr and Ec with $B = 0.1$.

$-f''(0)$													
M		$C = 0.5$						C = 1.5					
		Re_m=0.0		Re_m=0.2		Re_m=0.5		Re_m=0.0		Re_m=0.2		Re_m=0.5	
0		0.6673		0.6939		0.7707		-0.9095		-0.8752		-0.7746	
3		1.0910		1.1056		1.1485		-1.2533		-1.2308		-1.1642	
$-\theta'(0)$													
M	Pr	$C = 0.5$						$C = 1.5$					
		$Ec = 0.0$			$Ec = 0.2$			$Ec = 0.0$			$Ec = 0.2$		
		Re_m=0.0	Re_m=0.2	Re_m=0.5	Re_m=0.0	Re_m=0.2	Re_m=0.5	Re_m=0.0	Re_m=0.2	Re_m=0.5	Re_m=0.0	Re_m=0.2	Re_m=0.5
0	0.1	0.2148	0.2148	0.2140	0.2148	0.2148	0.2133	0.2898	0.2898	0.2890	0.2898	0.2898	0.2862
	0.7	0.5089	0.5089	0.5058	0.5089	0.5089	0.5010	0.7131	0.7131	0.7111	0.7131	0.7130	0.6985
	1.0	0.6220	0.6220	0.6186	0.6220	0.6220	0.6221	0.8437	0.8437	0.8415	0.8437	0.8436	0.8255
3	0.1	0.2103	0.2102	0.2100	0.2102	0.2103	0.2094	0.2921	0.2921	0.2916	0.2921	0.2920	0.2887
	0.7	0.4821	0.4821	0.4809	0.4821	0.4821	0.4769	0.7235	0.7235	0.7224	0.7235	0.7234	0.7089
	1.0	0.5888	0.5888	0.5874	0.5888	0.5888	0.5820	0.8566	0.8566	0.8553	0.8566	0.8565	0.8383

Chapter 3

MHD Forced Convection Boundary Layer Flow with a Flat Plate and Porous Substrate

3.1 Introduction

During the past several years, the requirements of modern technology have stimulated interest in fluid flow studies which involve interaction of several phenomena. One such study is related to the effects of forced convection flow through a porous substrate which plays an important role in many engineering applications including geothermal energy, petroleum reservoirs, environmental pollution, fuel cells, nano-manufacturing and nano-material processing. Vafai and Kim (1990) first discussed the external convection problem involving a relatively thin porous substrate attached to the surface of a flat plate. Huang and Vafai (1994) further studied the flow and heat transfer over an external boundary covered with a porous substrate. Ochoa-Tapia and Whitaker (1995) studied the boundary conditions at the porous medium or clear fluid by applying sophisticated volume-averaging technique which accounts for a jump in the stress at the interface. Kuznetsov (1997, 1998, 2000), Nield and Kuznetsov (2003), Nield and Bejan (2006), Aydin and Kaya (2008), Mukhopadhyay et al. (2012) and Wang (2013) reviewed the same problem of forced convection which is partly filled with a porous medium and partly with a clear fluid. The problem of forced convection of an electrically conducting fluid with a porous substrate and the flat plate under the influence of a magnetic field has attracted the interest of many

research works in view of its applications to astrophysics, engineering and to the boundary layer control in the field of aerodynamics.

The objective of the present chapter is to study the flow and heat transfer for an electrically conducting fluid with a porous substrate and to the flat plate under the influence of magnetic field. For simplicity, we use a Darcy model for the flow in the porous substrate, and the interface between the porous medium and the fluid clear of solid material, with the Beavers and Joseph (1967) boundary condition.

3.2 Formulation of the Problem

The boundary layer equations for a two-dimensional flow of an electrically conducting, viscous, incompressible fluid past a flat plate, in a uniform stream of velocity U_∞ and temperature T_∞ are constant, and the wall is maintained at constant temperature T_w, the thickness of the porous substrate is h, with an externally applied magnetic field of constant strength B_0 normal to the plate (Fig. 3.1), are [Cramer and Pai (1973)]-

$$\frac{\partial u}{\partial x}+\frac{\partial v}{\partial y}=0 \tag{3.1}$$

$$u\frac{\partial u}{\partial x}+v\frac{\partial u}{\partial y}=\upsilon\frac{\partial^2 u}{\partial y^2}-\frac{\sigma_e B_0^2 u}{\rho} \tag{3.2}$$

$$\rho\, C_p\left(u\frac{\partial T}{\partial x}+v\frac{\partial T}{\partial y}\right)=\kappa\frac{\partial^2 T}{\partial y^2}+\mu\left(\frac{\partial u}{\partial y}\right)^2+\sigma_e B_0^2 u^2 \tag{3.3}$$

where υ is the kinematic viscosity, σ_e the electrical conductivity, ρ the density, C_p the specific heat at constant pressure, κ the thermal conductivity and μ the coefficient of viscosity of the fluid under consideration. The other symbols have their usual meanings.

Since the flow of an in-viscid fluid (outside the boundary layer) is constant, pressure gradient in an in-viscid fluid and in the porous substrate are zero. Also, we are modeling the flow in the porous medium by Darcy's equation, which means that the velocity in the porous medium is zero. Also, we are imposing Beavers and Joseph (1967) boundary condition on the boundary, instead of no-slip condition as-

$$\left(\frac{\partial u}{\partial y}\right)_{y=0} = \left(\frac{\alpha_{BJ} u}{K^{1/2}}\right)_{y=0} \tag{3.4}$$

where α_{BJ} is the Beavers-Joseph constant and K is the permeability of the porous medium.

Therefore, in the present case, the boundary conditions are-

$$\begin{aligned} &y = 0: \quad u = \frac{K^{1/2}}{\alpha_{BJ}}\left(\frac{\partial \mathrm{u}}{\partial \mathrm{y}}\right), \; v = 0; \quad T = T_w \\ &y = \infty: \quad \frac{\partial u}{\partial y} = 0, \; \frac{\partial u}{\partial x} = -\frac{\sigma_e B_0^2}{\rho}; \quad T = T_\infty \end{aligned} \tag{3.5}$$

3.3 Analysis of the Velocity Boundary Layer

The boundary condition in (3.5), for the momentum equation at infinity, may be written as-

$$y=\infty:\ u=U(x)=U_{\infty}-\frac{\sigma_e B_0^2 x}{\rho}=U_{\infty}(1-\xi) \tag{3.6}$$

where,

$$\xi=\frac{\sigma_e B_0^2 x}{\rho U_{\infty}} \quad (\textit{magnetic interaction parameter}) \tag{3.7}$$

Introducing the stream function $\psi(x,y)$, such that

$$u=\frac{\partial\psi}{\partial y},\qquad v=-\frac{\partial\psi}{\partial x} \tag{3.8}$$

The equation of continuity (3.1) is identically satisfied and for the solution of the momentum equation (3.2), applying the generalized Falkner-Skan transformation as-

$$\psi=\sqrt{\upsilon x U}\,(1+\mathrm{g})^{-1/2}\ f(g,\eta) \tag{3.9}$$

$$\eta=y\sqrt{\frac{U}{\upsilon x}}\,(1+\mathrm{g})^{1/2} \tag{3.10}$$

where

$$g(\xi)=\frac{\xi}{U}\frac{dU}{d\xi} \quad (\textit{magnetic parameter}) \tag{3.11}$$

Hence,

$$u = U_\infty (1-g)^{-1} f_\eta \tag{3.12}$$

$$v = -\frac{1}{2}\sqrt{\frac{\upsilon U_\infty}{x}} g(1-g^2)^{-1/2} f - \frac{1}{2}\sqrt{\frac{\upsilon U_\infty}{x}} (1-g^2)^{-1/2} f$$

$$+ \frac{1}{2}\sqrt{\frac{\upsilon U_\infty}{x}} g(1-g)^{1/2}(1+g)^{-3/2} f - \sqrt{\frac{\upsilon U_\infty}{x}} g(1-g)^{1/2}(1+g)^{-1/2} f_g \tag{3.13}$$

$$+ \frac{y}{2x} U_\infty (1-g)^{-1} f_\eta - \frac{y}{2x} U_\infty g(1-g)^{-1} f_\eta - \frac{y}{2x} U_\infty g(1+g)^{-1} f_\eta$$

$$g(\xi) = -\frac{\xi}{1-\xi} \tag{3.14}$$

The momentum equation (3.2), after some simplifications, reduces to the form

$$\begin{aligned} 2(1+g)^2 f_{\eta\eta\eta} + (1+g+2g^2) f f_{\eta\eta} + 2g(1+g)\left(f_\eta - f_\eta^{\,2}\right) \\ = 2g(1-g^2)\left(f_\eta f_{g\eta} - f_g f_{\eta\eta}\right) \end{aligned} \tag{3.15}$$

with the corresponding boundary conditions-

$$\begin{aligned} &\eta = 0: \quad f = 0,\ f_\eta = \zeta\left(1+g+\tfrac{1}{2}g^2\right) f_{\eta\eta} \\ &\eta = \infty: \quad f_\eta = 1 \end{aligned} \tag{3.16}$$

where,

$$\zeta = \frac{1}{\alpha_{BJ}}\left(\frac{KU_\infty}{\upsilon x}\right)^{1/2} \quad (\textit{Porosity parameter}) \tag{3.17}$$

It may be noted that for a physically acceptable solution of the equation (3.15), the function $(1+g)$ introduced in equations (3.9) and (3.10) should be positive, which implies that $\xi = \dfrac{\sigma_e B_0^2 x}{\rho U_\infty} < \frac{1}{2}$. It follows that

$$g = -\frac{\xi}{1-\xi} < 1 \tag{3.18}$$

Again we assume that porosity parameter ζ is small and therefore a rapidly convergent series solution of equation (3.15) can be obtained if we expand $f(g,\eta)$ in power series of magnetic parameter g and porosity parameter ζ of the form-

$$f(g,\eta) = \sum_{i=0}^{\infty}\sum_{j=0}^{\infty} \zeta^i (-g)^j f_{ij}(\eta) \tag{3.19}$$

Substituting equation (3.19) and its derivatives in equation (3.15) and comparing the coefficients of like terms, we get the following set of equations-

I. Terms independent of ζ give-

$$2f_{00}''' + f_{00}f_{00}'' = 0 \tag{3.20}$$

$$2f_{01}''' + f_{00}f_{01}'' - 2f_{00}'f_{01}' + 3f_{00}''f_{01} = -f_{00}f_{00}'' + 2f_{00}' - 2f_{00}'^2 \tag{3.21}$$

$$\begin{aligned} &2f_{02}''' + f_{00}f_{02}'' - 4f_{00}'f_{02}' + 5f_{00}''f_{02} \\ &= -(f_{00} + 3f_{01})f_{01}'' + 2(f_{01}' + 1)f_{01}' - 5f_{00}''f_{01} - 3f_{00}f_{00}'' \\ &\quad - 2(f_{00}' - 1)f_{00}' \end{aligned} \tag{3.22}$$

The boundary conditions are-

$$\begin{aligned} &\eta = 0: \quad f_{0j} = 0,\ f'_{0j} = 0, \quad j \geq 0 \\ &\eta = \infty: \quad f'_{00} = 1,\ f'_{0j} = 0, \quad j > 0 \end{aligned} \tag{3.23}$$

II. Terms containing ζ give-

$$2f'''_{10} + f_{00}f''_{10} + f''_{00}f_{10} = 0 \tag{3.24}$$

$$\begin{aligned} &2f'''_{11} + f_{00}f''_{11} - 2f'_{00}f'_{11} + 3f''_{00}f_{11} \\ &\quad = -\left(f_{00} + 3f_{01}\right)f''_{10} - 2\left(2f'_{00} - f'_{01} - 1\right)f'_{10} - \left(f''_{00} + f''_{01}\right)f_{10} \end{aligned} \tag{3.25}$$

$$\begin{aligned} &2f'''_{12} + f_{00}f''_{12} - 4f'_{00}f'_{12} + 5f''_{00}f_{12} \\ &\quad = -\left(f_{00} + 3f_{01}\right)f''_{11} + 2\left(2f'_{01} + 1\right)f'_{11} - \left(5f''_{00} + 3f''_{01}\right)f_{11} \\ &\quad -\left(3f_{00} + 5f_{01} + 5f_{02}\right)f''_{10} - 2\left(2f'_{00} - 2f'_{02} - 1\right)f'_{10} \\ &\quad -\left(3f''_{00} + f''_{01} + f''_{02}\right)f_{10} \end{aligned} \tag{3.26}$$

The boundary conditions are-

$$\begin{aligned} &\eta = 0: \quad f_{1j} = 0,\ f'_{10} = f''_{00},\ f'_{11} = f''_{01} - f''_{00},\ f'_{12} = f''_{02} - f''_{01} + \tfrac{1}{2}f''_{00} \\ &\eta = \infty: \quad f'_{1j} = 0, \quad j \geq 0 \end{aligned} \tag{3.27}$$

The equations (3.20) and (3.24) are those of Nield and Kuznetsov (2003) for a non-magnetic case. The remaining equations are linear ordinary differential equations. These have been solved numerically by standard techniques with the help of computer

programming. The velocity profiles for various values of g are plotted against η in Fig. 3.2 and 3.3.

3.4 Analysis of the Thermal Boundary Layer

Since the porous substrate is attached with the plate, there are two thermal boundary layers- one in the porous substrate, known as the porous thermal boundary layer, and other above the porous substrate, known as ordinary thermal boundary layer.

(i) Porous Thermal Boundary Layer

Due to stagnate fluid, the energy equation is considered a simple conduction equation for the temperature T_p, therefore under boundary layer approximations, the energy equation in the porous boundary layer reduces to-

$$\kappa \frac{\partial^2 T_p}{\partial y^2} = 0 \tag{3.28}$$

We have the boundary condition

$$y = -h: \quad T_p = T_w \tag{3.29}$$

and the matching conditions

$$y = 0: \quad T = T_p, \quad \kappa \frac{\partial T}{\partial y} = \kappa_p \frac{\partial T_p}{\partial y} \tag{3.30}$$

Let

$$\theta_p = \frac{T_p - T_\infty}{T_w - T_\infty} \tag{3.31}$$

The boundary and matching conditions become

$$\eta = -\lambda\zeta\left(1 + g + \tfrac{1}{2}g^2\right): \quad \theta_p = 1 \tag{3.32}$$

$$\eta = 0: \quad \theta = \theta_p, \quad \frac{\partial\theta}{\partial\eta} = \kappa_m \frac{\partial\theta_p}{\partial\eta} \tag{3.33}$$

where

$$\lambda = \frac{\alpha_{BJ} h}{\sqrt{K}} \tag{3.34}$$

$$\kappa_m = \frac{\kappa_p}{\kappa} \tag{3.35}$$

The energy equation (3.28) becomes

$$\frac{\partial^2\theta_p}{\partial\eta^2} = 0 \tag{3.36}$$

The solution of equation (3.36), satisfying (3.32) to first order in ζ is

$$\theta_p = 1 + \{A(\lambda\zeta + \eta) + B\zeta\eta\}\left(1 + g + \tfrac{1}{2}g^2\right) \tag{3.37}$$

where A and B are constants.

The matching conditions then give-

$$\eta = 0: \quad \theta = 1 + A\lambda\zeta\left(1 + g + \tfrac{1}{2}g^2\right), \quad \theta_\eta = \kappa_m\left(A + B\zeta\right)\left(1 + g + \tfrac{1}{2}g^2\right) \tag{3.38}$$

(ii) Ordinary Thermal Boundary Layer

By introducing dimensionless temperature distribution

$$\frac{T - T_\infty}{T_w - T_\infty} = \theta(g, \eta, \zeta) \tag{3.39}$$

The energy equation (3.3) after some simplification reduces to-

$$\begin{aligned} &2\left(1-g^2\right)^2\theta_{\eta\eta} + \Pr\left(1-g\right)^2\left(1+g+2g^2\right)f\theta_\eta + \Pr\zeta\left(1-g\right)^2\left(1+g\right)f_\eta\theta_\zeta \\ &\qquad = 2\Pr g\left(1-g\right)^2\left(1-g^2\right)\left(f_\eta\theta_g - f_g\theta_\eta\right) - 2\Pr Ec\left(1+g\right)^2 f_{\eta\eta}^2 \\ &\qquad\quad + 2\Pr Ec\; g\left(1+g\right)f_\eta^2 \end{aligned} \tag{3.40}$$

with the boundary conditions-

$$\begin{aligned} &\eta = 0: \quad \theta = 1 \\ &\eta = \infty: \quad \theta = 0 \end{aligned} \tag{3.41}$$

where $\Pr = \dfrac{\mu C_p}{\kappa}$ is the Prandtl number and $Ec = \dfrac{U_\infty^2}{C_p\left(T_w - T_\infty\right)}$ the Eckert number.

For small magnetic parameter g and porosity parameter ζ, a series solution of the equation (3.40) similar to the velocity boundary layer can be obtained by taking $\theta(g, \eta, \zeta)$ as

$$\theta(g,\eta,\zeta)=\sum_{i=0}^{\infty}\sum_{j=0}^{\infty}\zeta^{i}(-g)^{j}\theta_{ij}(\eta) \tag{3.42}$$

Substituting equations (3.19) and (3.42) with derivatives in equation (3.40) and comparing the coefficients of like terms, we get the following set of equations-

I. Terms independent of ζ give-

$$2\theta_{00}''+\Pr f_{00}\theta_{00}'=-2\Pr Ecf_{00}''^{2} \tag{3.43}$$

$$\begin{aligned}&2\theta_{01}''+\Pr f_{00}\theta_{01}'-2\Pr f_{00}'\theta_{01}\\&\quad=-\Pr(f_{00}+3f_{01})\ \theta_{00}'-2\Pr Ec\left(2f_{00}''f_{01}''-2f_{00}''^{2}+f_{00}'^{2}\right)\end{aligned} \tag{3.44}$$

$$\begin{aligned}&2\theta_{02}''+\Pr f_{00}\theta_{02}'-4\Pr f_{00}'\theta_{02}\\&\quad=-\Pr(f_{00}+3f_{01})\theta_{01}'+2\Pr(2f_{00}'+f_{01}')\theta_{01}\\&\quad-\Pr(3f_{00}+5f_{01}+5f_{02})\theta_{00}'\\&\quad-2\Pr Ec\left(2f_{00}''f_{02}''+f_{01}''^{2}-4f_{00}''f_{01}''+2f_{00}'f_{01}'+3f_{00}''^{2}-f_{00}'^{2}\right)\end{aligned} \tag{3.45}$$

The boundary and the matching conditions are-

$$\begin{aligned}&\eta=0:\ \ \theta_{00}=1,\ \ \theta_{0j}=0,\ \ \theta_{00}'=\kappa_{m}A,\ \ \theta_{01}'=-\kappa_{m}A,\ \ \theta_{02}'=\tfrac{1}{2}\kappa_{m}A,\ \ \mathrm{j}>0\\&\eta=\infty:\ \ \theta_{0j}=0,\ \ j\geq 0\end{aligned} \tag{3.46}$$

II. Terms containing ζ give-

$$2\theta_{10}''+\Pr f_{00}\theta_{10}'+\Pr f_{00}'\theta_{10}=-\Pr f_{10}\theta_{00}'-4\Pr Ecf_{00}''f_{10}'' \tag{3.47}$$

$$
\begin{aligned}
&2\theta_{11}'' + \Pr f_{00}\theta_{11}' - \Pr f_{00}'\theta_{11} \\
&\quad = -\Pr\left(f_{00}+3f_{01}\right)\theta_{10}' - \Pr\left(f_{00}'+f_{01}'\right)\theta_{10} - \Pr f_{10}\theta_{01}' + 2\Pr f_{10}'\theta_{01} \\
&\quad -\Pr\left(f_{10}+3f_{11}\right)\theta_{00}' - 4\Pr Ec\left(f_{00}''f_{11}'' - 2f_{00}''f_{10}'' + f_{01}''f_{10}'' + f_{00}'f_{10}'\right)
\end{aligned}
\tag{3.48}
$$

$$
\begin{aligned}
&2\theta_{12}'' + \Pr f_{00}\theta_{12}' - 3\Pr f_{00}'\theta_{12} \\
&\quad = -\Pr\left(f_{00}+3f_{01}\right)\theta_{11}' + \Pr\left(3f_{00}'+f_{01}'\right)\theta_{11} - \Pr\left(3f_{00}+5f_{01}+5f_{02}\right)\theta_{10}' \\
&\quad -\Pr\left(f_{00}'+f_{01}'+f_{02}'\right)\theta_{10} - \Pr f_{10}\theta_{02}' + 4\Pr f_{10}'\theta_{02} \ -\Pr\left(f_{10}+3f_{11}\right)\theta_{01}' \\
&\quad +2\Pr\left(2f_{10}'+f_{11}'\right)\theta_{01} - \Pr\left(3f_{10}+5f_{11}+5f_{12}\right)\theta_{00}' \\
&\quad -4\Pr Ec\left(f_{00}''f_{12}'' - 2f_{00}''f_{11}'' + f_{01}''f_{11}'' + f_{00}'f_{11}' + 3f_{00}''f_{10}'' - 2f_{01}''f_{10}''\right. \\
&\quad \left. + f_{02}''f_{10}'' - f_{00}'f_{10}' + f_{01}'f_{10}'\right)
\end{aligned}
\tag{3.49}
$$

The boundary and the matching conditions are-

$$
\begin{aligned}
&\eta = 0: \ \ \theta_{10} = A\lambda,\ \theta_{11} = -A\lambda,\ \theta_{12} = \tfrac{1}{2}A\lambda,\ \theta_{10}' = \kappa_m B,\ \theta_{11}' = -\kappa_m B,\ \theta_{12}' = \tfrac{1}{2}\kappa_m B \\
&\eta = \infty: \ \ \theta_{1j} = 0,\ j \geq 0
\end{aligned}
\tag{3.50}
$$

Equations (3.43) to (3.50) with the boundary and matching conditions have been solved numerically by standard techniques and the corresponding temperature profiles against η are shown graphically in Fig. 3.4 to 3.7 for different g.

3.5 Surface Heat Transfer

The heat flux at the boundary is

$$q = \kappa \left(\frac{\partial T}{\partial y} \right)_{y=0} \tag{3.51}$$

If the Nusselt number is defined by

$$Nu = -\frac{qx}{\kappa \left(T_w - T_\infty \right)} \tag{3.52}$$

which, in the present case becomes

$$Nu^* = -\left(1 + g + \tfrac{1}{2} g^2 \right) \sum_{i=0}^{\infty} \sum_{j=0}^{\infty} \zeta^i \left(-g \right)^j \theta'_{ij}(0) \tag{3.53}$$

where

$$Nu^* = \frac{Nu}{\sqrt{\mathrm{Re}}} \tag{3.54}$$

and

$$\mathrm{Re} = \frac{U_\infty x}{\upsilon} \qquad (\textit{local Reynolds number}) \tag{3.55}$$

The Nusselt numbers for various values of magnetic parameter g against Prandtl number Pr are shown in Fig. 3.8 and 3.9.

3.6 Results and Discussion

From Figures 3.2 and 3.3 it is evident that the velocity increases with the increasing value of the magnetic parameter g. It is further observed that in the presence of the

porous substrate the velocity profiles decrease more rapidly with the increase in the magnetic parameter g. Similarly, for the temperature distribution i.e. from the Fig. 3.4 and 3.5, it is observed that the temperature distribution increases with the increasing value of the magnetic parameter g for $\eta < 1$ and afterwards it decreases with the increasing value of the magnetic parameter g whereas the temperature distribution decreases with the increasing values of the Prandtl number Pr and the Eckert number Ec respectively. The Fig. 3.6 and 3.7 also shows the variation of temperature distribution in the presence of porous substrate, the temperature distribution decreases with the increase in the magnetic parameter g. Also, in Fig. 3.6 it can be seen that for $1 < \eta < 3$, the temperature distribution decreases for the increasing value of the Prandtl number Pr and the temperature distribution increases for the increasing values of the Prandtl number Pr for other value of η. But in Fig. 3.7, it can be seen that the temperature distribution increases with the increase in the Eckert number Ec. For $\eta < 2.5$ the temperature distribution decreases with the increase in η and for $\eta > 2.5$, reverse phenomenon occurs. The Fig. 3.8 and 3.9 show the variation of the Nusselt number against the Prandtl number Pr. It is observed that the Nusselt number increases with the increasing value of the magnetic parameter g. Further it is observed that for the given magnetic parameter g, the Nusselt number increases with the Prandtl number Pr faster than corresponding to the absence of the porous substrate.

3.7 Conclusions

In this chapter, it is concluded that in the porous substrate the effect of the magnetic field is to retard the flow for $\eta \leq 2.5$ whereas it accelerates the flow for $\eta > 2.5$. The Nusselt number increases with the increasing values of both the magnetic parameter and the Prandtl number.

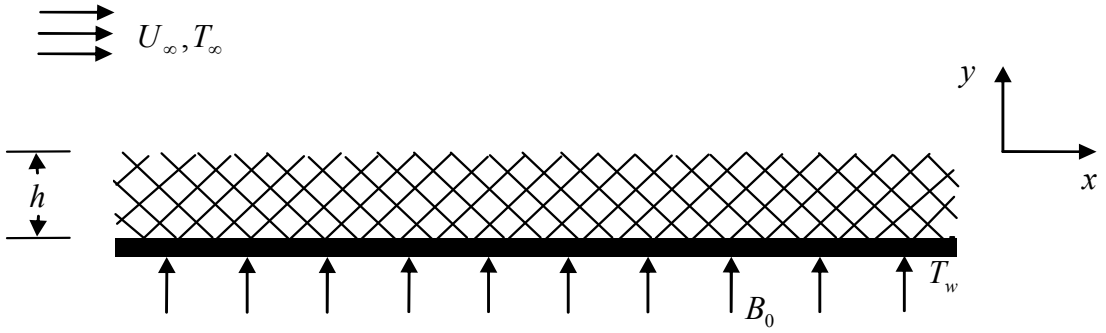

Fig. 3.1 The schematic of the problem and coordinate system.

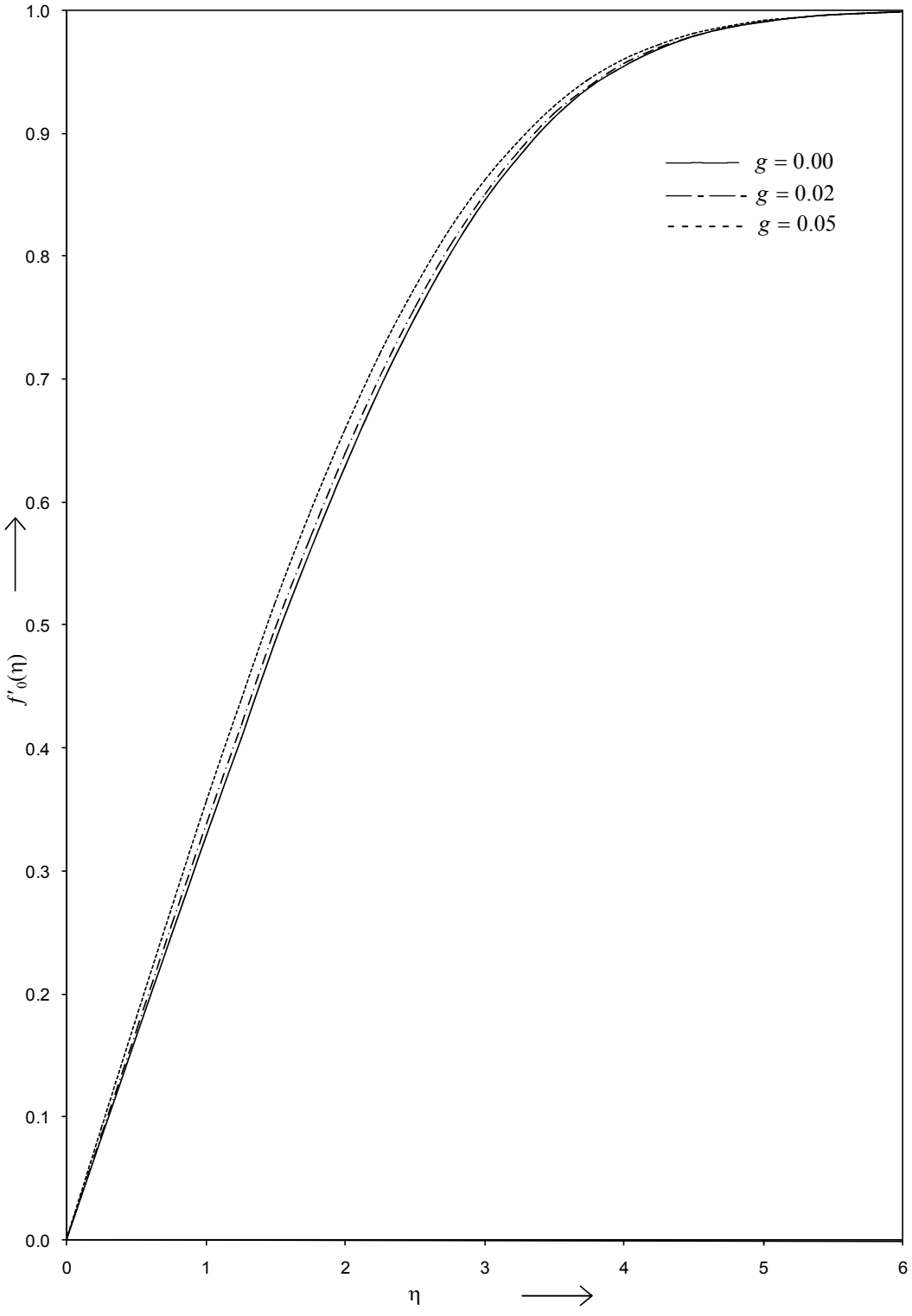

Fig. 3.2 Velocity distribution (non-porous) against η for various values of g.

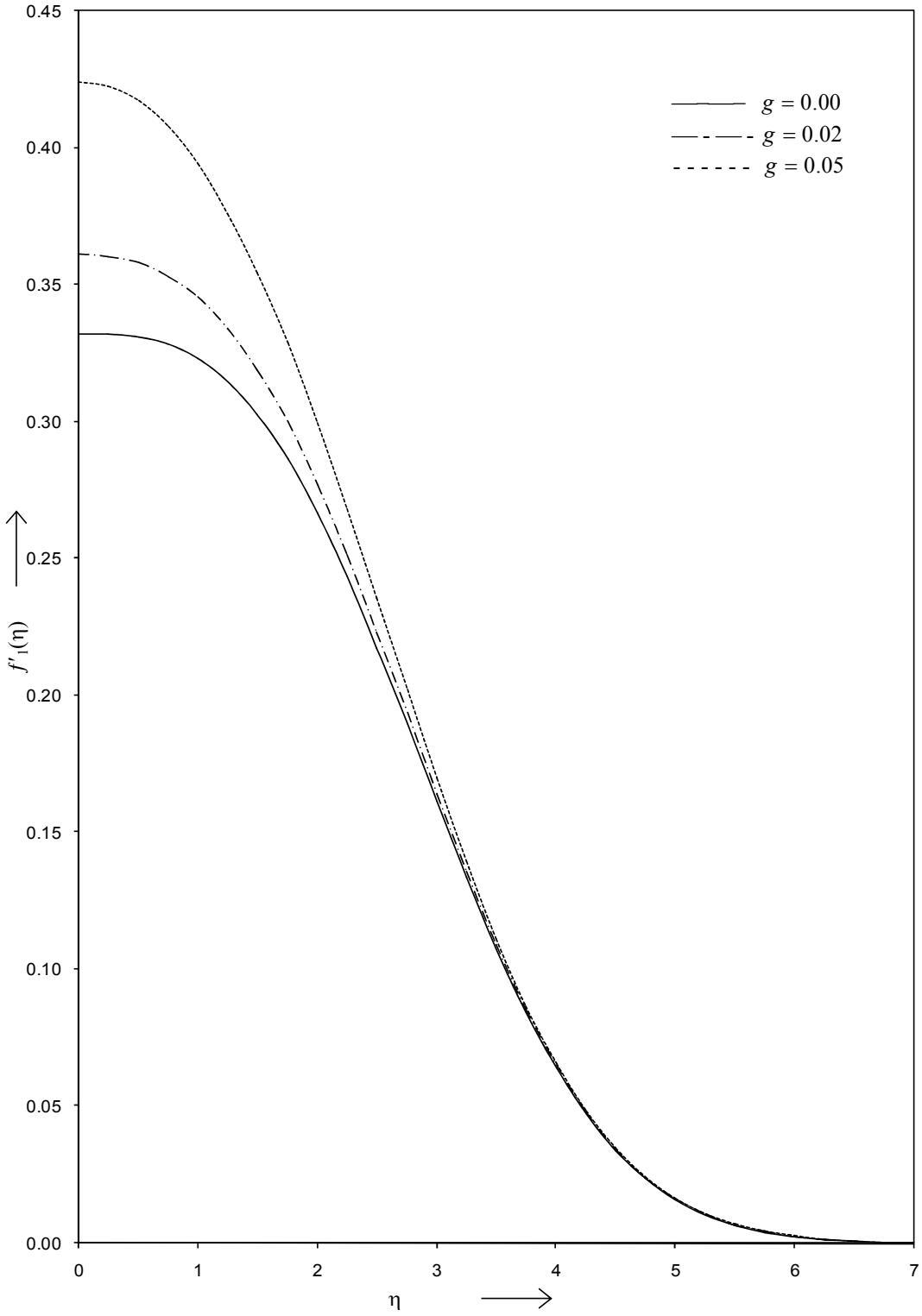

Fig. 3.3 Velocity distribution (porous) against η for various values of g.

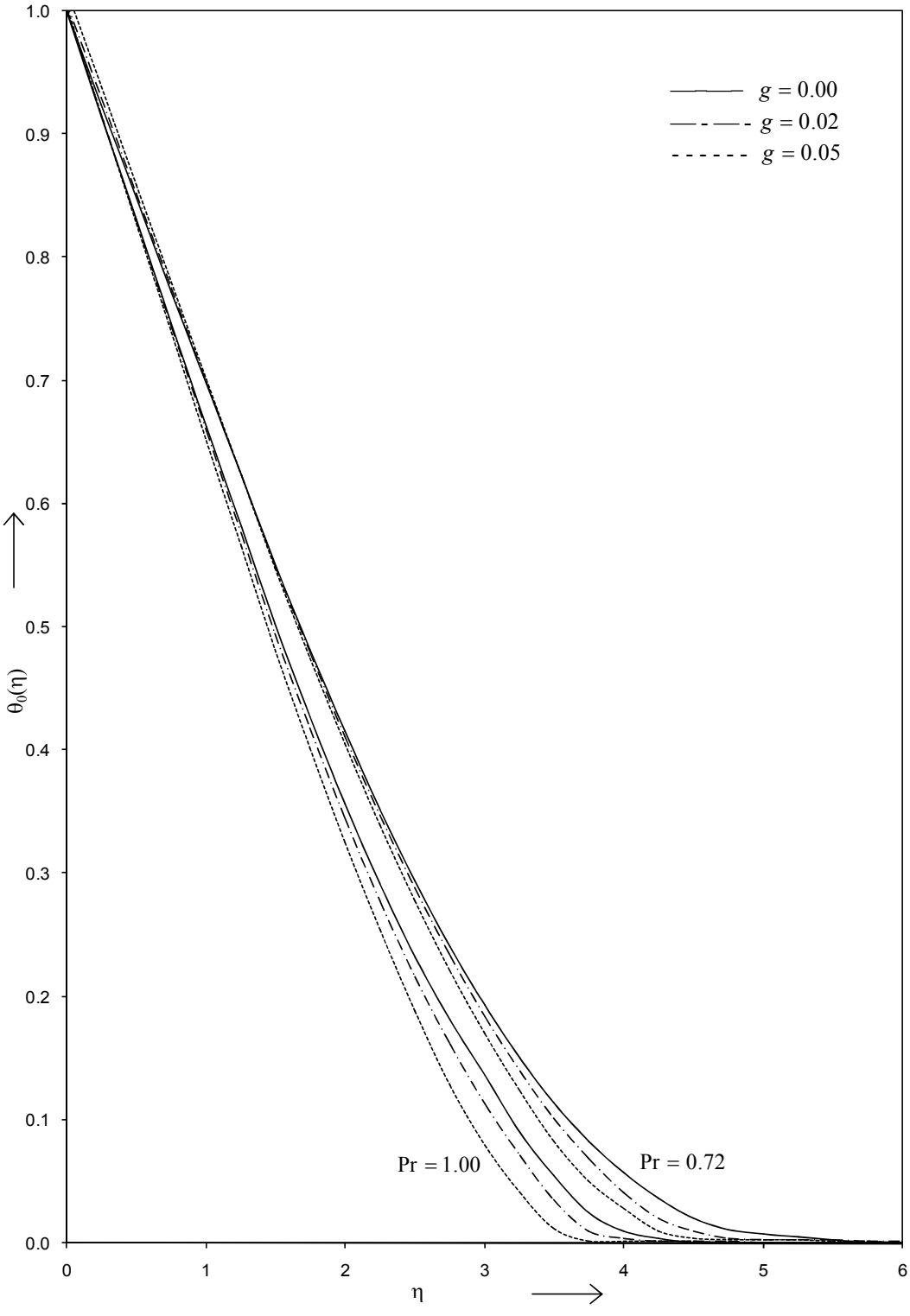

Fig. 3.4 Temperature distribution (non-porous) against η for various values of g and Pr with $Ec = 0.0$.

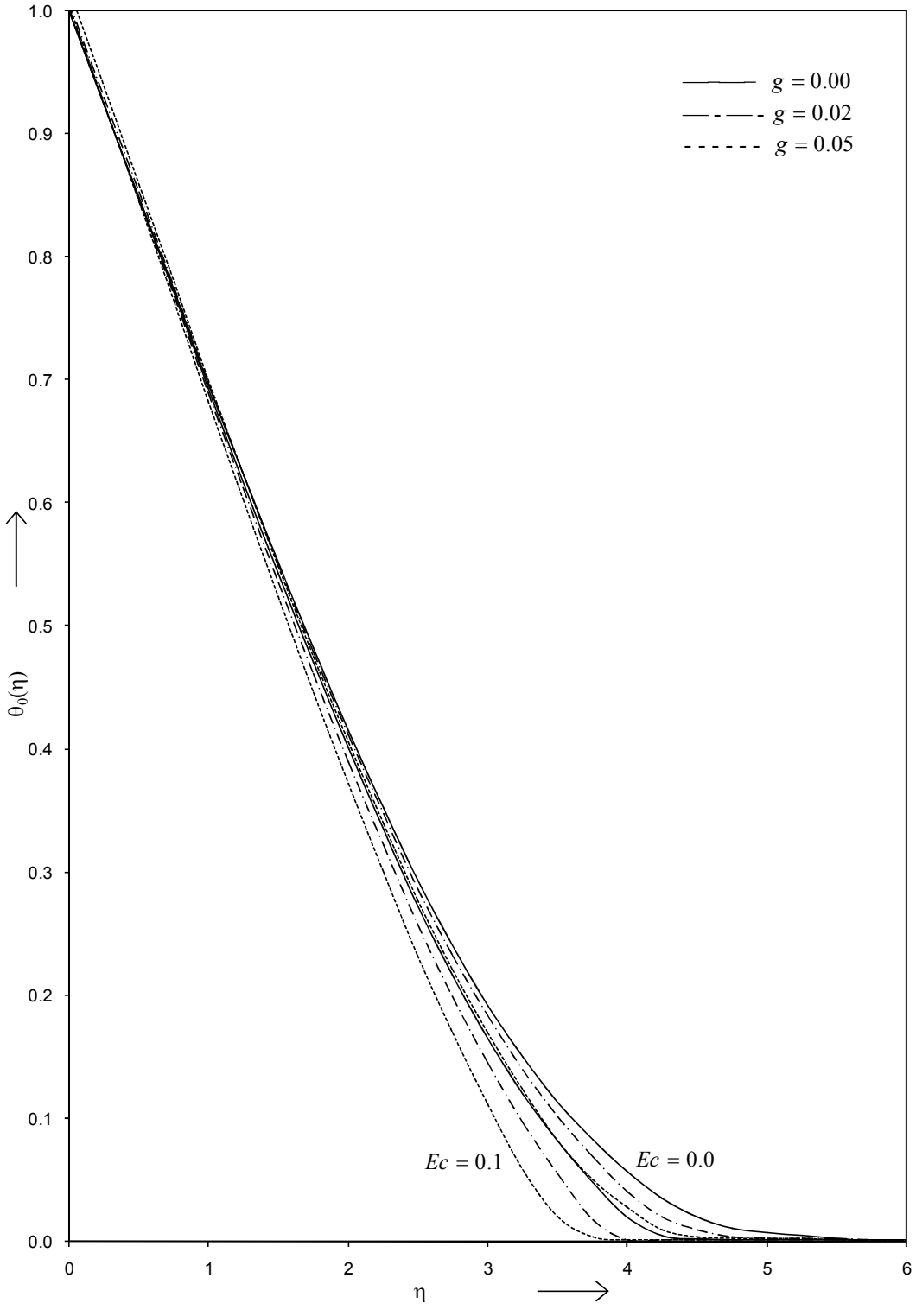

Fig. 3.5 Temperature distribution (non-porous) against η for various values of g and Ec with $\Pr = 0.72$.

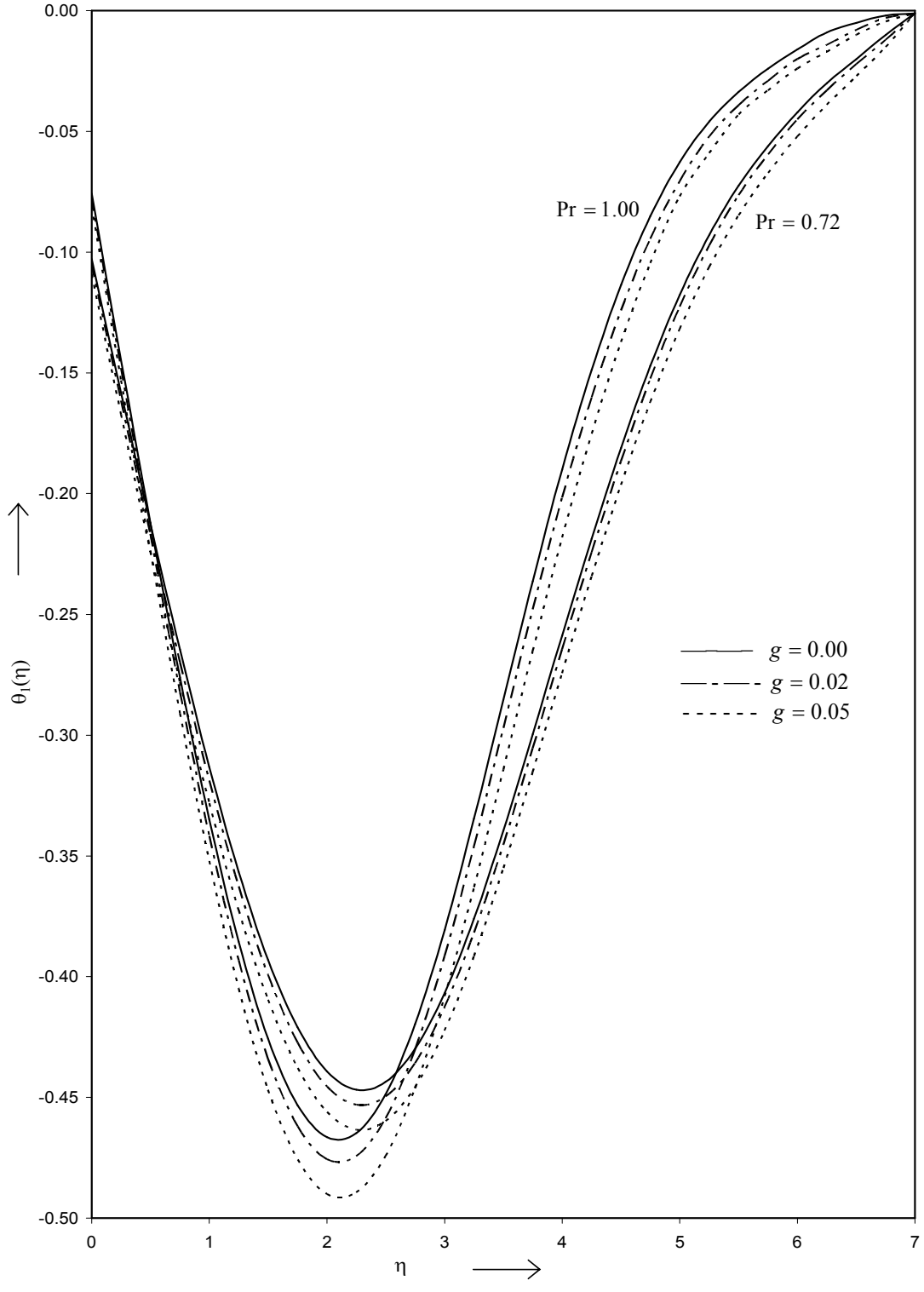

Fig. 3.6 Temperature distribution (porous) against η for various values of g and Pr with $Ec = 0.0$.

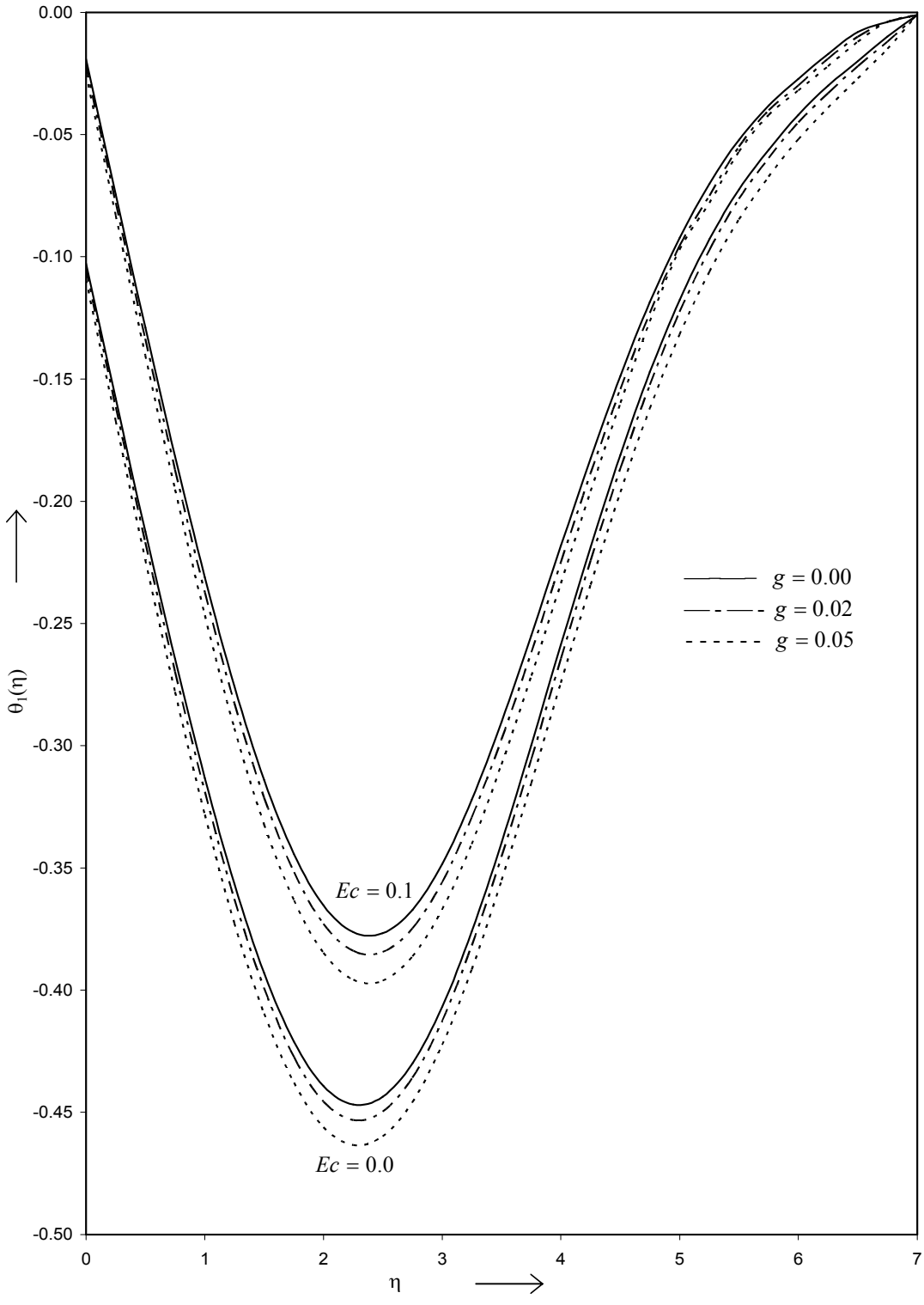

Fig. 3.7 Temperature distribution (porous) against η for various values of g and Ec with $\Pr = 0.72$.

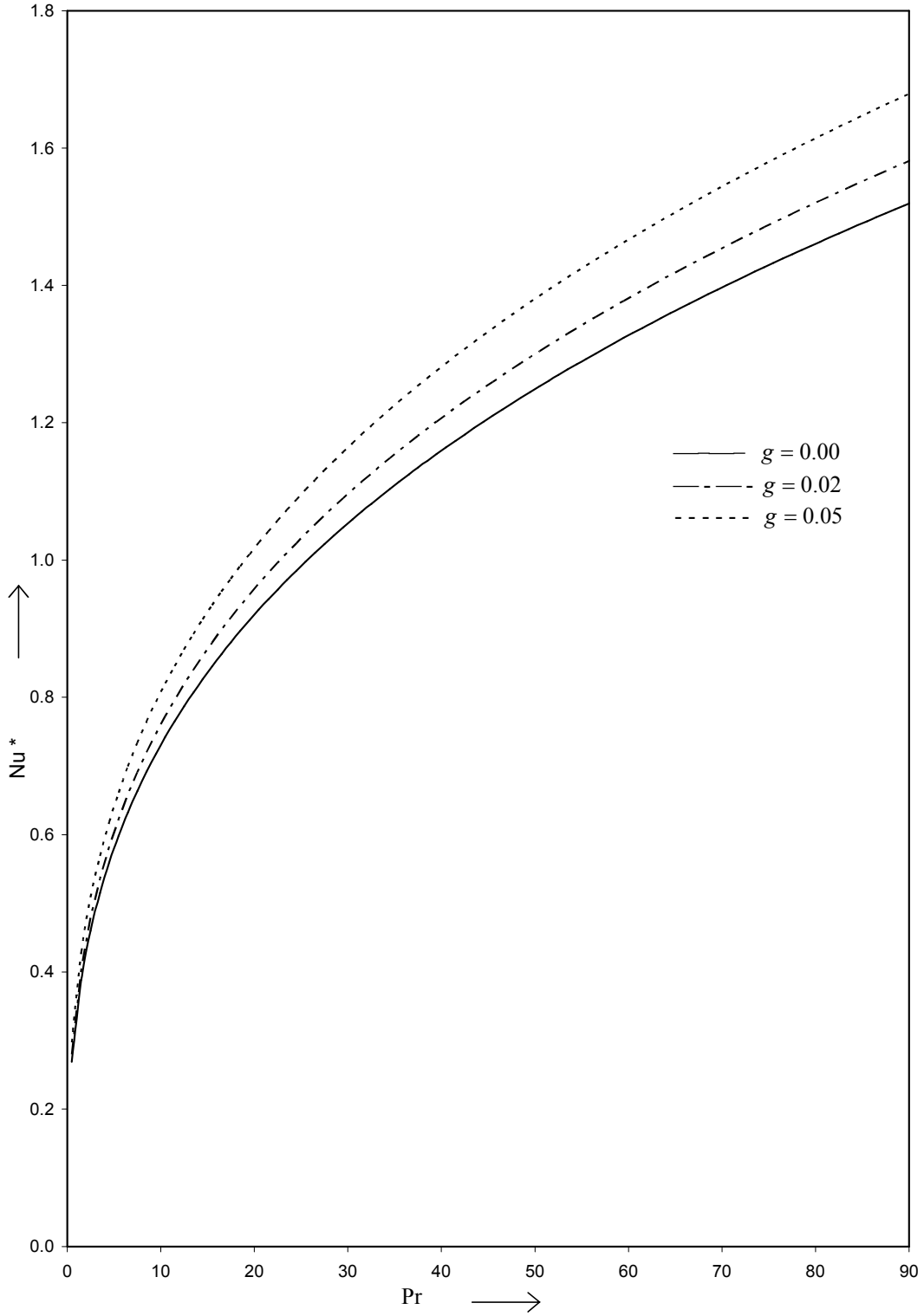

Fig. 3.8 Nusselt number (non-porous) against Pr for various values of g.

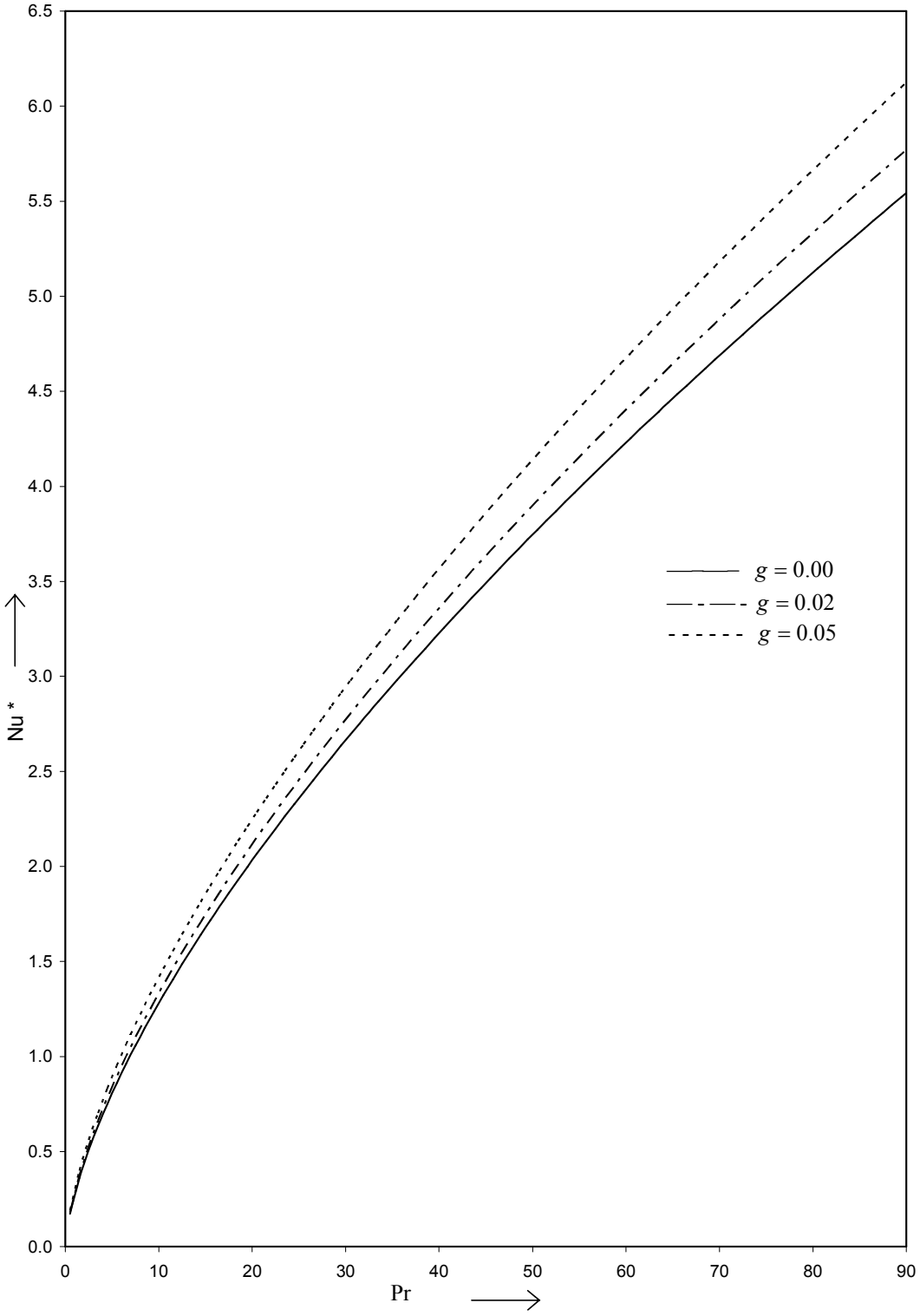

Fig. 3.9 Nusselt number (porous) against Pr for various values of g.

Chapter 4

MHD Stagnation Point Flow and Heat Transfer over a Permeable Surface

4.1 Introduction

In recent years, the requirements of modern technology have stimulated interest in fluid flow studies which involve interaction of several phenomena. One such study is stagnation point flow over a permeable surface which plays an important role in many engineering problems, petroleum industries, ground water flows, extrusion of a polymer sheet from a dye and boundary layer control. More importantly, the quality of the products, in the above mentioned processes, depends on the kinematics of stretching and the simultaneous heat and mass transfer rates during the fabrication process. Crane (1970) studied the flow over a linearly stretching sheet in an ambient fluid and gave a similarity solution in closed analytical form for the study of two-dimensional problem. Heat transfer in the flow over a permeable surface has been investigated by several authors such as Gupta and Gupta (1977), Carragher and Crane (1982), Chiam (1994), Magyari and Keller (2000), Mahapatra and Gupta (2002), Elbashbeshy and Bazid (2003), Liao and Pop (2004), Jat and Chaudhary (2007, 2008) and Bhattacharyya and Layek (2011).

The object of the present chapter is to study the stagnation point flow and heat transfer for an electrically conducting fluid over a permeable surface in the presence of a magnetic field. The fluid is acted upon by an external uniform magnetic field and

a uniform injection or suction is directed normal to the plane of the wall. The wall and stream temperatures are assumed to be constants. Numerical results are obtained for velocity, temperature, skin friction and surface heat transfer using Shooting method.

4.2 Mathematical Model

Consider the steady two-dimensional stagnation point flow $(u,v,0)$ of a viscous incompressible electrically conducting fluid near a stagnation point over a permeable surface placed in the plane $y=0$ of a Cartesian coordinates system with the $x-$ axis along the surface, in a uniform injection or suction velocity $\pm v_0$ at the boundary of the surface and in the presence of an externally applied normal magnetic field of constant strength $(0,H_0,0)$. The stretching surface has a uniform temperature T_w while the velocity of the flow external to the boundary layer is u_e and temperature T_∞. The system of boundary layer equations (which model Fig. 4.1) are given by-

$$\frac{\partial u}{\partial x}+\frac{\partial v}{\partial y}=0 \tag{4.1}$$

$$u\frac{\partial u}{\partial x}+v\frac{\partial u}{\partial y}=u_e\frac{du_e}{dx}+\upsilon\frac{\partial^2 u}{\partial y^2}-\frac{\sigma_e\,\mu_e^2\,H_0^2\,u}{\rho} \tag{4.2}$$

$$\rho C_p\left(u\frac{\partial T}{\partial x}+v\frac{\partial T}{\partial y}\right)=\kappa\frac{\partial^2 T}{\partial y^2}+\mu\left(\frac{\partial u}{\partial y}\right)^2+\sigma_e\,\mu_e^2\,H_0^2\,u^2 \tag{4.3}$$

where υ is the kinematic viscosity, σ_e the electrical conductivity, μ_e the magnetic permeability, ρ the density, C_p the specific heat at constant pressure, κ the thermal

conductivity and μ the coefficient of viscosity of the fluid under consideration. The other symbols have their usual meanings.

The boundary conditions are-

$$\begin{aligned} &y = 0: \;\; u = 0,\; v = \pm v_0; \;\; T = T_w \\ &y = \infty: \;\; u = u_e = ax,\; v = -ay; \;\; T = T_\infty \end{aligned} \tag{4.4}$$

where a is a constant proportional to the free stream velocity far away from the stretching surface.

4.3 Similarity Analysis

The continuity equation (4.1) is identically satisfied by stream function $\psi(x, y)$, defined as

$$u = \frac{\partial \psi}{\partial y}, \qquad v = -\frac{\partial \psi}{\partial x} \tag{4.5}$$

For the solution of the momentum and the energy equations (4.2) and (4.3), the following dimensionless variables are defined-

$$\psi(x, y) = \sqrt{a\upsilon}\; x\, f(\eta) \tag{4.6}$$

$$\eta = \sqrt{\frac{a}{\upsilon}}\; y \tag{4.7}$$

$$\theta(\eta) = \frac{T - T_\infty}{T_w - T_\infty} \tag{4.8}$$

Equations (4.5) to (4.8), transform equations (4.2) and (4.3) into

$$f''' + f\,f'' - f'^2 - \mathrm{Re}_m^2\, f' + 1 = 0 \tag{4.9}$$

$$\theta'' + \mathrm{Pr}\, f\theta' + \mathrm{Pr}\, Ec\, f''^2 + \mathrm{Pr}\, Ec\, \mathrm{Re}_m^2\, f'^2 = 0 \tag{4.10}$$

where the prime (') denotes differentiation with respect to η, $\mathrm{Re}_m = \mu_e H_0 \sqrt{\frac{\sigma_e}{\rho a}}$ the magnetic parameter, $\mathrm{Pr} = \frac{\mu C_p}{\kappa}$ the Prandtl number and $Ec = \frac{u_e^{\,2}}{C_p\left(T_w - T_\infty\right)}$ the Eckert number.

The corresponding boundary conditions are-

$$\begin{aligned} &\eta = 0: \;\; f = A,\; f' = 0;\;\; \theta = 1 \\ &\eta = \infty: \;\; f' = 1;\;\; \theta = 0 \end{aligned} \tag{4.11}$$

where $A = \pm \frac{v_0}{\sqrt{a\upsilon}}$ is the suction parameter.

For numerical solution of the equations (4.9) and (4.10), we apply the following power series in a small magnetic parameter Re_m^2 as-

$$f(\eta) = \sum_{i=0}^{\infty} \left(\mathrm{Re}_m^2\right)^i f_i(\eta) \tag{4.12}$$

$$\theta(\eta) = \sum_{j=0}^{\infty} \left(\mathrm{Re}_m^2\right)^j \theta_j(\eta) \tag{4.13}$$

Substituting equations (4.12) and (4.13) and its derivatives in equations (4.9) and (4.10) and then equating the coefficients of like powers of Re_m^2, we get the following set of equations-

$$f_0''' + f_0 f_0'' - f_0'^2 + 1 = 0 \tag{4.14}$$

$$\theta_0'' + \mathrm{Pr}\, f_0 \theta_0' = -\mathrm{Pr}\, Ec\, f_0''^2 \tag{4.15}$$

$$f_1''' + f_0 f_1'' - 2 f_0' f_1' + f_0'' f_1 = f_0' \tag{4.16}$$

$$\theta_1'' + \mathrm{Pr}\, f_0 \theta_1' = -\mathrm{Pr}\, f_1 \theta_0' - \mathrm{Pr}\, Ec \left(2 f_0'' f_1'' + f_0'^2 \right) \tag{4.17}$$

$$f_2''' + f_0 f_2'' - 2 f_0' f_2' + f_0'' f_2 = -f_1 f_1'' + \left(f_1' + 1 \right) f_1' \tag{4.18}$$

$$\theta_2'' + \mathrm{Pr}\, f_0 \theta_2' = -\mathrm{Pr} \left(f_1 \theta_1' + f_2 \theta_0' \right) - \mathrm{Pr}\, Ec \left(2 f_0'' f_2'' + f_1''^2 + 2 f_0' f_1' \right) \tag{4.19}$$

with the boundary conditions-

$$\begin{aligned} &\eta = 0: \quad f_0 = A,\ f_i = 0,\ f_j' = 0; \quad \theta_0 = 1,\ \theta_i = 0 \\ &\eta = \infty: \quad f_0' = 1,\ f_i' = 0; \quad \theta_j = 0 \qquad\qquad i > 0,\ j \geq 0 \end{aligned} \tag{4.20}$$

The equation (4.14) was obtained by Jat and Chaudhary (2007) for the non-magnetic case, in the absence of the suction parameter and the slip factor. The remaining equations are linear ordinary differential equations and have been solved numerically by Shooting method. The velocity and temperature distributions for various values of the parameters are shown in Fig. 4.2 and Fig. 4.3 to Fig. 4.4 respectively.

4.4 Skin Friction and Nusselt Number

The physical quantities of interest, the local skin friction coefficient C_f and the local Nusselt number Nu i.e. surface heat transfer are given by-

$$C_f = \frac{\tau_w}{\rho u_e^2 / 2} = \frac{\mu \left(\frac{\partial u}{\partial y} \right)_{y=0}}{\rho u_e^2 / 2} \tag{4.21}$$

and

$$Nu = -\frac{x \left(\frac{\partial T}{\partial y} \right)_{y=0}}{\left(T_w - T_\infty \right)} \tag{4.22}$$

which, in the present case, can be expressed in the following forms

$$C_f = \frac{2}{\sqrt{\mathrm{Re}}} f''(0)$$

$$= \frac{2}{\sqrt{\mathrm{Re}}} \sum_{i=0}^{\infty} \left(\mathrm{Re}_m^2 \right)^i f_i''(0) \tag{4.23}$$

and

$$Nu = -\sqrt{\mathrm{Re}}\ \theta'(0)$$

$$= -\sqrt{\mathrm{Re}} \sum_{j=0}^{\infty} \left(\mathrm{Re}_m^2 \right)^j \theta_j'(0) \tag{4.24}$$

where $\mathrm{Re} = \frac{u_e x}{\upsilon}$ is the local Reynolds number.

Numerical values of the functions $f''(0)$ and $\theta'(0)$, which are proportional to local skin friction and local heat transfer rate at the surface respectively for various values of the parameters are presented in Table 4.1.

4.5 Discussion of the Results

The Figure 4.2 shows the variation of velocity distribution against η for various values of the suction parameter A and the magnetic parameter Re_m. It may be observed that the velocity increases as the suction parameter A increases, whereas it decreases as the magnetic parameter Re_m increases for a fixed η.

The Figures 4.3 to 4.4 show the variation of the temperature distribution against η for various values of the parameters such as the suction parameter A, the magnetic parameter Re_m, the Prandtl number Pr and the Eckert number Ec. From these figures it may be observed that the temperature distribution decreases with the increasing value of the suction parameter A and same phenomena occur for the Prandtl number Pr. It is further observed that in Fig. 4.3 the temperature distribution decreases with the increasing value of the magnetic parameter Re_m. In Fig. 4.4, for fixed suction parameter A temperature distribution decreases with the increasing value of the Eckert number Ec and reverse phenomena occurs for the magnetic parameter Re_m.

The numerical values of the functions $f''(0)$ and $-\theta'(0)$ for various values of the suction parameter A, the magnetic parameter Re_m, the Prandtl number Pr and the Eckert number Ec are presented in Table 4.1. It may be observed from the table that the boundaries values $f''(0)$ for non-magnetic flow, in the absence of the suction parameter and the slip factor, are same as those obtained by Jat and Chaudhary (2007). Further, it may be observed from the table that the function $f''(0)$ increases with the increasing values of the suction parameter A, similar results are obtained for $-\theta'(0)$ whereas the value of $f''(0)$ decreases with the increasing value of the magnetic parameter Re_m while opposite results are observed for $-\theta'(0)$. Further $-\theta'(0)$ decreases with the increasing value of the Eckert number Ec and same for the Prandtl number Pr if $A<0$.

4.6 Conclusions

In this chapter, the steady two-dimensional stagnation point flow and heat transfer of a viscous incompressible electrically conducting fluid over a permeable surface has been analyzed. The similarity equations are obtained and solved numerically by a Shooting method. The effects of the suction parameter, the magnetic parameter, the Prandtl number and the Eckert number are studied in detail. The velocity boundary layer thickness increases with the increasing value of the suction parameter while the reverse phenomenon is observed for thermal boundary layer thickness. Further concluded when the Eckert number equal to zero the velocity as well as thermal boundary layer thickness decreases with the increasing value of the magnetic

parameter and the Prandtl number, whereas for the Eckert number not equal to zero, thermal boundary layer thickness increases with the increasing value of the magnetic parameter and decreases with the increasing value of the Eckert number. On other hand from the results it can be concluded that skin friction and Nusselt number varies similarly as velocity boundary layer thickness and thermal boundary layer thickness respectively with different parameters.

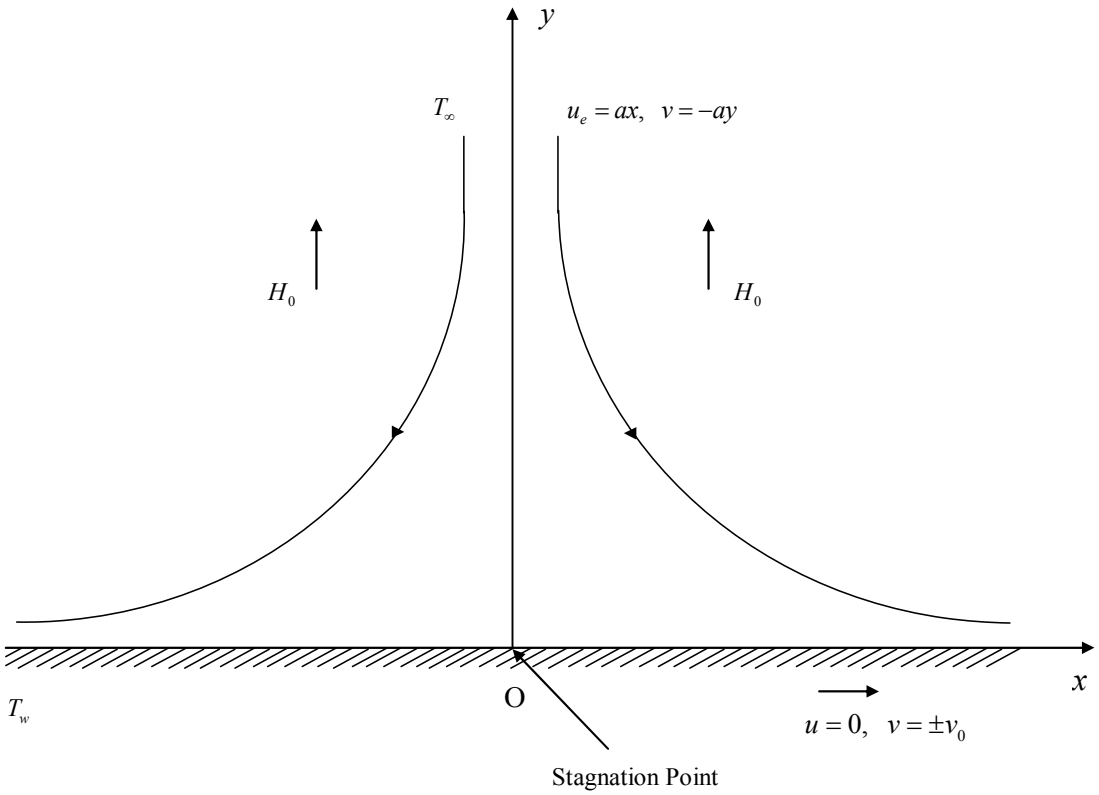

Fig. 4.1 A sketch of the physical problem.

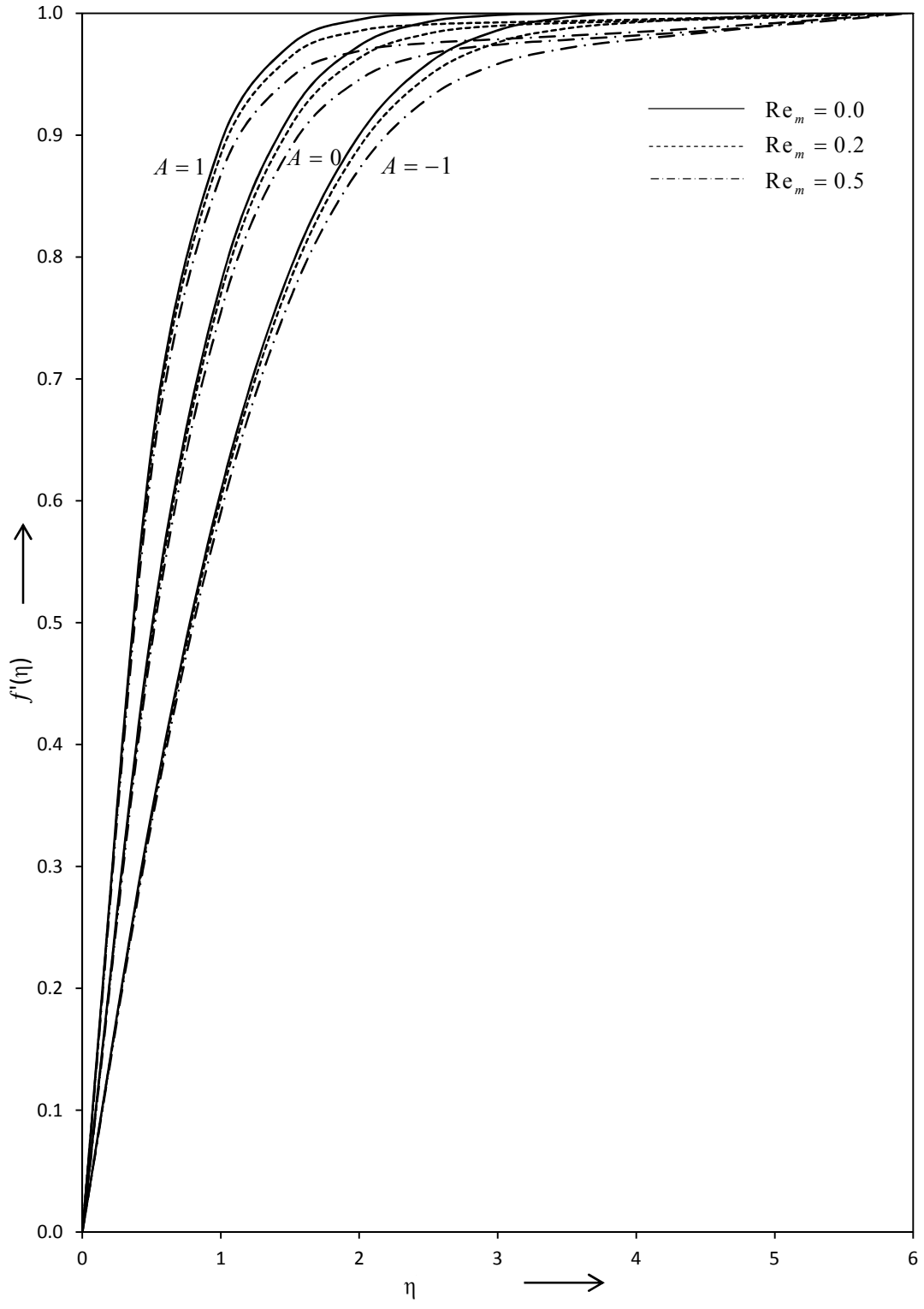

Fig. 4.2 Variation of velocity with η for several values of A and Re_m.

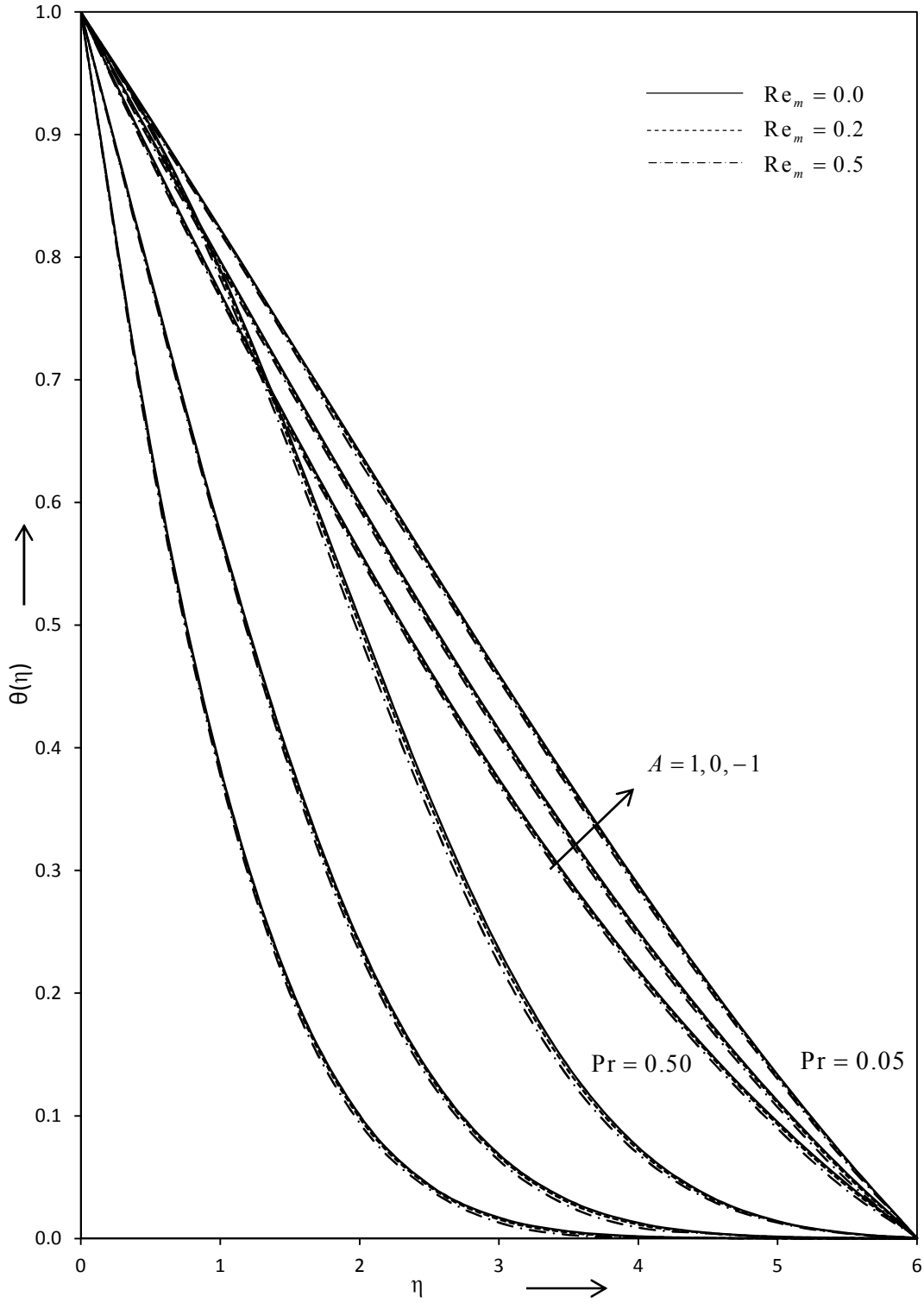

Fig. 4.3 Variation of temperature with η for several values of A, Re_m and Pr when $Ec = 0.00$.

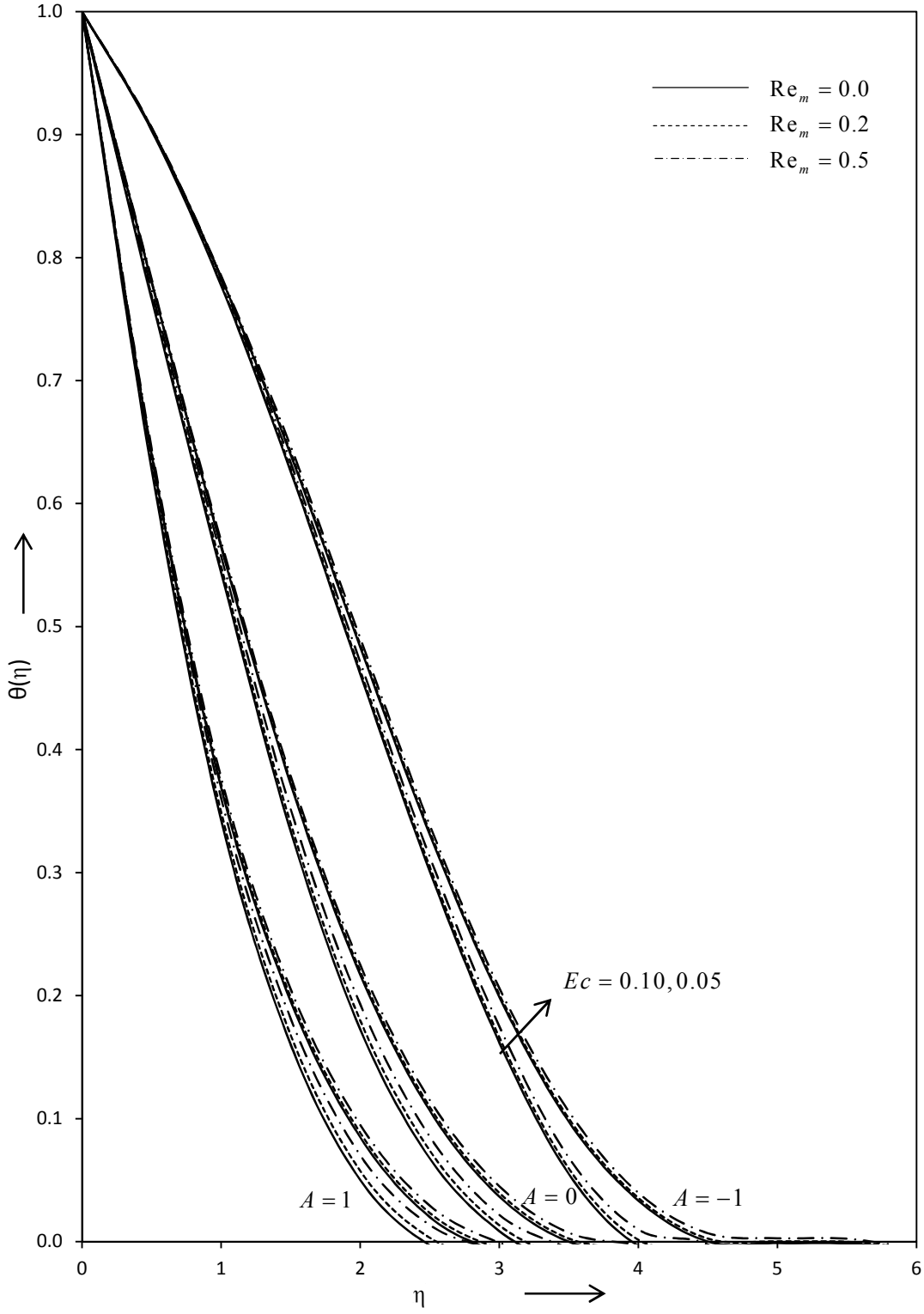

Fig. 4.4 Variation of temperature with η for several values of A, Re_m and Ec when $\mathrm{Pr} = 0.50$.

Table 4.1 Computed values of $f''(0)$ and $-\theta'(0)$ for several values of A, Re_m, Pr and Ec.

Pr	$-\theta'(0)$								
	$A = -1$								
	$Re_m = 0.0$			$Re_m = 0.2$			$Re_m = 0.5$		
	$f''(0) = 0.7566$			$f''(0) = 0.7512$			$f''(0) = 0.7419$		
	$Ec = 0.00$	$Ec = 0.05$	$Ec = 0.10$	$Ec = 0.00$	$Ec = 0.05$	$Ec = 0.10$	$Ec = 0.00$	$Ec = 0.05$	$Ec = 0.10$
0.05	0.1724	0.1724	0.1724	0.1728	0.1724	0.1720	0.1735	0.1722	0.1710
0.50	0.1642	0.1642	0.1642	0.1666	0.1645	0.1624	0.1703	0.1643	0.1583
1.00	0.1597	0.1597	0.1597	0.1627	0.1619	0.1613	0.1690	0.1625	0.1580
2.00	0.1553	0.1553	0.1553	0.1569	0.1561	0.1550	0.1671	0.1613	0.1567

Table 4.1 Computed values of $f''(0)$ and $-\theta'(0)$ for several values of A, Re_m, Pr and Ec. – Contd. 1

Pr	$-\theta'(0)$								
	$A = 0$								
	$Re_m = 0.0$			$Re_m = 0.2$			$Re_m = 0.5$		
	$f''(0) = 1.2326$			$f''(0) = 1.2213$			$f''(0) = 1.2016$		
	$Ec = 0.00$	$Ec = 0.05$	$Ec = 0.10$	$Ec = 0.00$	$Ec = 0.05$	$Ec = 0.10$	$Ec = 0.00$	$Ec = 0.05$	$Ec = 0.10$
0.05	0.2030	0.2030	0.2030	0.2032	0.2027	0.2022	0.2036	0.2022	0.2007
0.50	0.4334	0.4334	0.4334	0.4352	0.4314	0.4277	0.4381	0.4276	0.4171
1.00	0.5528	0.5528	0.5528	0.5547	0.5533	0.5529	0.5597	0.5574	0.5563
2.00	0.6739	0.6739	0.6739	0.6752	0.6748	0.6744	0.6789	0.6758	0.6752

Table 4.1 Computed values of $f''(0)$ and $-\theta'(0)$ for several values of A, Re_m, Pr and Ec. – Contd. 2

Pr	$-\theta'(0)$								
	$A = 1$								
	$Re_m = 0.0$			$Re_m = 0.2$			$Re_m = 0.5$		
	$f''(0) = 1.8894$			$f''(0) = 1.8708$			$f''(0) = 1.8383$		
	$Ec = 0.00$	$Ec = 0.05$	$Ec = 0.10$	$Ec = 0.00$	$Ec = 0.05$	$Ec = 0.10$	$Ec = 0.00$	$Ec = 0.05$	$Ec = 0.10$
0.05	0.2349	0.2349	0.2349	0.2350	0.2344	0.2338	0.2352	0.2336	0.2319
0.50	0.8018	0.8018	0.8018	0.8028	0.7976	0.7924	0.8044	0.7900	0.7755
1.00	0.9570	0.9570	0.9570	0.9608	0.9601	0.9599	0.9632	0.9623	0.9617
2.00	0.9825	0.9825	0.9825	0.9903	0.9889	0.9884	0.9974	0.9953	0.9931

Chapter 5

Magnetohydrodynamic Boundary Layer Flow over an Exponentially Stretching Sheet with Radiation Effects

5.1 Introduction

The study of laminar boundary layer flow over a stretching sheet has received much interest in recent years due to its numerous applications in industrial manufacturing processes such as wire drawing, hot rolling, manufacturing of plastic and rubber surfaces, condensation process of metallic plate in a cooling bath and glass, fibers spinning and many others. In all these cases, during such processes both stretching and simultaneous cooling or heating have a decisive influence on the quality of the final products. Sakiadis (1961) probably was first who studied the problem of boundary layer flow over a continuous solid surface moving with constant velocity. Crane (1970) extended this concept to the flow over a linearly stretching sheet and obtained a similar solution in closed analytical form for the steady two dimensional problem. Gupta and Gupta (1977), Carragher and Crane (1982), Magyari and Keller (1999), Elbashbeshy (2001), Mahapatra and Gupta (2002), Pop et al. (2004), Ishak et al. (2006) and Jat and Chaudhary (2008) studied the boundary layer flow problems over stretching sheet taking into various aspects of the problem. Recently, various aspects of such problem have been investigated either analytically or numerically by several researchers such as Bidin and Nazar (2009), Jat and Chaudhary (2010) and Bachok et al. (2012).

The effects of thermal radiation on boundary layer flow and heat transfer problems play a significant role when technological processes take place at high temperature, for example in electrical power generation, solar power technology, astrophysical flows etc.

Realizing the increasing technical applications of the magnetohydrodynamic effects, we have studied in the chapter the radiation effects on two dimensional boundary layer flow of an incompressible viscous electrically conducting fluid over an exponentially stretching sheet in the presence of uniform transverse magnetic field by using Rosseland approximation. The results of velocity, temperature, skin friction and surface heat transfer for different parameters were obtained.

5.2 Problem Formulation

Consider the steady two-dimensional boundary layer flow $(u,v,0)$ of an incompressible viscous electrically conducting fluid over an exponentially stretching sheet. The $x-$ axis is taken along the continuous stretching surface in the direction of motion and $y-$ axis is perpendicular to it. A uniform magnetic field of constant strength $(0,H_0,0)$ is assumed to be applied normal to the stretching surface as shown in Fig. 5.1. The magnetic Reynolds number is assumed to be small and therefore no magnetic induction is present. The surface is assumed to be highly elastic and is stretched in the $x-$ direction with a velocity u_w and surface temperature T_w. All the fluid properties are assumed to be constant throughout the motion. Therefore, under

the usual boundary layer approximations, the governing boundary layer equations with the radiation effects are

$$\frac{\partial u}{\partial x}+\frac{\partial v}{\partial y}=0 \tag{5.1}$$

$$u\frac{\partial u}{\partial x}+v\frac{\partial u}{\partial y}=\upsilon\frac{\partial^2 u}{\partial y^2}-\frac{\sigma_e\,\mu_e^2\,H_0^2\,u}{\rho} \tag{5.2}$$

$$\rho C_p\left(u\frac{\partial T}{\partial x}+v\frac{\partial T}{\partial y}\right)=\kappa\frac{\partial^2 T}{\partial y^2}+\mu\left(\frac{\partial u}{\partial y}\right)^2-\frac{\partial q_r}{\partial y}+\sigma_e\,\mu_e^2\,H_0^2\,u^2 \tag{5.3}$$

where υ is the kinematic viscosity, σ_e the electrical conductivity, μ_e the magnetic permeability, ρ the density, C_p the specific heat at constant pressure, κ the thermal conductivity, μ the coefficient of viscosity and q_r the relative heat flux of the fluid under consideration. The other symbols have their usual meanings.

The boundary conditions are-

$$\begin{aligned} &y=0:\ u=u_w=U_0e^{x/L},\ v=0;\ \ T=T_w=T_\infty+T_0e^{x/2L}\\ &y=\infty:\ u=0;\ \ T=T_\infty \end{aligned} \tag{5.4}$$

where U_0 is the reference velocity, L is the reference length, T_∞ is the temperature far away from the sheet and T_0 is the reference temperature.

Using Rosseland approximation [Rosseland (1936)], the radiation heat flux q_r simplifies as-

$$q_r = -\frac{4\sigma^*}{3k^*}\frac{\partial T^4}{\partial y} \tag{5.5}$$

where σ^* is the Stefan-Boltzmann constant and k^* is the mean absorption coefficient. Assuming that the temperature difference within the flow is such that the terms T^4 may be expressed as a linear function of temperature. Hence, expanding T^4 in a Taylor series about T_∞ and neglecting higher order terms gives-

$$T^4 = 4T_\infty^3 T - 3T_\infty^4 \tag{5.6}$$

using equations (5.5) and (5.6), equation (5.3) reduces to-

$$\rho C_p\left(u\frac{\partial T}{\partial x}+v\frac{\partial T}{\partial y}\right)=\left(\kappa+\frac{16\sigma^* T_\infty^3}{3k^*}\right)\frac{\partial^2 T}{\partial y^2}+\mu\left(\frac{\partial u}{\partial y}\right)^2+\sigma_e\,\mu_e^2\,H_0^2\,u^2 \tag{5.7}$$

5.3 Mathematical Analysis

The continuity equation (5.1) is identically satisfied by stream function $\psi(x,y)$, defined as

$$u=\frac{\partial \psi}{\partial y}, \qquad v=-\frac{\partial \psi}{\partial x} \tag{5.8}$$

For the solution of the momentum and the energy equations (5.2) and (5.7), the following dimensionless variables are defined-

$$\psi(x,y)=\sqrt{2\upsilon L U_0}\; e^{x/2L}\, f(\eta) \tag{5.9}$$

$$\eta = \sqrt{\frac{U_0}{2\upsilon L}}\, e^{x/2L}\, y \tag{5.10}$$

$$\theta(\eta) = \frac{T - T_\infty}{T_0\, e^{x/2L}} \tag{5.11}$$

Equations (5.8) to (5.11), transform equations (5.2) and (5.7) into

$$f''' + f\, f'' - 2f'^2 - 2\,\mathrm{Re}_m^2\, f' = 0 \tag{5.12}$$

$$\left(1 + \frac{4}{3}K\right)\theta'' + \mathrm{Pr}\, f\, \theta' - \mathrm{Pr}\, f'\, \theta + \mathrm{Pr}\, Ec\, f''^2 + 2\,\mathrm{Pr}\, Ec\,\mathrm{Re}_m^2\, f'^2 = 0 \tag{5.13}$$

where the prime (') denotes differentiation with respect to η, $\mathrm{Re}_m = \mu_e H_0 \sqrt{\frac{\sigma_e L}{\rho u_w}}$ is the magnetic parameter, $K = \frac{4\sigma^* T_\infty^3}{k^* \kappa}$ the radiation parameter, $\mathrm{Pr} = \frac{\mu C_p}{\kappa}$ the Prandtl number and $Ec = \frac{u_w^2}{C_p\left(T_w - T_\infty\right)}$ the Eckert number.

The corresponding boundary conditions are-

$$\begin{aligned} &\eta = 0: \quad f = 0,\ f' = 1;\ \theta = 1 \\ &\eta = \infty: \quad f' = 0;\ \theta = 0 \end{aligned} \tag{5.14}$$

For numerical solution of the equations (5.12) and (5.13), through a perturbation technique, by assuming the following power series in a small magnetic parameter Re_m^2 as-

$$f(\eta)=\sum_{i=0}^{\infty}\left(\mathrm{Re}_m^2\right)^i f_i(\eta) \tag{5.15}$$

$$\theta(\eta)=\sum_{j=0}^{\infty}\left(\mathrm{Re}_m^2\right)^j \theta_j(\eta) \tag{5.16}$$

Substituting equations (5.15) and (5.16) and its derivatives in equations (5.12) and (5.13) and then equating the coefficients of like powers of Re_m^2, we get the following set of equations-

$$f_0'''+f_0 f_0''-2f_0'^2=0 \tag{5.17}$$

$$\left(1+\frac{4}{3}K\right)\theta_0''+\mathrm{Pr}\, f_0\,\theta_0'-\mathrm{Pr}\, f_0'\theta_0=-\mathrm{Pr}\, Ec\, f_0''^2 \tag{5.18}$$

$$f_1'''+f_0 f_1''-4f_0' f_1'+f_0'' f_1=2f_0' \tag{5.19}$$

$$\left(1+\frac{4}{3}K\right)\theta_1''+\mathrm{Pr}\, f_0\,\theta_1'-\mathrm{Pr}\, f_0'\theta_1=-\mathrm{Pr}\left(f_1\theta_0'-f_1'\theta_0\right)-2\,\mathrm{Pr}\, Ec\left(f_0''f_1''+f_0'^2\right) \tag{5.20}$$

$$f_2'''+f_0 f_2''-4f_0' f_2'+f_0'' f_2=-f_1 f_1''+2\left(f_1'+1\right)f_1' \tag{5.21}$$

$$\left(1+\frac{4}{3}K\right)\theta_2''+\mathrm{Pr}\, f_0\,\theta_2'-\mathrm{Pr}\, f_0'\theta_2=\mathrm{Pr}\left(-f_1\theta_1'+f_1'\theta_1-f_2\theta_0'+f_2'\theta_0\right)-\mathrm{Pr}\, Ec\left(2f_0''f_2''+f_1''^2+4f_0' f_1'\right) \tag{5.22}$$

with the boundary conditions-

$$\eta = 0: \;\; f_i = 0,\; f_0' = 1,\; f_j' = 0; \;\; \theta_0 = 1,\; \theta_j = 0$$

$$\eta = \infty: \;\; f_i' = 0; \;\; \theta_i = 0 \qquad\qquad i \geq 0,\; j > 0 \tag{5.23}$$

The equations (5.17) and (5.18) were obtained by Bidin and Nazar (2009) for the non-magnetic case and the remaining equations are linear ordinary differential equations and have been solved numerically by Runge-Kutta method of fourth order. The velocity and temperature distributions for various values of the parameters are shown in Fig. 5.2 and Fig. 5.3 to 5.7 respectively.

5.4 Local Skin Friction and Surface Heat Transfer

The physical quantities of interest the local skin friction coefficient C_f and the local Nusselt number Nu i.e. surface heat transfer are given by-

$$C_f = \frac{\tau_w}{\rho u_w^2 / 2} = \frac{\mu \left(\frac{\partial u}{\partial y} \right)_{y=0}}{\rho u_w^2 / 2} \tag{5.24}$$

and

$$Nu = -\frac{L \left(\frac{\partial T}{\partial y} \right)_{y=0}}{\left(T_w - T_\infty \right)} \tag{5.25}$$

which, in the present case, can be expressed in the following forms

$$C_f = \sqrt{\frac{2}{\mathrm{Re}}}\; f''(0)$$

$$= \sqrt{\frac{2}{\mathrm{Re}}} \sum_{i=0}^{\infty} \left(\mathrm{Re}_m^2\right)^i f_i''(0) \tag{5.26}$$

and

$$Nu = -\sqrt{\frac{\mathrm{Re}}{2}}\, \theta'(0)$$

$$= -\sqrt{\frac{\mathrm{Re}}{2}} \sum_{j=0}^{\infty} \left(\mathrm{Re}_m^2\right)^j \theta_j'(0) \tag{5.27}$$

where $\mathrm{Re} = \frac{u_w L}{\upsilon}$ is the local Reynolds number.

Numerical values of the functions $f''(0)$ and $\theta'(0)$, which are proportional to local skin friction and local heat transfer rate at the surface respectively for various values of the parameters are presented in Table 5.1.

5.5 Results and Discussion

The Figure 5.2 shows the variation of velocity distribution against η for various values of the magnetic parameter Re_m. It is observed that the velocity distribution decreases with increasing value of the magnetic parameter Re_m.

The Figure 5.3 to 5.7 show the variation of the temperature distribution against η for various values of the parameters such as the magnetic parameter Re_m, the radiation parameter K, the Prandtl number Pr and the Eckert number Ec. From these figures

it may be observed that the temperature distribution decreases with the decreasing values of the magnetic parameter Re_m, the radiation parameter K and the Eckert number Ec, and reverse phenomenon occurs for the Prandtl number Pr.

In Table 5.1 the numerical values of the function $-f''(0)$ and $-\theta'(0)$ for various values the magnetic parameter Re_m, the radiation parameter K, the Prandtl number Pr and the Eckert number Ec are given. It is observed from the table that the boundary values $f''(0)$ and $\theta'(0)$ for the non-magnetic flow are the same as those obtained by Bidin and Nazar (2009). Further it is observed that the function $f''(0)$ decreases with the increasing value of the magnetic parameter Re_m. Also the function $\theta'(0)$ increases with the increasing value of the magnetic parameter Re_m, the radiation parameter K, and the Eckert number Ec respectively taking other parameters constant and the reverse phenomenon occurs for the Prandtl number Pr.

5.6 Conclusions

The present study gives numerical solutions for the effects of radiation on steady two-dimensional laminar boundary layer flow of an incompressible, viscous, electrically conducting fluid over an exponentially stretching sheet in the presence of uniform magnetic field. The effects of different parameters such as the magnetic parameter, the radiation parameter, the Prandtl number and the Eckert number are studied in detail. It concludes that the velocity boundary layer thickness as well as the skin friction coefficient decreases with the increasing value of the magnetic parameter

whereas the reverse phenomenon occurs for the thermal boundary layer thickness and the surface heat transfer. Further the thermal boundary layer thickness and the surface heat transfer increases with the increasing value of the radiation parameter and the Eckert number whereas the reverse phenomenon occurs for the Prandtl number.

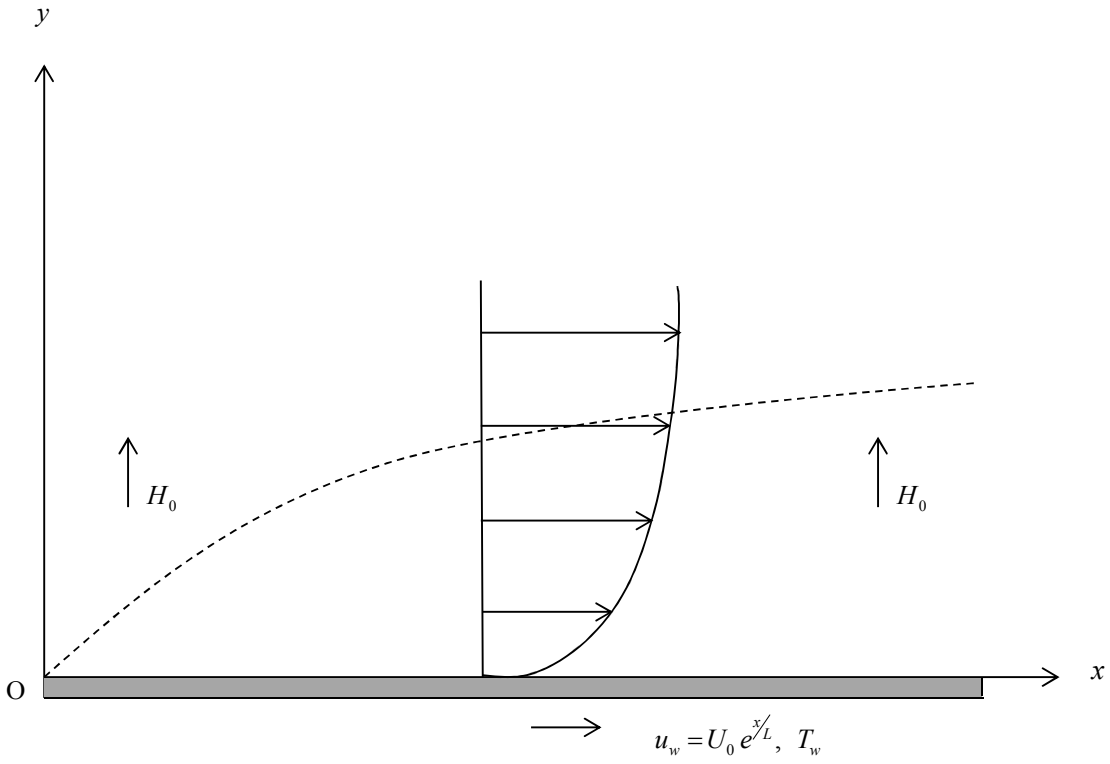

Fig. 5.1 Flow configuration and the coordinate system.

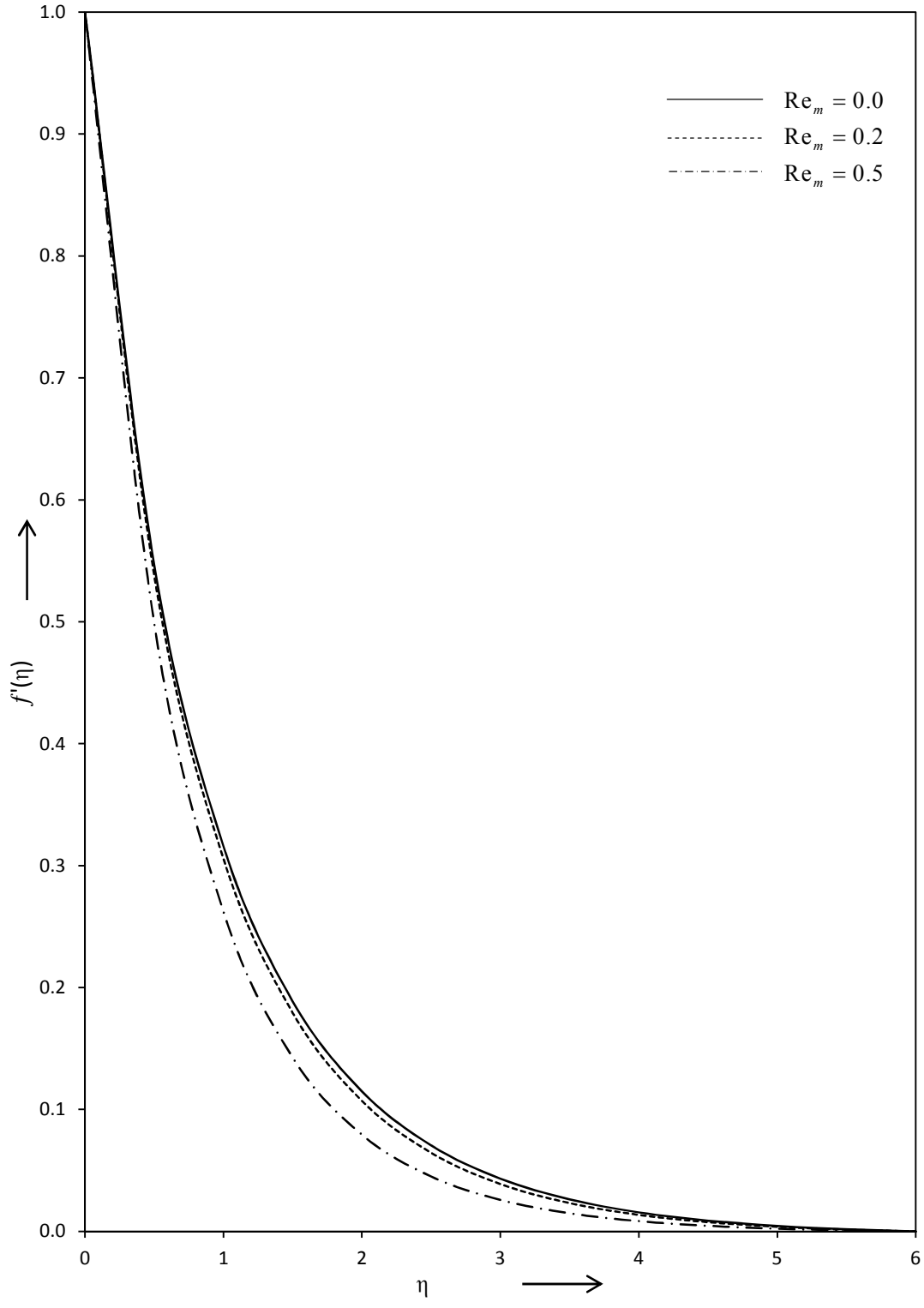

Fig. 5.2 Effects of Re_m on velocity profiles against η.

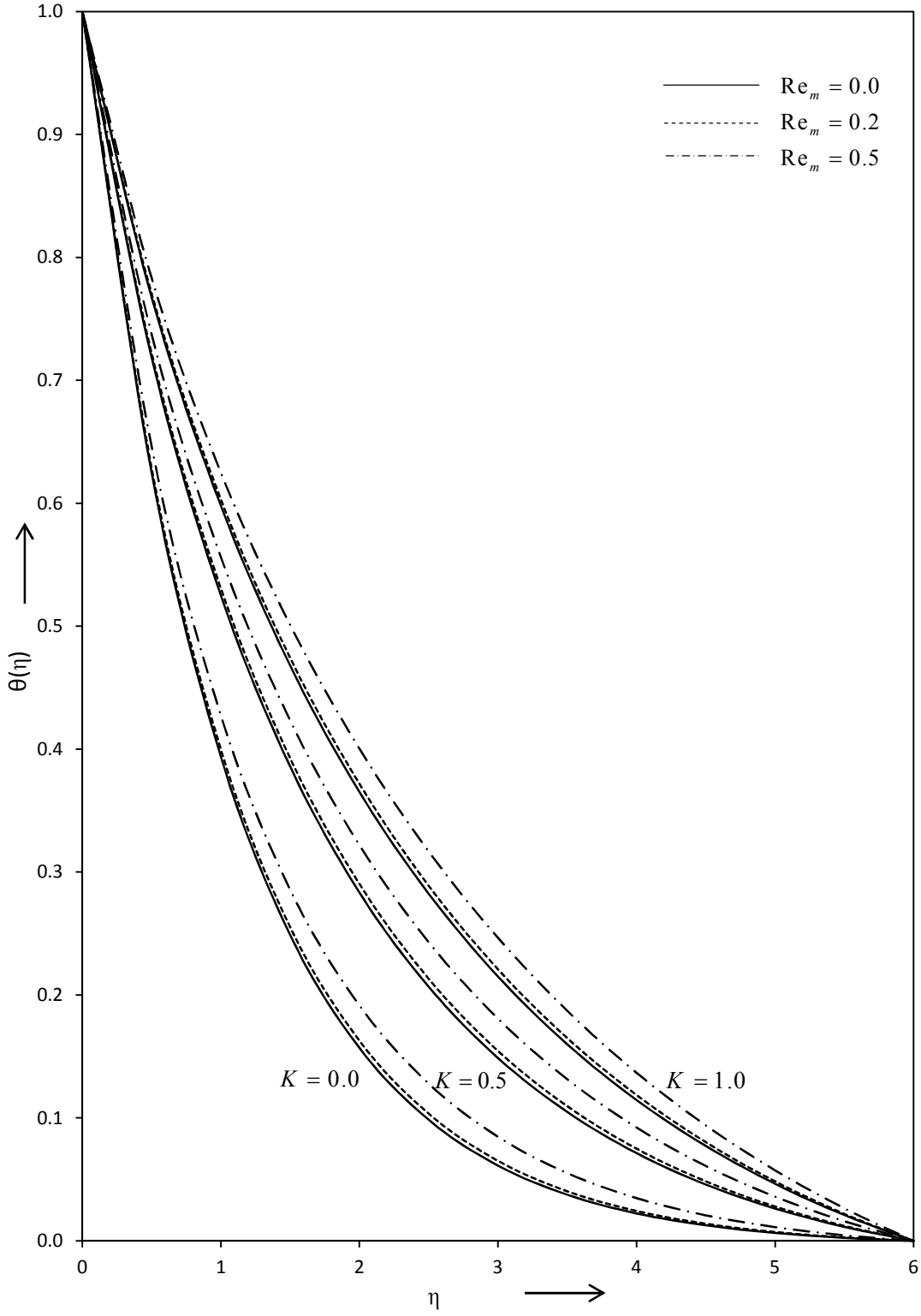

Fig. 5.3 Effects of Re_m and K on temperature profiles against η for $\mathrm{Pr}=1$ and $Ec=0.0$.

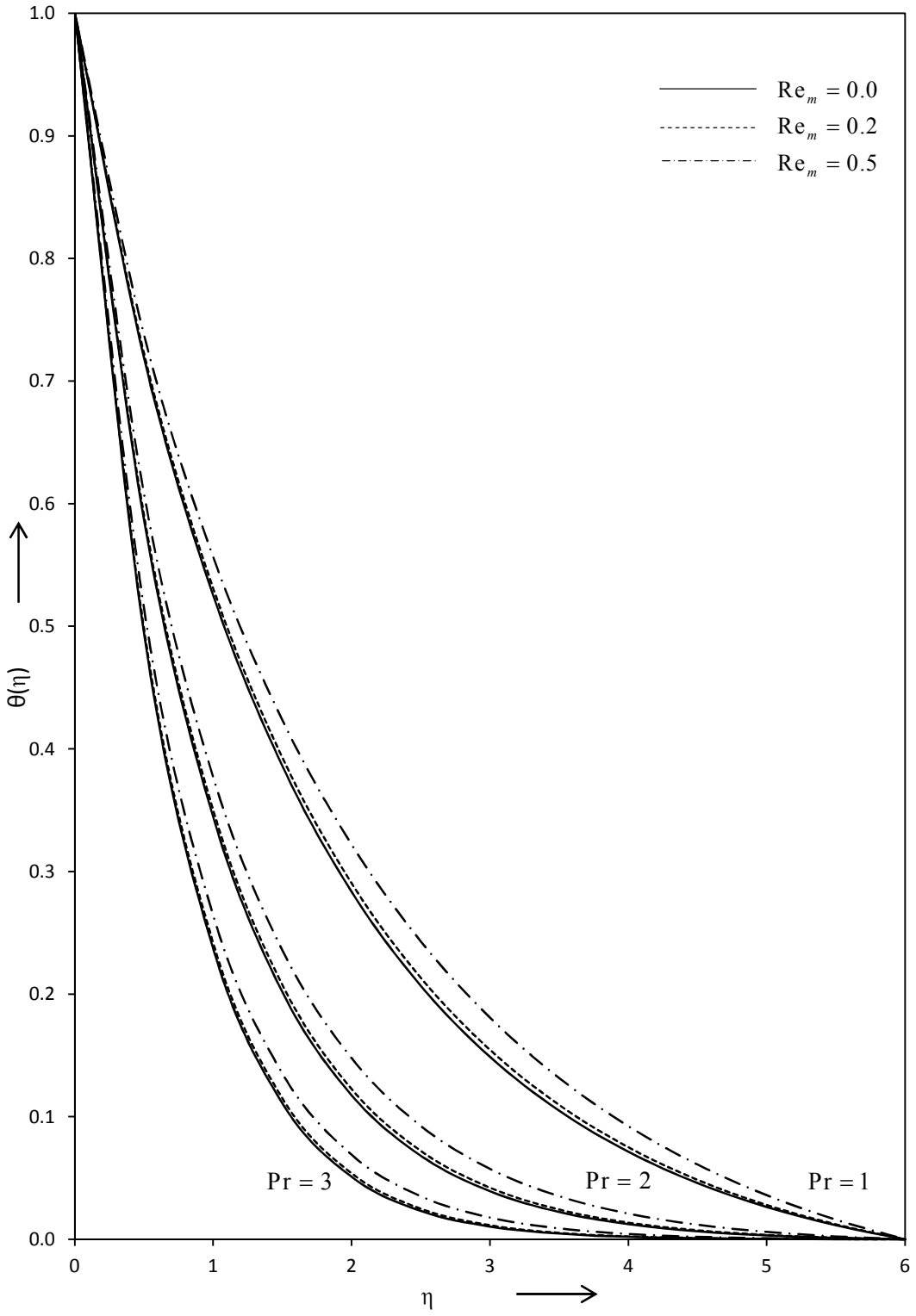

Fig. 5.4 Effects of Re_m and Pr on temperature profiles against η for $K = 0.5$ and $Ec = 0.0$.

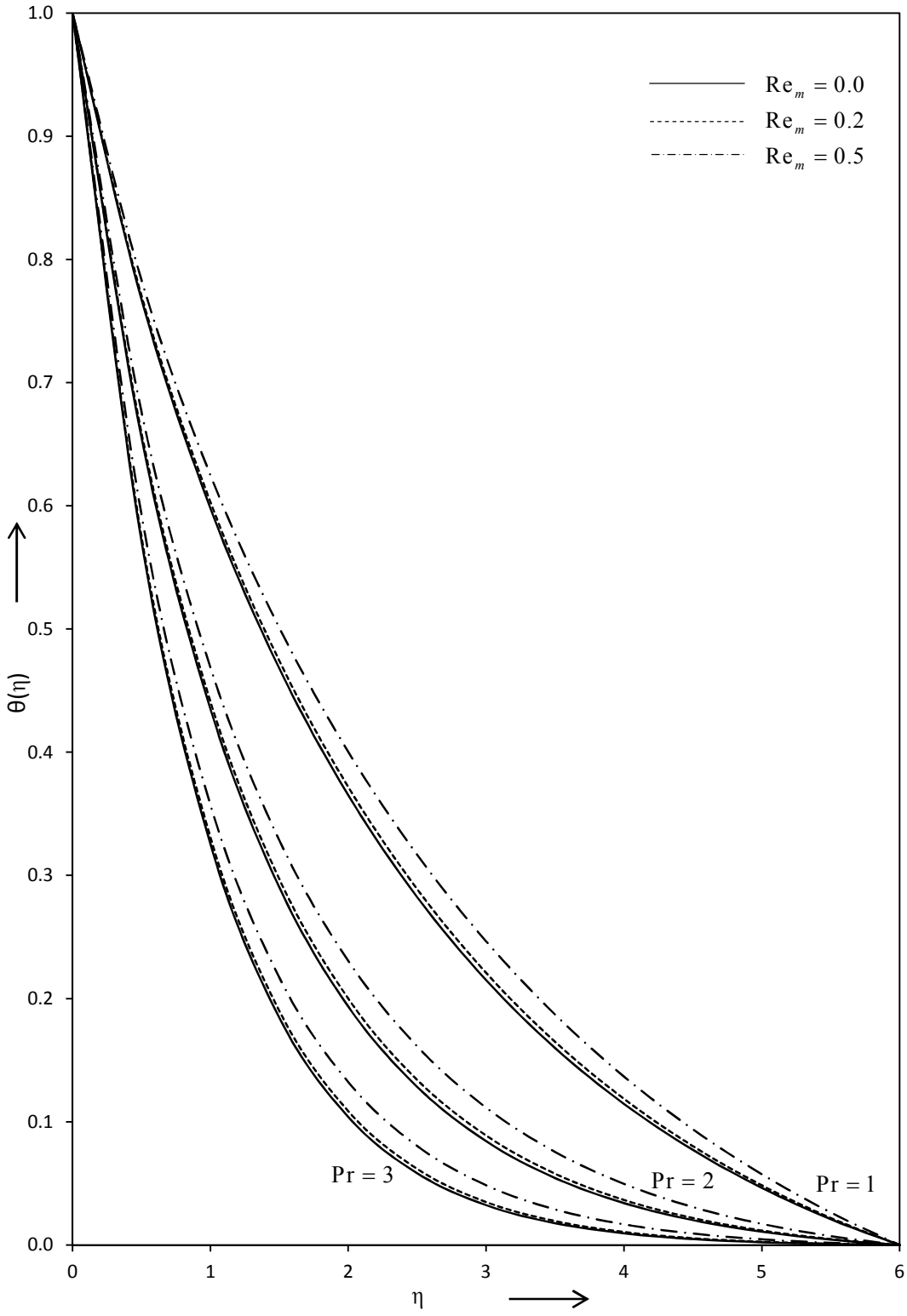

Fig. 5.5 Effects of Re_m and Pr on temperature profiles against η for $K = 1.0$ and $Ec = 0.0$.

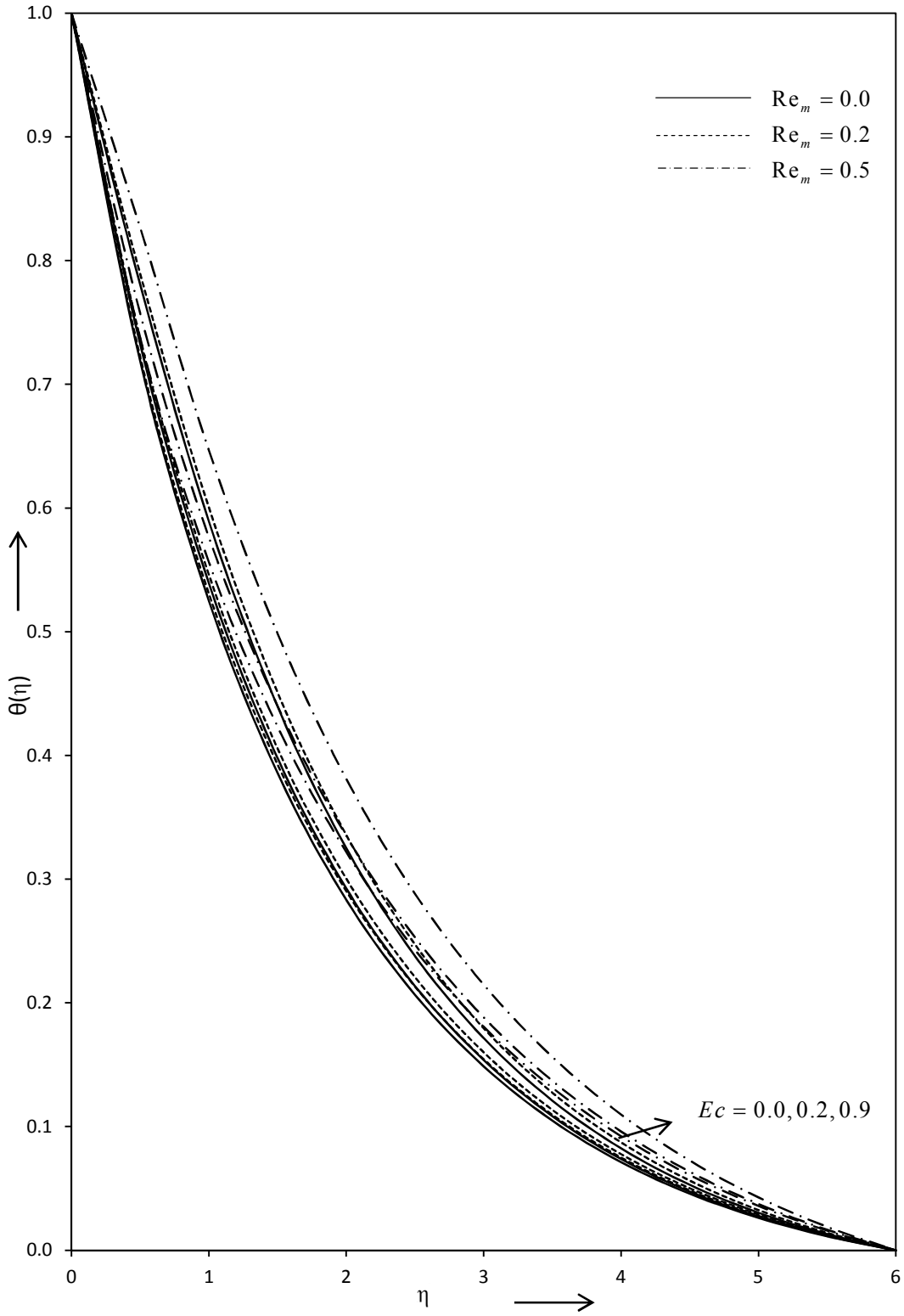

Fig. 5.6 Effects of Re_m and Ec on temperature profiles against η for $K = 0.5$ and $\mathrm{Pr} = 1$.

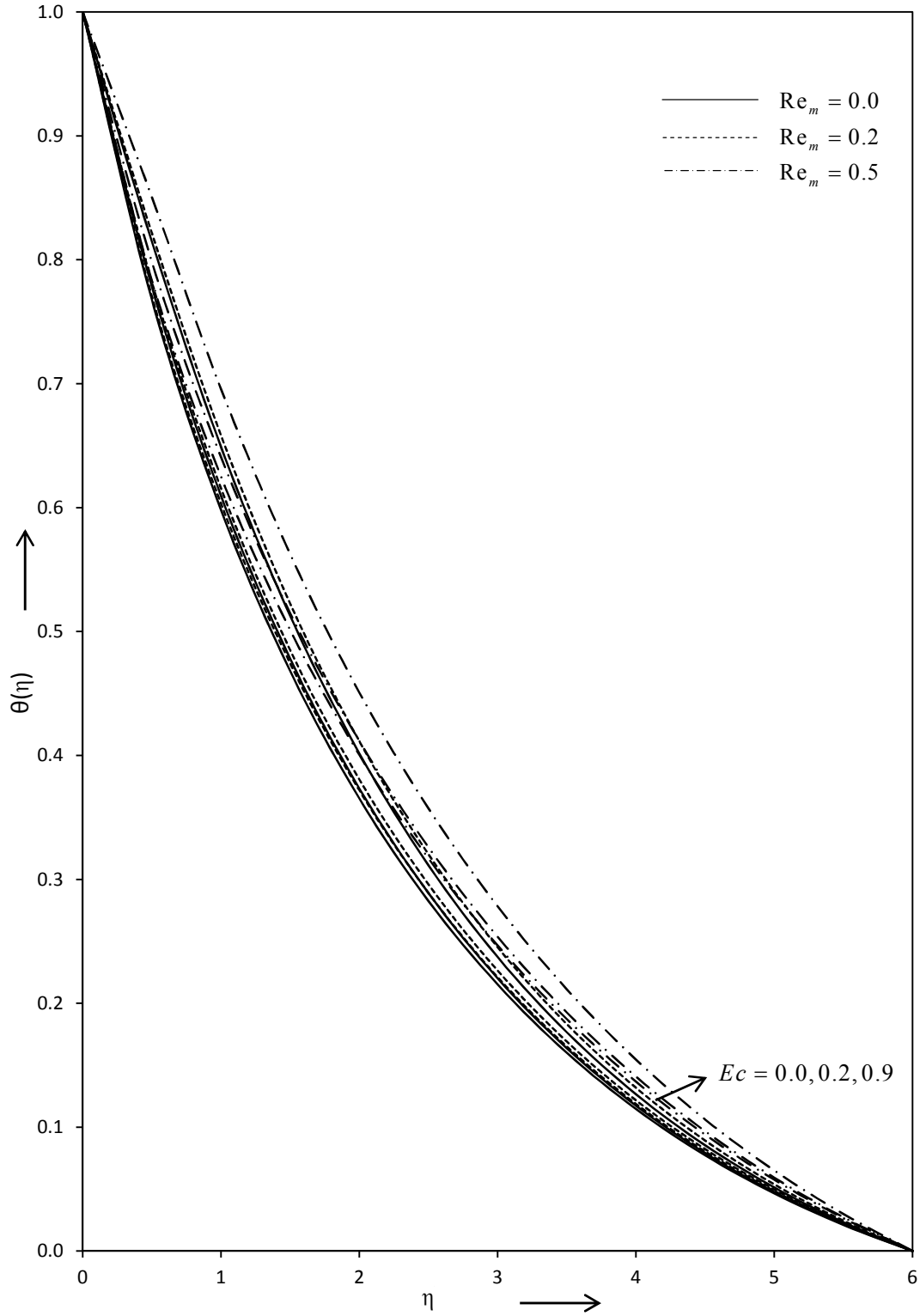

Fig. 5.7 Effects of Re_m and Ec on temperature profiles against η for $K = 1.0$ and $\mathrm{Pr} = 1$.

Table 5.1 Values of $-f''(0)$ and $-\theta'(0)$ for different values of Re_m, K, Pr and Ec.

$-f''(0)$									
$Re_m = 0.0$			$Re_m = 0.2$			$Re_m = 0.5$			
1.2821			1.3135			1.4642			
$-\theta'(0)$									
K	Pr	$Ec = 0.0$			$Ec = 0.2$			$Ec = 0.9$		
		$Re_m = 0.0$	$Re_m = 0.2$	$Re_m = 0.5$	$Re_m = 0.0$	$Re_m = 0.2$	$Re_m = 0.5$	$Re_m = 0.0$	$Re_m = 0.2$	$Re_m = 0.5$
0.0	1	0.9559	0.9555	0.9429	0.8634	0.8627	0.8372	0.5395	0.5376	0.4672
	2	1.4712	1.4709	1.4580	1.3051	1.3041	1.2679	0.7236	0.7204	0.6023
	3	1.8689	1.8685	1.8559	1.6377	1.6365	1.5911	0.8287	0.8244	0.6643
0.5	1	0.6860	0.6857	0.6746	0.6270	0.6265	0.6074	0.4207	0.4194	0.3720
	2	1.0737	1.0734	1.0605	0.9655	0.9647	0.9368	0.5867	0.5846	0.5038
	3	1.3805	1.3802	1.3673	1.2282	1.2273	1.1930	0.6953	0.6924	0.5832
1.0	1	0.5528	0.5525	0.5432	0.5094	0.5090	0.4938	0.3576	0.3566	0.3208
	2	0.8653	0.8550	0.8526	0.7844	0.7838	0.7602	0.5012	0.4995	0.4368
	3	1.1215	1.1211	1.1082	1.0067	1.0059	0.9770	0.6050	0.6027	0.5177

Chapter 6

MHD Slip Flow Past a Shrinking Sheet

6.1 Introduction

The viscous flow and heat transfer in the boundary layer region due to a stretching sheet has wide theoretical and technical applications in manufacturing process and in industries such as extraction of polymer sheet, paper production, wire drawing, glass-fiber production, the cooling and drying of paper and textiles. Furthermore, the continuous surface heat and mass transfer problems are many practical applications in polymer processing and electro-chemistry. The study of heat transfer and flow field is necessary for determining the quality of the final products of such process. Crane (1970) was first who considered steady boundary layer flow of a viscous incompressible fluid over a linearly stretching plate and gave an exact similarity solution in closed analytical form. The effects of heat and mass transfer and magnetic field under various physical conditions have been investigated by several authors such as Chen and Char (1988), Chiam (1994), Andersson (2002), Ariel et al. (2006), Jat and Chaudhary (2007, 2008), Wang (2008), Fang et al. (2010), Nadeem et al. (2010), Bhattacharyya and Layek (2011) and Bhattacharyya et al. (2011). Recently Mahapatra et al. (2012) studied the oblique stagnation-point flow and heat transfer towards a shrinking sheet with thermal radiation.

Based on the above mentioned investigations and applications, this chapter is concerned with a steady, two dimensional stagnation flow of an electrically

conducting fluid past a shrinking sheet in the presence of a magnetic field. The numerical results of velocity, temperature, skin friction and surface heat transfer for different parameters such as the velocity ratio parameter, the slip parameter, the magnetic parameter, the Prandtl number and the Eckert number were obtained.

6.2 Mathematical Formulation

Consider the steady two-dimensional laminar flow $(u,v,0)$ of a viscous incompressible electrically conducting fluid towards a linearly shrinking sheet such that the sheet is shrinked in its own plane with velocity proportional to the distance from the stagnation point in the presence of an externally applied normal magnetic field of constant strength $(0,H_0,0)$. The shrinking surface has a linear velocity u_w and uniform temperature T_w, while the velocity of the flow external to the boundary layer is u_e and temperature T_∞ as shown in Fig. 6.1. Therefore, under the usual boundary layer approximations, the governing equations of motion are-

$$\frac{\partial u}{\partial x}+\frac{\partial v}{\partial y}=0 \tag{6.1}$$

$$u\frac{\partial u}{\partial x}+v\frac{\partial u}{\partial y}=u_e\frac{du_e}{dx}+\upsilon\frac{\partial^2 u}{\partial y^2}-\frac{\sigma_e\mu_e^2 H_0^2 u}{\rho} \tag{6.2}$$

$$\rho C_p\left(u\frac{\partial T}{\partial x}+v\frac{\partial T}{\partial y}\right)=\kappa\frac{\partial^2 T}{\partial y^2}+\mu\left(\frac{\partial u}{\partial y}\right)^2+\sigma_e\mu_e^2 H_0^2 u^2 \tag{6.3}$$

where υ is the kinematic viscosity, σ_e the electrical conductivity, μ_e the magnetic permeability, ρ the density, C_p the specific heat at constant pressure, κ the thermal conductivity and μ the coefficient of viscosity of the fluid under consideration. The other symbols have their usual meanings.

The boundary conditions are-

$$\begin{aligned} &y = 0: \ u = u_w = cx + L\left(\frac{\partial u}{\partial y}\right), \ v = 0; \ \ T = T_w \\ &y = \infty: \ u = u_e = ax; \ \ T = T_\infty \end{aligned} \tag{6.4}$$

where c is a proportionality constant of the velocity of shrinking sheet, L is a slip length and a is a constant proportional to the free stream velocity for away from the sheet.

6.3 Similarity Transformation

The continuity equation (6.1) is identically satisfied by stream function $\psi(x, y)$, defined as

$$u = \frac{\partial \psi}{\partial y}, \qquad v = -\frac{\partial \psi}{\partial x} \tag{6.5}$$

For the solution of the momentum and the energy equations (6.2) and (6.3), the following dimensionless variables are defined-

$$\psi(x, y) = \sqrt{a\upsilon}\, x\, f(\eta) \tag{6.6}$$

$$\eta = \sqrt{\frac{a}{\upsilon}}\, y \tag{6.7}$$

$$\theta(\eta) = \frac{T - T_\infty}{T_w - T_\infty} \tag{6.8}$$

Equations (6.5) to (6.8), transform equations (6.2) and (6.3) into

$$f''' + f\, f'' - f'^2 - \mathrm{Re}_m^2\, f' + 1 = 0 \tag{6.9}$$

$$\theta'' + \mathrm{Pr}\, f\theta' + \mathrm{Pr}\, Ec\, f''^2 + \mathrm{Pr}\, Ec\, \mathrm{Re}_m^2\, f'^2 = 0 \tag{6.10}$$

where the prime (') denotes differentiation with respect to η, $\mathrm{Re}_m = \mu_e H_0 \sqrt{\frac{\sigma_e}{\rho a}}$ is the magnetic parameter, $\mathrm{Pr} = \frac{\mu C_p}{\kappa}$ the Prandtl number and $Ec = \frac{u_e^2}{C_p\left(T_w - T_\infty\right)}$ the Eckert number.

The corresponding boundary conditions are-

$$\begin{aligned} &\eta = 0: \;\; f = 0,\; f' = \frac{c}{a} + \delta f''; \;\; \theta = 1 \\ &\eta = \infty: \;\; f' = 1; \;\; \theta = 0 \end{aligned} \tag{6.11}$$

where $\frac{c}{a}$ is the velocity ratio parameter and $\delta = L\sqrt{\frac{a}{\upsilon}}$ is the slip parameter.

For numerical solution of the equations (6.9) and (6.10), we apply the following power series in a small magnetic parameter Re_m^2 as-

$$f(\eta)=\sum_{i=0}^{\infty}\left(\mathrm{Re}_m^2\right)^i f_i(\eta) \tag{6.12}$$

$$\theta(\eta)=\sum_{j=0}^{\infty}\left(\mathrm{Re}_m^2\right)^j \theta_j(\eta) \tag{6.13}$$

Substituting equations (6.12) and (6.13) and its derivatives in equations (6.9) and (6.10) and then equating the coefficients of like powers of Re_m^2, we get the following set of equations-

$$f_0'''+f_0 f_0''-f_0'^2+1=0 \tag{6.14}$$

$$\theta_0''+\mathrm{Pr}\, f_0\,\theta_0'=-\mathrm{Pr}\, Ec\, f_0''^2 \tag{6.15}$$

$$f_1'''+f_0 f_1''-2f_0'f_1'+f_0''f_1=f_0' \tag{6.16}$$

$$\theta_1''+\mathrm{Pr}\, f_0\,\theta_1'=-\mathrm{Pr}\, f_1\,\theta_0'-\mathrm{Pr}\, Ec\left(2f_0''f_1''+f_0'^2\right) \tag{6.17}$$

$$f_2'''+f_0f_2''-2f_0'f_2'+f_0''f_2=-f_1f_1''+\left(f_1'+1\right)f_1' \tag{6.18}$$

$$\theta_2''+\mathrm{Pr}\, f_0\,\theta_2'=-\mathrm{Pr}\left(f_1\theta_1'+f_2\theta_0'\right)-\mathrm{Pr}\, Ec\left(2f_0''f_2''+f_1''^2+2f_0'f_1'\right) \tag{6.19}$$

with the boundary conditions-

$$\begin{aligned}&\eta=0:\ \ f_i=0,\ f_0'=\frac{c}{a}+\delta f_0'',\ f_j'=\delta f_j'';\ \ \theta_0=1,\ \theta_j=0\\ &\eta=\infty:\ \ f_0'=1,\ f_j'=0;\ \ \theta_i=0 \qquad\qquad i\geq 0,\ j>0\end{aligned} \tag{6.20}$$

The equation (6.14) was also obtained by Bhattacharyya et al. (2011) for the non-magnetic case and the remaining equations are linear ordinary differential equations

and have been solved numerically by Newton's shooting method with fourth-order Runge-Kutta integration scheme for various values of the parameters.

The velocity and temperature distributions for various values of the parameters are shown in Fig. 6.2 to 6.4 and Fig. 6.5 to 6.6 respectively.

6.4 Local Skin Friction and Local Nusselt Number

The physical quantities of interest the local skin friction coefficient C_f and the local Nusselt number Nu i.e. surface heat transfer are given by-

$$C_f = \frac{\tau_w}{\rho u_e^2 / 2} = \frac{\mu \left(\frac{\partial u}{\partial y} \right)_{y=0}}{\rho u_e^2 / 2} \tag{6.21}$$

and

$$Nu = -\frac{x \left(\frac{\partial T}{\partial y} \right)_{y=0}}{\left(T_w - T_\infty \right)} \tag{6.22}$$

which, in the present case, can be expressed in the following forms

$$C_f = \frac{2}{\sqrt{\mathrm{Re}}} f''(0)$$

$$= \frac{2}{\sqrt{\mathrm{Re}}} \sum_{i=0}^{\infty} \left(\mathrm{Re}_m^2 \right)^i f_i''(0) \tag{6.23}$$

and

$$Nu = -\sqrt{\mathrm{Re}}\ \theta'(0)$$

$$= -\sqrt{\mathrm{Re}} \sum_{j=0}^{\infty} \left(\mathrm{Re}_m^2\right)^j \theta_j'(0) \tag{6.24}$$

where $\mathrm{Re} = \frac{u_e x}{\upsilon}$ is the local Reynolds number.

Numerical values of the functions $f''(0)$ and $\theta'(0)$, which are proportional to local skin friction and local heat transfer rate at the surface respectively for various values of the parameters are presented in Table 6.1 and 6.2.

6.5 Numerical Results and Discussion

The velocity profiles $f'(\eta)$ for various values of the velocity ratio parameter $\frac{c}{a}$, the slip parameter δ and the magnetic parameter Re_m are shown in Fig. 6.2 to 6.4. It is observed that the velocity boundary layer thickness increases with the increasing values of the velocity ratio parameter $\frac{c}{a}$ and the slip parameter δ, whereas it decreases as the magnetic parameter Re_m increases for a fixed η.

The temperature profiles $\theta(\eta)$ for various values of the velocity ratio parameter $\frac{c}{a}$, the slip parameter δ, the magnetic parameter Re_m, the Prandtl number Pr and the Eckert number Ec are plotted in Fig. 6.5 to 6.6. It is observed that for the slip parameter $\delta = 0.5$ the thermal boundary layer thickness decreases with the increasing

values of the velocity ratio parameter $\frac{c}{a}$, the Prandtl number Pr and the Eckert number Ec and the reverse phenomenon is observed for the magnetic parameter Re_m.

The numerical values of the function $f''(0)$ for various values of the velocity ratio parameter $\frac{c}{a}$, the slip parameter δ and the magnetic parameter Re_m are presented in Table 6.1. It is observed from the table that the boundary values $f''(0)$ for the non-magnetic flow are the same as those obtained by Bhattacharyya et al. (2011). Further it may be observed from the table that the function $f''(0)$ decreases with the increasing value of the magnetic parameter Re_m when $\frac{c}{a} > -0.9$ and opposite phenomenon occurs when $\frac{c}{a} < -0.9$ and same phenomenon occurs for the velocity ratio parameter $\frac{c}{a}$ at fixed slip parameter δ. Again $f''(0)$ decreases with increasing value of the slip parameter δ when the velocity ratio parameter $\frac{c}{a}$ is fixed.

The numerical values of the function $-\theta'(0)$ for various values of the velocity ratio parameter $\frac{c}{a}$, the magnetic parameter Re_m, the Prandtl number Pr and the Eckert number Ec with the slip parameter $\delta = 0.5$ are presented in Table 6.2 It may be observed from the table that the function $-\theta'(0)$ increases with the increasing value

of the velocity ratio parameter $\frac{c}{a}$, and the Prandtl number Pr but opposite phenomenon occurs for the magnetic parameter Re_m and the Eckert number Ec.

6.6 Conclusions

In this chapter, the stagnation flow for two-dimensional of electrically conducting fluid past a shrinking sheet with slip boundaries in the presence of a magnetic field is studied. The similarity equations are derived and solved numerically. It is found that the velocity boundary layer thickness increases with the increasing values of the velocity ratio parameter, the slip parameter. Further we observed that the magnetic parameter decreases with the increasing value of the velocity boundary layer thickness but the reverse phenomenon occurs for thermal boundary layer thickness. Also it observed that the thermal boundary layer thickness decreases with increasing values of the velocity ratio parameter, the Prandtl number and the Eckert number. On other hand from the results it can be concluded that skin friction and Nusselt number varies similarly as velocity boundary layer thickness and thermal boundary layer thickness respectively with different parameters.

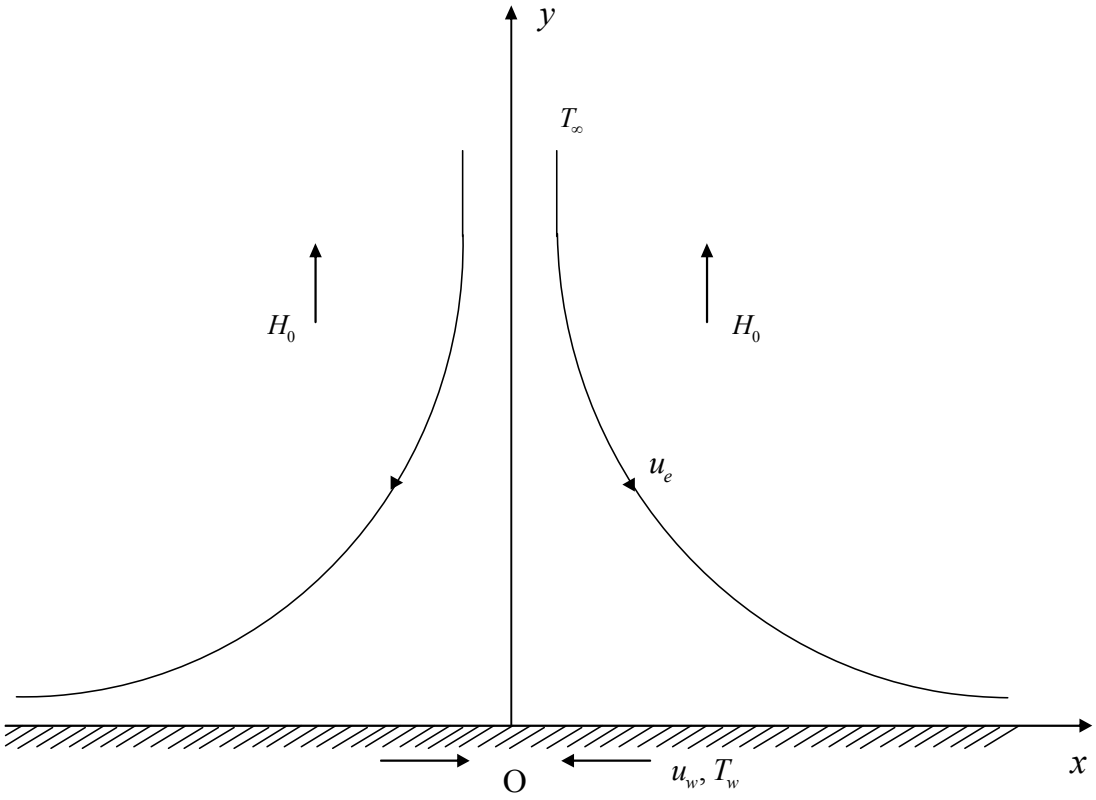

Fig. 6.1 Physical model of two-dimensional stagnation point flow past a shrinking sheet.

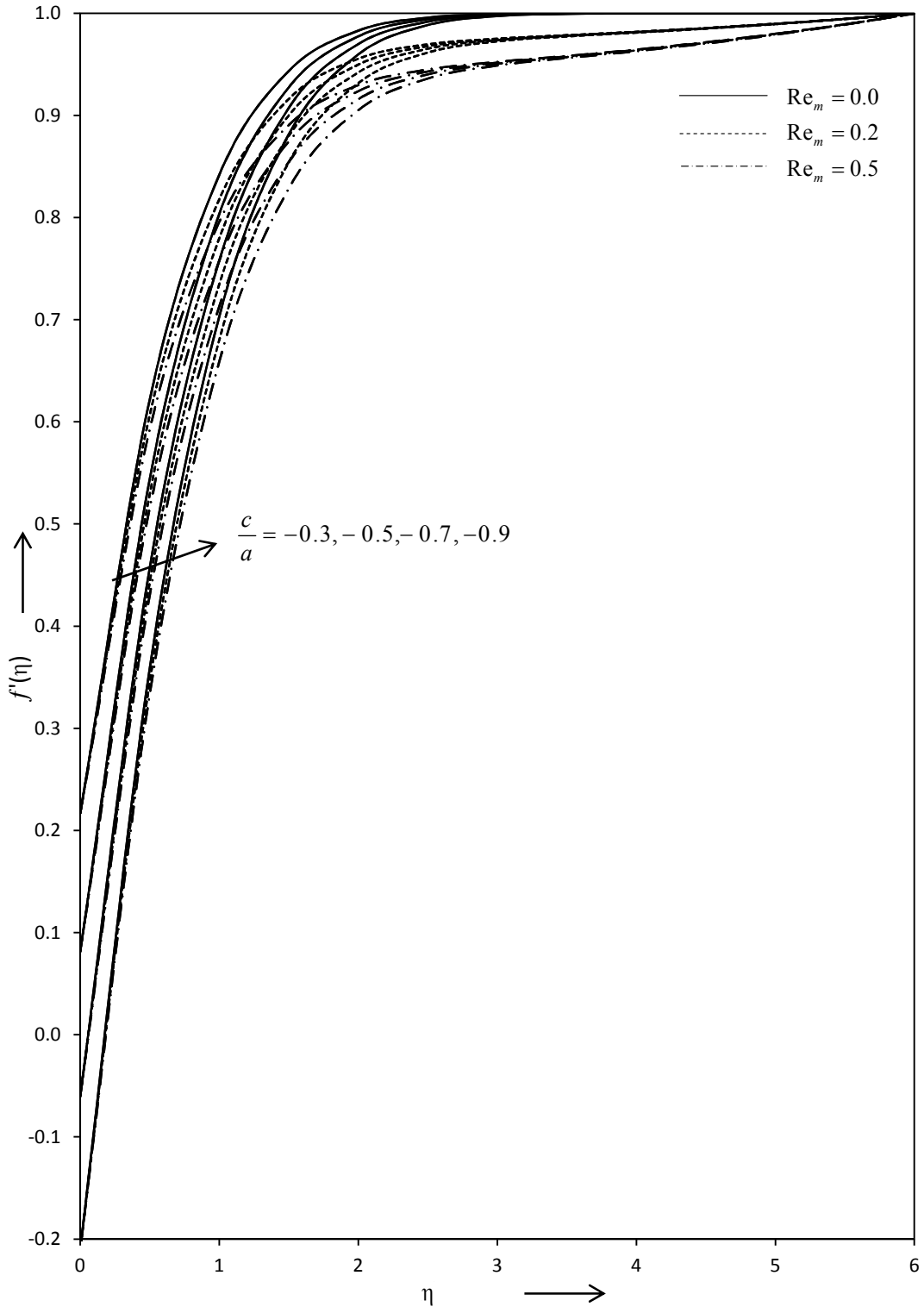

Fig. 6.2 Influence of $\frac{c}{a}$ and Re_m on velocity against η when $\delta = 0.5$.

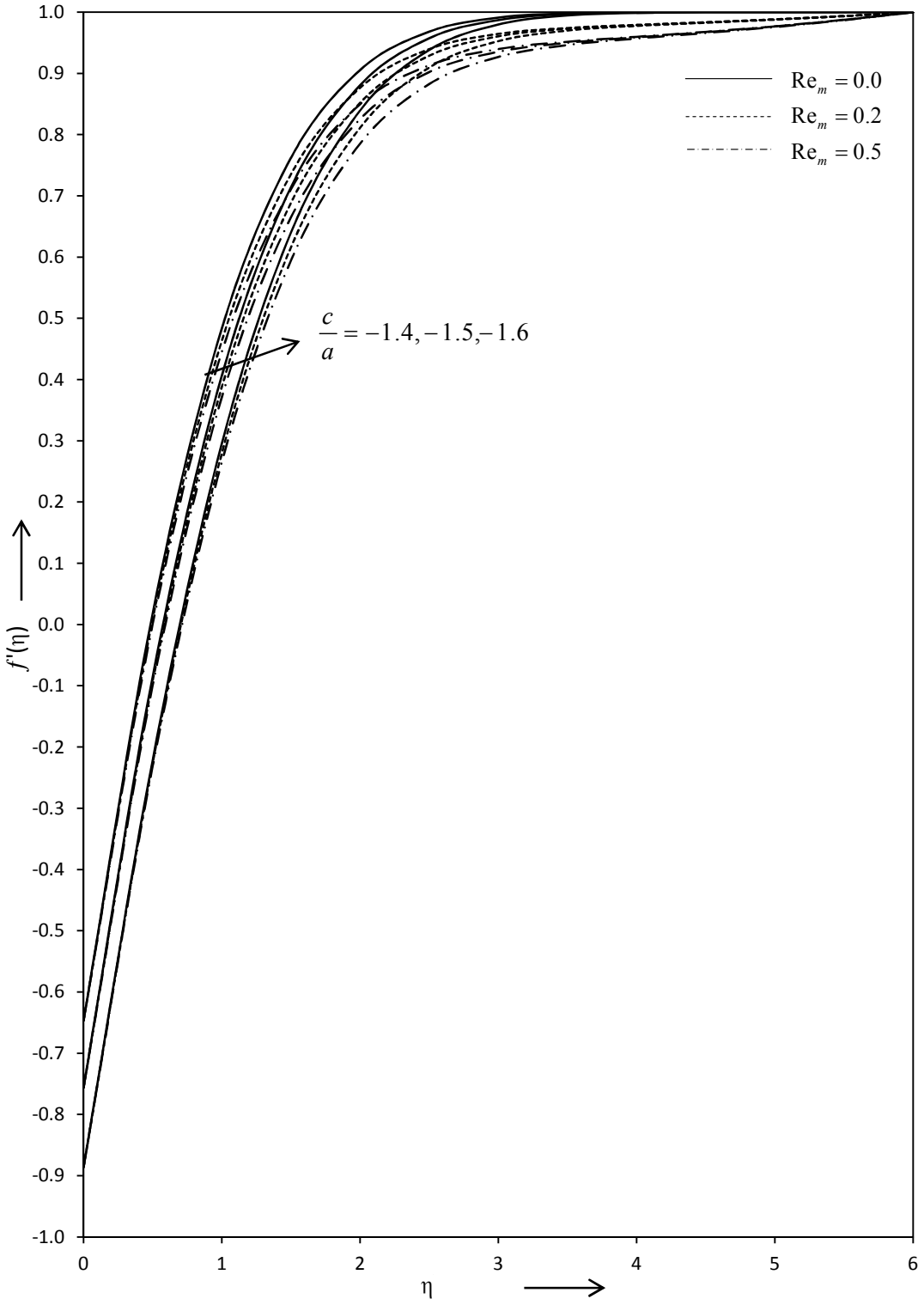

Fig. 6.3 Influence of $\frac{c}{a}$ and Re_m on velocity against η when $\delta = 0.5$.

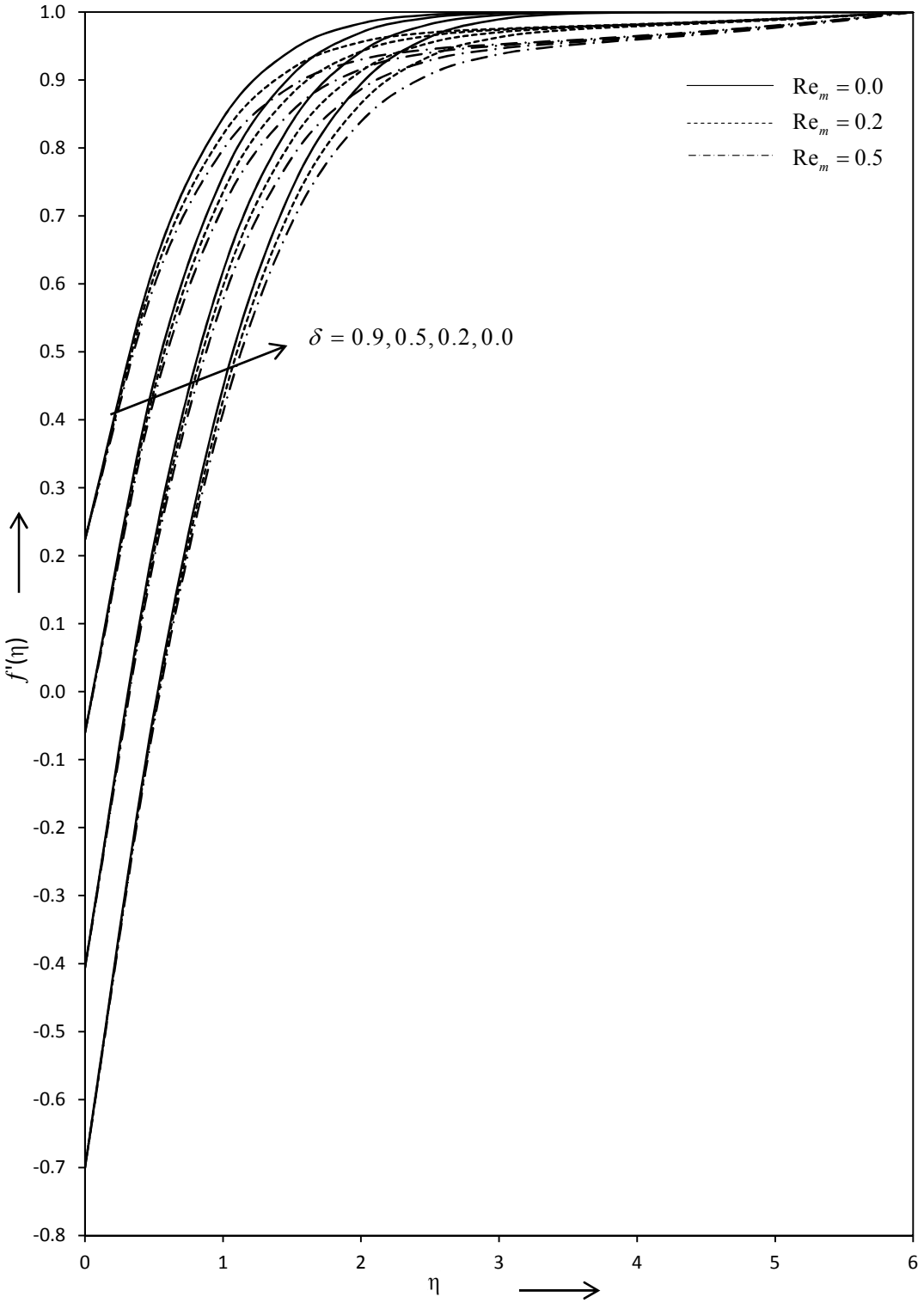

Fig. 6.4 Influence of δ and Re_m on velocity against η when $\frac{c}{a} = -0.7$.

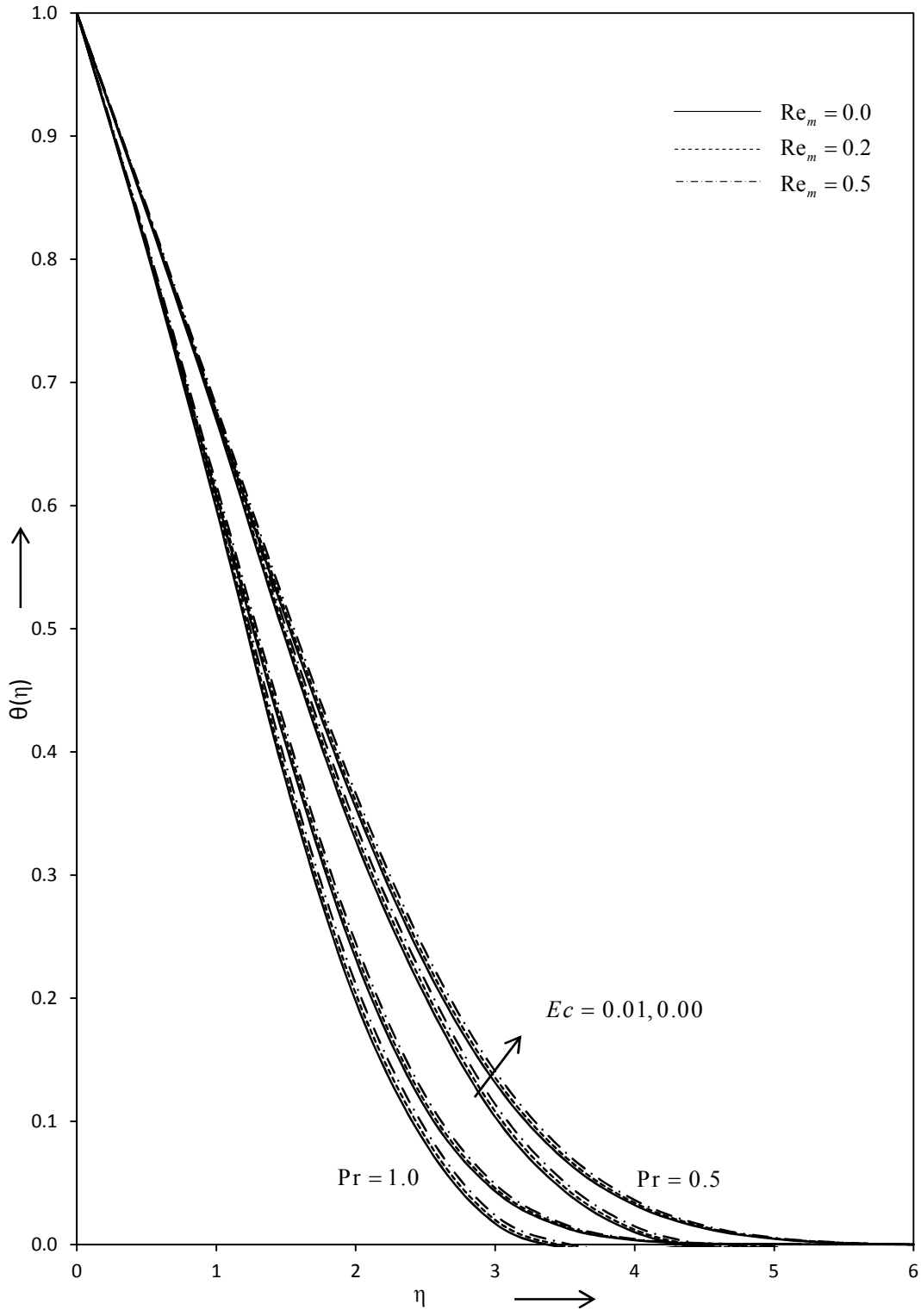

Fig. 6.5 Influence of Re_m, Pr and Ec on temperature against η when $\frac{c}{a} = -1.4$ and $\delta = 0.5$.

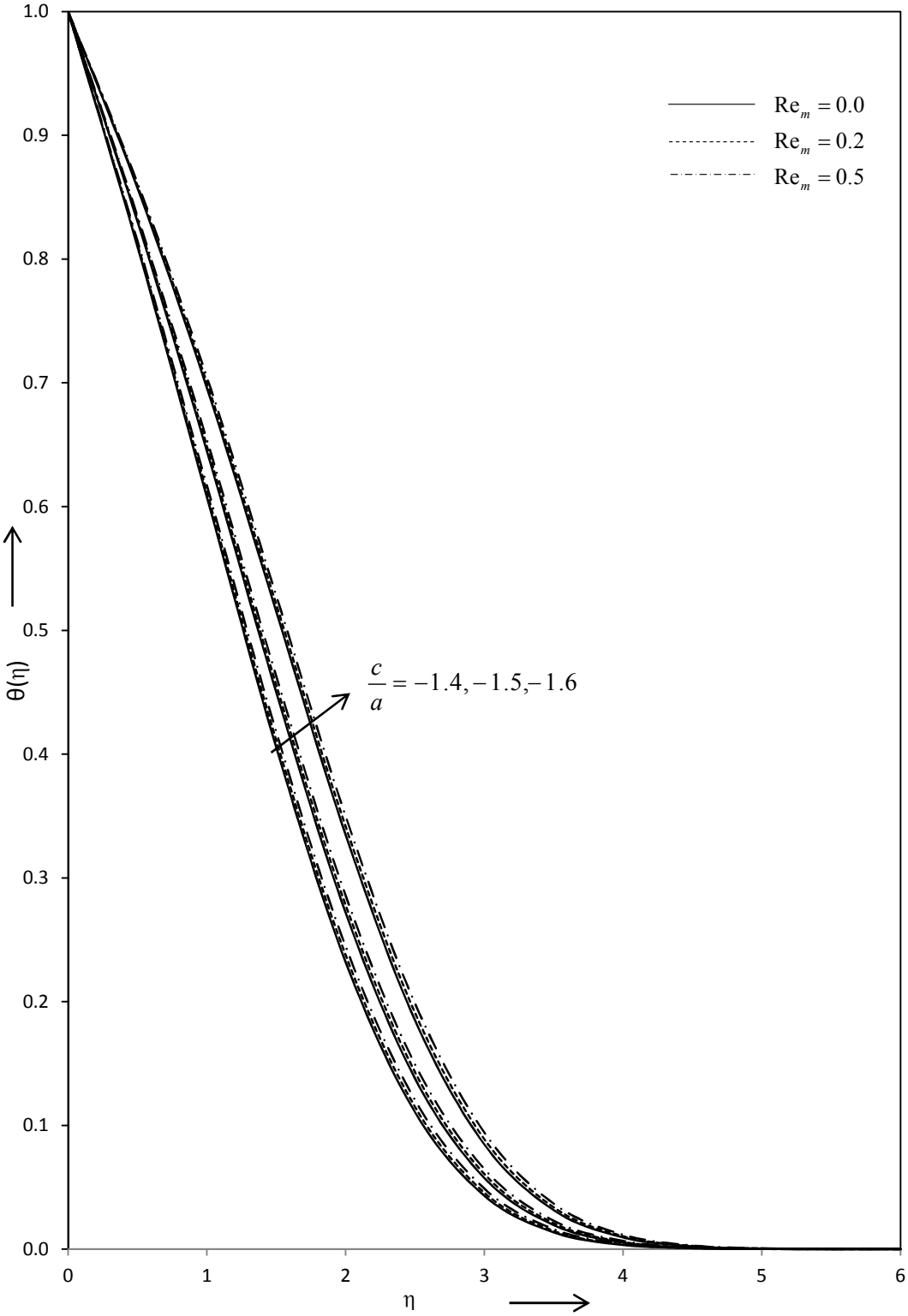

Fig. 6.6 Influence of $\frac{c}{a}$ and Re_m on temperature against η when $\delta = 0.5$, $\mathrm{Pr} = 1.0$ and $Ec = 0.00$.

Table 6.1 Numerical values of $f''(0)$ for several values of $\frac{c}{a}$, δ and Re_m.

δ	$\frac{c}{a}$	$f''(0)$		
		$\mathrm{Re}_m = 0.0$	$\mathrm{Re}_m = 0.2$	$\mathrm{Re}_m = 0.5$
0.5	-0.3	1.0340	0.9986	0.9658
	-0.5	1.1631	1.1304	1.1002
0.0	-0.7	1.5004	1.4895	1.4804
0.2	-0.7	1.4706	1.4496	1.4306
0.5	-0.7	1.2796	1.2499	1.2225
0.9	-0.7	1.0268	0.9913	0.9583
0.5	-0.9	1.3798	1.3536	1.3296
	-1.4	-0.2202	-0.2086	-0.1976
	-1.5	-0.1465	-0.1347	-0.1233
	-1.6	-0.0351	-0.0231	-0.011

Table 6.2 Numerical values of $-\theta'(0)$ for several values of $\frac{c}{a}$, Re_m, Pr and Ec with $\delta = 0.5$.

Pr	Ec	$-\theta'(0)$								
		$\frac{c}{a} = -1.4$			$\frac{c}{a} = -1.5$			$\frac{c}{a} = -1.6$		
		$Re_m = 0.0$	$Re_m = 0.2$	$Re_m = 0.5$	$Re_m = 0.0$	$Re_m = 0.2$	$Re_m = 0.5$	$Re_m = 0.0$	$Re_m = 0.2$	$Re_m = 0.5$
0.1	0.00	0.2109	0.2098	0.2084	0.1780	0.1695	0.1680	0.1492	0.1420	0.1395
	0.01	0.2109	0.2097	0.2083	0.1780	0.1691	0.1678	0.1492	0.1406	0.1391
	0.05	0.2109	0.2095	0.2080	0.1780	0.1685	0.1673	0.1492	0.1398	0.1385
0.5	0.00	0.3180	0.3148	0.3109	0.2672	0.2632	0.2622	0.2293	0.2291	0.2102
	0.01	0.3180	0.3147	0.3106	0.2672	0.2624	0.2614	0.2293	0.2285	0.2101
	0.05	0.3180	0.3140	0.3092	0.2672	0.2620	0.2602	0.2293	0.2273	0.2093
1.0	0.00	0.3725	0.3683	0.3632	0.3311	0.3271	0.3222	0.2767	0.2730	0.2686
	0.01	0.3725	0.3681	0.3627	0.3311	03268	0.3216	0.2767	0.2728	0.2680
	0.05	0.3725	0.3672	0.3607	0.3311	0.3259	0.3195	0.2767	0.2716	0.2656

Chapter 7

Unsteady Magnetohydrodynamic Boundary Layer Flow near the Stagnation Point towards a Shrinking Surface

7.1 Introduction

Stagnation flow of an incompressible viscous fluid over a shrinking sheet has many important practical applications in engineering and industrial processes, such as the extrusion of a polymer in a melt-spinning process, continuous casting of metals, the aerodynamic extrusion of plastic sheets, the cooling of metallic sheets or electronic chips and many others. In all these cases, a study of fluid flow and heat transfer has important significance because the quality of the final product depends on the rate of cooling and the process of stretching.

In recent years, the boundary layer flow due to a shrinking sheet has attraction of many researchers because of its useful applications. A very interesting example in which the shrinking sheet situation occurs is of a rising shrinking balloon. Shrinking film is also a common application of shrinking sheet problems in engineering and industries. Shrinking film is very useful in packaging of bulk products because it can be unwrapped easily with adequate heat.

From the stretching case, the flow of shrinking sheet is different and the fluid is attracted towards a slot. Physically, the generated velocity at shrinking sheet has an

unsteady flow due to the application of inadequate suction and is not confined within the boundary layer.

In view of all these applications, Sakiadis (1961) initiated the study of boundary layer flow over a continuous solid surface moving with constant speed. Later Crane (1970) considered the problem of the flow over a linearly stretching sheet in an ambient fluid and gave a similarity solution in closed analytical form for the steady two-dimensional problem. Gupta and Gupta (1977) and Vleggaar (1977) have investigated the solution of stretching flow problems at the constant surface temperature while Soundalgekar and Ramana Murty (1980) and Grubka and Bobba (1985) have analysed the solution of stretching flow problems with a variable surface temperature. Many researchers such as Magyari and Keller (1999), Elbashbeshy and Bazid (2003), Jat and Chaudhary (2008, 2009, 2010), Bachok et al. (2011) and Zheng et al. (2011) have analyzed the stretching sheet problems with different aspects of fluid, such as the heat transfer, the permeability of the surface and the unsteadiness flow. Mahapatra and Nandy (2011, 2013) studied the unsteady stagnation-point flow and heat transfer over an unsteady shrinking sheet. Recently Aly and Vajravelu (2014) and Chaudhary and Kumar (2014) discussed numerical solutions of boundary layer flow problems over different surfaces in a porous medium. More recently Nandy et al. (2014) and Rosca and Pop (2015) investigated the unsteady boundary layer flow over a permeable stretching or shrinking surface.

Realizing the increasing technical applications of the magnetohydrodynamic effects, the aim of the present chapter is concerned with a steady, two-dimensional unsteady

stagnation flow of an electrically conducting fluid over a shrinking surface in the presence of a uniform transverse magnetic field.

7.2 Flow Formulation

Consider an unsteady two-dimensional steady flow $(u,v,0)$ of a viscous incompressible electrically conducting fluid near a stagnation point over a continuously shrinking surface placed in the plane $y=0$ of a Cartesian coordinate system in the presence of time dependent free stream. The $x-$axis is taken along the shrinking surface in the direction of motion and $y-$axis is perpendicular to it. A uniform magnetic field of constant strength $(0,H_0,0)$ is assumed to be applied normal to the shrinking surface (Fig. 7.1). The surface is assumed to be highly elastic and is shrinking in the $x-$direction with a velocity is u_w and surface temperature T_w while the velocity of the flow, external to the boundary layer is u_e and temperature T_∞. Therefore, under the usual boundary layer and Boussinesq approximations, the systems of boundary layer equations are given by

$$\frac{\partial u}{\partial x}+\frac{\partial v}{\partial y}=0 \tag{7.1}$$

$$\frac{\partial u}{\partial t}+u\frac{\partial u}{\partial x}+v\frac{\partial u}{\partial y}=\frac{\partial u_e}{\partial t}+u_e\frac{\partial u_e}{\partial x}+\upsilon\frac{\partial^2 u}{\partial y^2}-\frac{\sigma_e\,\mu_e^2\,H_0^2\,u}{\rho} \tag{7.2}$$

$$\rho C_p\left(\frac{\partial T}{\partial t}+u\frac{\partial T}{\partial x}+v\frac{\partial T}{\partial y}\right)=\kappa\frac{\partial^2 T}{\partial y^2}+\mu\left(\frac{\partial u}{\partial y}\right)^2+\sigma_e\,\mu_e^2\,H_0^2\,u^2 \tag{7.3}$$

where υ is the kinematic viscosity, σ_e the electrical conductivity, μ_e the magnetic permeability, ρ the density, C_p the specific heat at constant pressure, κ the thermal conductivity and μ the coefficient of viscosity of the fluid under consideration. The other symbols have their usual meanings.

The boundary conditions are-

$$\begin{aligned} &y=0:\ u=u_w=\frac{cx}{1+\gamma t},\ v=0;\ \ T=T_w \\ &y=\infty:\ u=u_e=\frac{ax}{1+\gamma t};\ \ T=T_\infty \end{aligned} \tag{7.4}$$

where c is a constant, γ is the shrinking rate and a is the strength of the stagnation point flow.

7.3 Similarity Solution

The continuity equation (7.1) is identically satisfied by stream function $\psi(x,y,t)$, defined as

$$u=\frac{\partial\psi}{\partial y},\qquad v=-\frac{\partial\psi}{\partial x} \tag{7.5}$$

For the solution of the momentum and the energy equations (7.2) and (7.3), the following dimensionless variables are defined-

$$\psi(x,y,t)=\sqrt{\frac{a\upsilon}{1+\gamma t}}\ x f(\eta) \tag{7.6}$$

$$\eta = \sqrt{\frac{a}{\upsilon(1+\gamma t)}}\ y \tag{7.7}$$

$$\theta(\eta) = \frac{T - T_\infty}{T_w - T_\infty} \tag{7.8}$$

Equations (7.5) to (7.8), transform equations (7.2) and (7.3) into

$$f''' + \left(f + \frac{1}{2}\eta\beta\right) f'' + \left(\beta - \alpha\,\mathrm{Re}_m^2 - f'\right) f' + 1 - \beta = 0 \tag{7.9}$$

$$\theta'' + \mathrm{Pr}\left(f + \frac{1}{2}\eta\beta\right)\theta' + \frac{1}{\alpha^2}\mathrm{Pr}\,Ec\,f''^2 + \frac{1}{\alpha}\mathrm{Pr}\,Ec\,\mathrm{Re}_m^2\,f'^2 = 0 \tag{7.10}$$

where the prime (') denotes differentiation with respect to η, $\beta = \frac{\gamma}{a}$ is the unsteadiness parameter, $\alpha = \frac{c}{a}$ the velocity parameter, $\mathrm{Re}_m = \mu_e H_0 \sqrt{\frac{\sigma_e x}{\rho u_w}}$ the magnetic parameter, $\mathrm{Pr} = \frac{\mu C_p}{\kappa}$ the Prandtl number and $Ec = \frac{{u_w}^2}{C_p\left(T_w - T_\infty\right)}$ the Eckert number.

The corresponding boundary conditions are-

$$\begin{aligned} &\eta = 0: \quad f = 0,\ f' = \alpha;\quad \theta = 1 \\ &\eta = \infty: \quad f' = 1;\quad \theta = 0 \end{aligned} \tag{7.11}$$

For numerical solution of the equations (7.9) and (7.10), through a perturbation technique, by assuming the following power series in a small magnetic parameter Re_m^2 as-

$$f(\eta)=\sum_{i=0}^{\infty}\left(\mathrm{Re}_m^2\right)^i f_i(\eta) \tag{7.12}$$

$$\theta(\eta)=\sum_{j=0}^{\infty}\left(\mathrm{Re}_m^2\right)^j \theta_j(\eta) \tag{7.13}$$

Substituting equations (7.12) and (7.13) and its derivatives in equations (7.9) and (7.10) and then equating the coefficients of like powers of Re_m^2, we get the following set of equations-

$$f_0'''+\left(f_0+\frac{1}{2}\eta\beta\right)f_0''+\left(\beta-f_0'\right)f_0'=\beta-1 \tag{7.14}$$

$$\theta_0''+\mathrm{Pr}\left(f_0+\frac{1}{2}\eta\beta\right)\theta_0'=-\frac{1}{\alpha^2}\mathrm{Pr}\,Ec\,f_0''^2 \tag{7.15}$$

$$f_1'''+\left(f_0+\frac{1}{2}\eta\beta\right)f_1''+\left(\beta-2f_0'\right)f_1'+f_0''f_1=\alpha f_0' \tag{7.16}$$

$$\theta_1''+\mathrm{Pr}\left(f_0+\frac{1}{2}\eta\beta\right)\theta_1'=-\mathrm{Pr}\,f_1\theta_0'-\frac{1}{\alpha^2}\mathrm{Pr}\,Ec\left(2f_0''f_1''+\alpha f_0'^2\right) \tag{7.17}$$

$$f_2'''+\left(f_0+\frac{1}{2}\eta\beta\right)f_2''+\left(\beta-2f_0'\right)f_2'+f_0''f_2=-f_1f_1''+\left(f_1'+\alpha\right)f_1' \tag{7.18}$$

$$\theta_2''+\mathrm{Pr}\left(f_0+\frac{1}{2}\eta\beta\right)\theta_2'=-\mathrm{Pr}\left(f_1\theta_1'+f_2\theta_0'\right)-\frac{1}{\alpha^2}\mathrm{Pr}\,Ec\left(2f_0''f_2''+f_1''^2+2\alpha f_0'f_1'\right) \tag{7.19}$$

with the boundary conditions-

$$\eta = 0: \;\; f_i = 0,\; f_0' = \alpha,\; f_j' = 0;\;\; \theta_0 = 1,\; \theta_j = 0$$
$$\eta = \infty: \;\; f_0' = 1,\; f_j' = 0;\;\; \theta_i = 0 \qquad\qquad i \geq 0,\; j > 0 \tag{7.20}$$

The equation (7.14) was also obtained by Mahapatra and Nandy (2011) for the non-magnetic case and the remaining equations are linear ordinary differential equations and have been solved numerically by Runge-Kutta method of fourth order. The velocity and temperature distributions for various values of the parameters are shown in Fig. 7.2 and Fig. 7.3 to 7.6 respectively.

7.4 Skin Friction and Heat Transfer Rate

The physical quantities of interest, the local skin friction coefficient C_f and the local Nusselt number Nu i.e. surface heat transfer are given by-

$$C_f = \frac{\tau_w}{\rho u_w^2 / 2} = \frac{\mu \left(\frac{\partial u}{\partial y} \right)_{y=0}}{\rho u_w^2 / 2} \tag{7.21}$$

and

$$Nu = -\frac{x \left(\frac{\partial T}{\partial y} \right)_{y=0}}{\left(T_w - T_\infty \right)} \tag{7.22}$$

which, in the present case, can be expressed in the following forms

$$C_f = \frac{2}{\alpha^{3/2} \sqrt{\mathrm{Re}}} \, f''(0)$$

$$= \frac{2}{\alpha^{3/2}\sqrt{\mathrm{Re}}} \sum_{i=0}^{\infty} \left(\mathrm{Re}_m^2\right)^i f_i''(0) \tag{7.23}$$

and

$$Nu = -\sqrt{\frac{\mathrm{Re}}{\alpha}}\, \theta'(0)$$

$$= -\sqrt{\frac{\mathrm{Re}}{\alpha}} \sum_{j=0}^{\infty} \left(\mathrm{Re}_m^2\right)^j \theta_j'(0) \tag{7.24}$$

where $\mathrm{Re} = \frac{u_w x}{\upsilon}$ is the local Reynolds number.

Numerical values of the functions $f''(0)$ and $\theta'(0)$, which are proportional to local skin friction and local heat transfer rate at the surface respectively for various values of the parameters are presented in Table 7.1 and 7.2.

7.5 Computational Results and Discussion

The Figure 7.2 shows the variation of velocity distribution against η for various values of the unsteadiness parameter β, the velocity parameter α and the magnetic parameter Re_m. It may be observed that, for the fixed value of the velocity parameter α, velocity distribution increases with the decreasing value of the unsteadiness parameter β, and opposite phenomenon occur for the magnetic parameter Re_m.

The Figures 7.3 to 7.6 show the variation of temperature distribution against η for the various values of the parameters such as the unsteadiness parameter β, the velocity parameter α, the magnetic parameter Re_m, the Prandtl number Pr and the Eckert number Ec. From these figures it may be observed that the temperature distribution decreases with increasing values of the unsteadiness parameter β, the velocity parameter α, the magnetic parameter Re_m, the Prandtl number Pr and the Eckert number Ec.

In Table 7.1 the numerical values of the function $f''(0)$ for various values of the unsteadiness parameter β, the velocity parameter α and the magnetic parameter Re_m are given. It may be observed from the table that the boundary values $f''(0)$ for the non-magnetic flow are the same as those obtained by Mahapatra and Nandy (2011). The value of the function $f''(0)$ decreases with the increasing values of the unsteadiness parameter β and the magnetic parameter Re_m respectively taking other parameters constant and reverse phenomenon occurs for the velocity parameter α.

Table 7.2 gives the numerical values of the function $-\theta'(0)$ for the various values of the unsteadiness parameter β, the velocity parameter α, the magnetic parameter Re_m, the Prandtl number Pr and the Eckert number Ec. It may be observed from the table that the boundary values $-\theta'(0)$ for the non-magnetic flow are same as those obtained by Mahapatra and Nandy (2011). The value of the function $-\theta'(0)$ increases with the increasing value of the unsteadiness parameter β, considering other

parameters constant and same phenomenon occurs for the velocity parameter α, the magnetic parameter Re_m, the Prandtl number $\mathrm{Pr} < 0.5$ and the Eckert number Ec. It is further observed that the function $-\theta'(0)$ decreases with an increasing value of the Prandtl number $\mathrm{Pr} > 0.5$ for fixed other parameters.

7.6 Conclusions

The present work extends the two-dimensional unsteady stagnation flow of an electrically conducting fluid, over shrinking surface in the presence of magnetic field. Under some special conditions, the problem will reduce the results obtained by previous researchers. The effects of different parameters such as the unsteadiness parameter, the velocity parameter, the magnetic parameter, the Prandtl number and the Eckert number are studied in detail. The velocity as well as thermal boundary layer thickness decreases with the increasing values of the unsteadiness parameter, the velocity parameter, the magnetic parameter, the Prandtl number and the Eckert number whereas in the velocity reverse phenomenon occurs for the magnetic parameter. From the results it can be concluded that skin friction and Nusselt number varies according to the velocity and thermal boundary layers thickness respectively with different parameters.

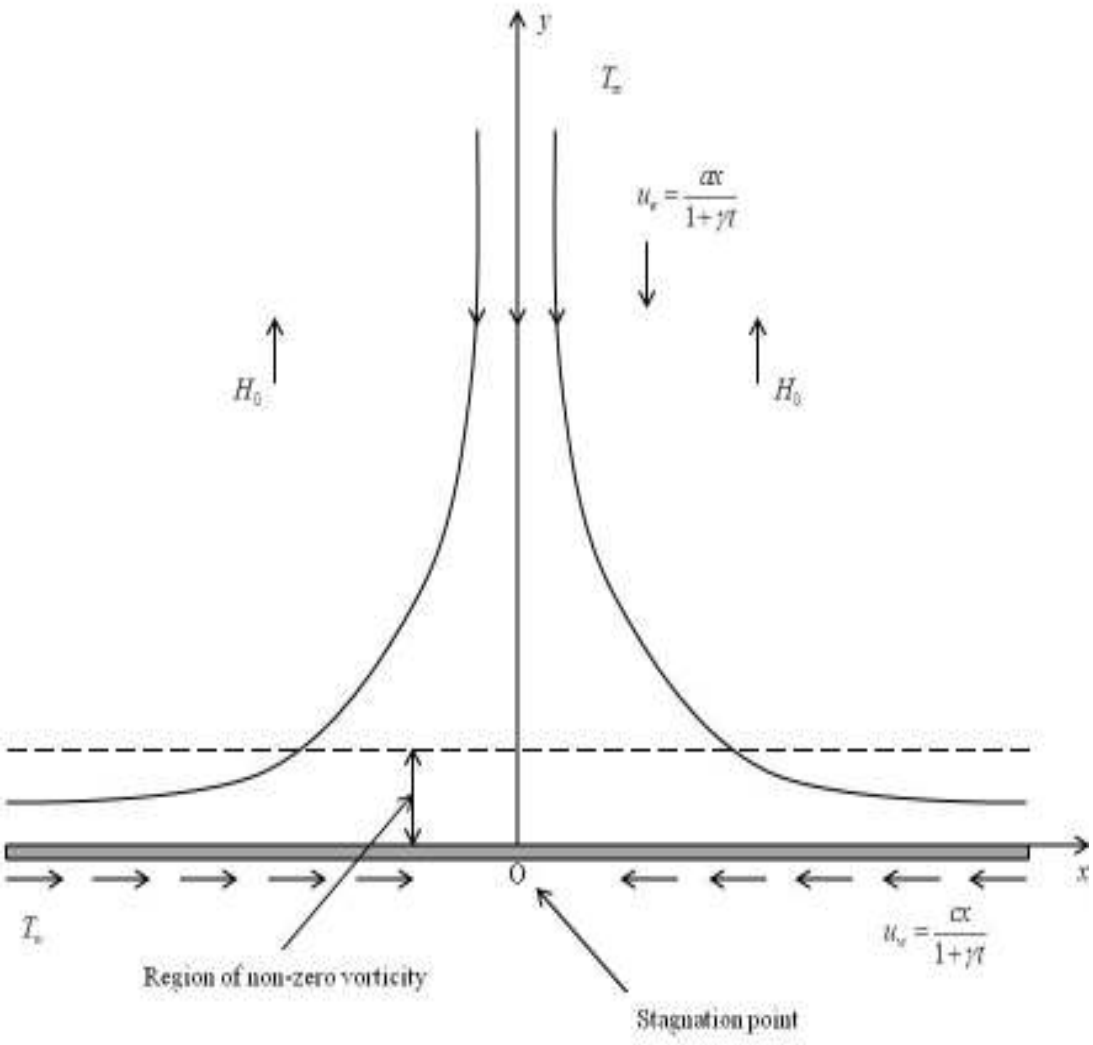

Fig. 7.1 Coordinate system for the shrinking surface.

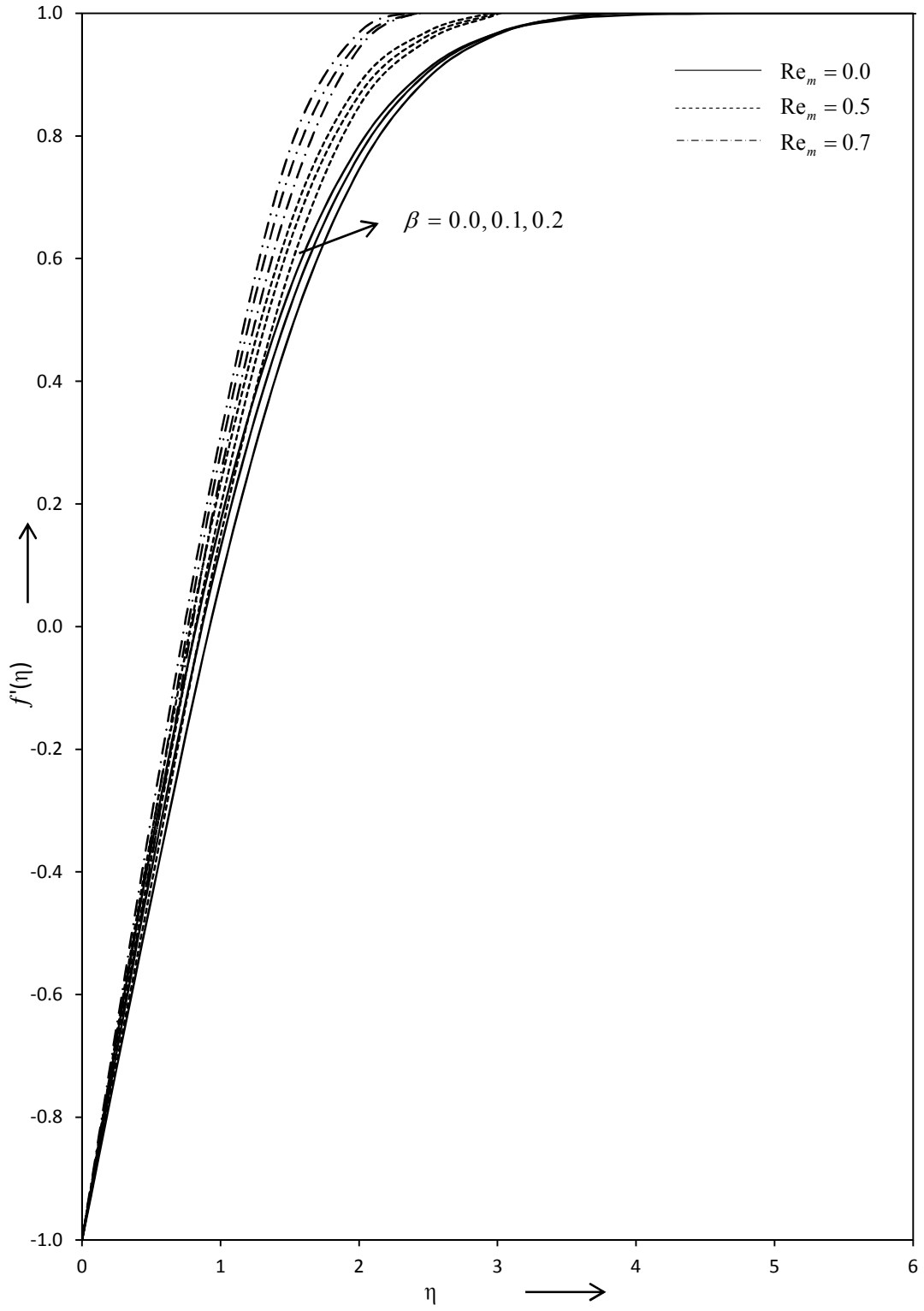

Fig. 7.2 Behavior of velocity distribution against η for various values of β and Re_m with $\alpha = -0.1$.

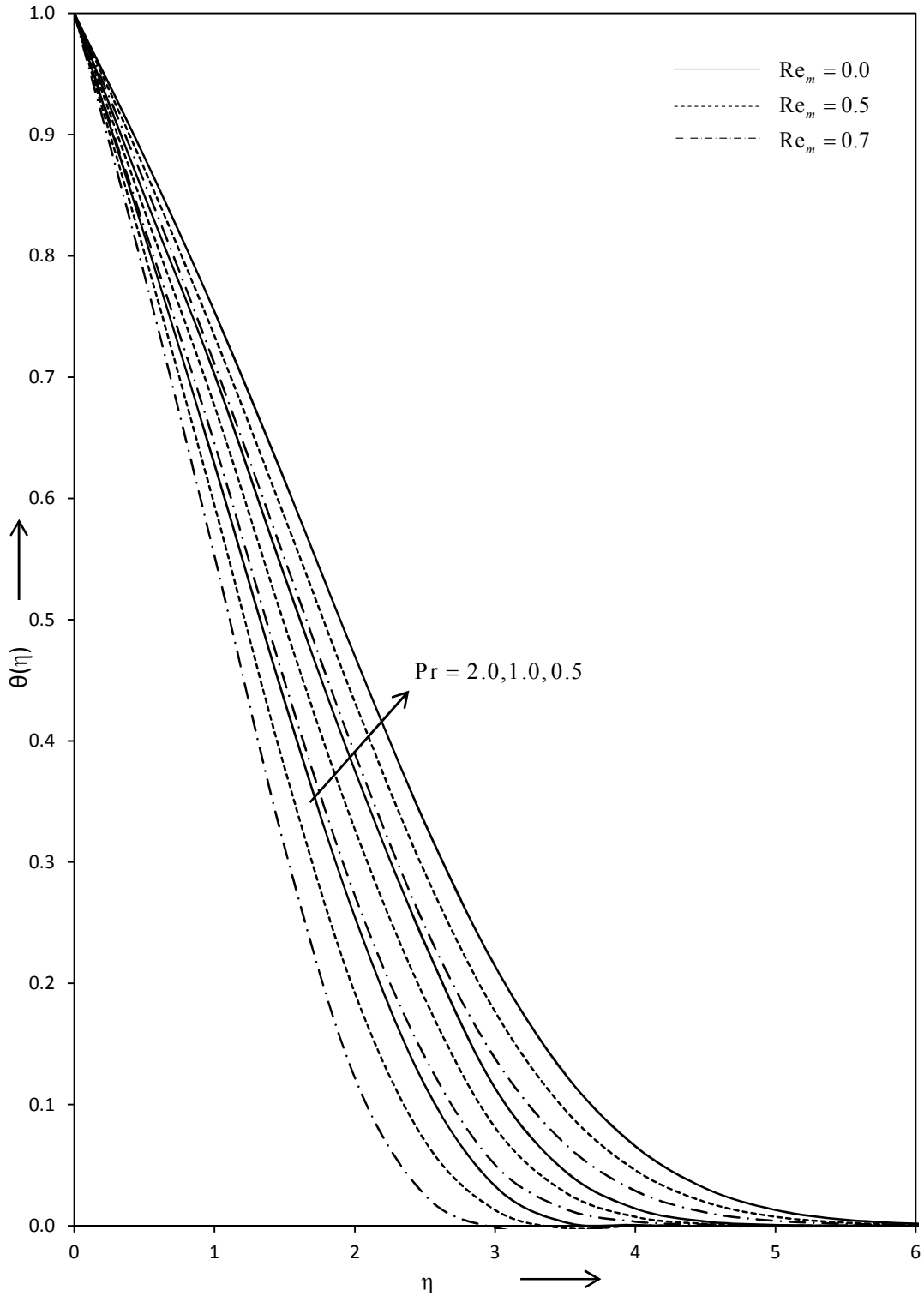

Fig. 7.3 Behavior of temperature distribution against η for various values of Re_m and Pr with $\beta = 0.1$, $\alpha = -1.0$ and $Ec = 0.000$.

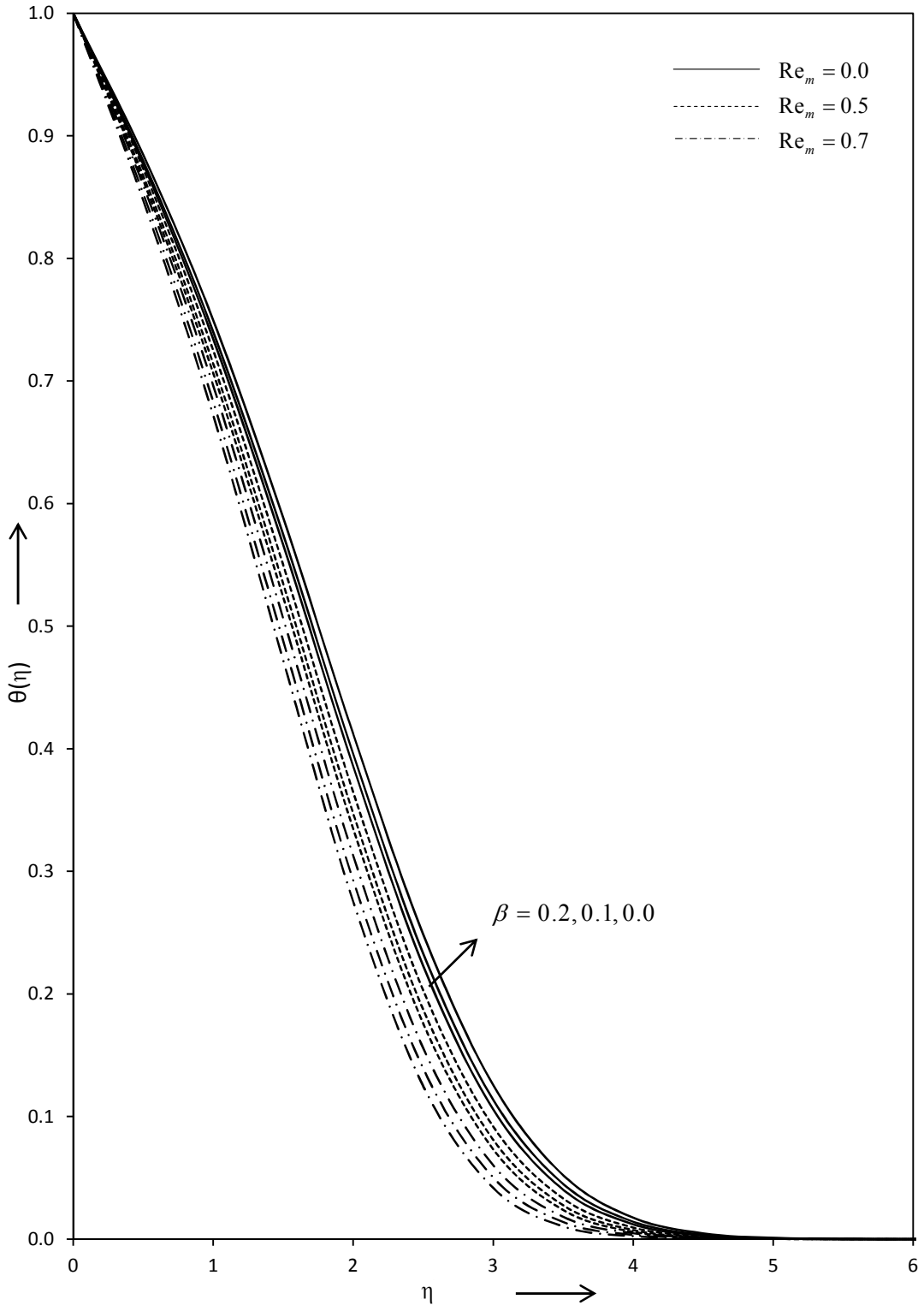

Fig. 7.4 Behavior of temperature distribution against η for various values of β and Re_m with $\alpha = -1.0$, $\mathrm{Pr} = 1.0$ and $Ec = 0.000$.

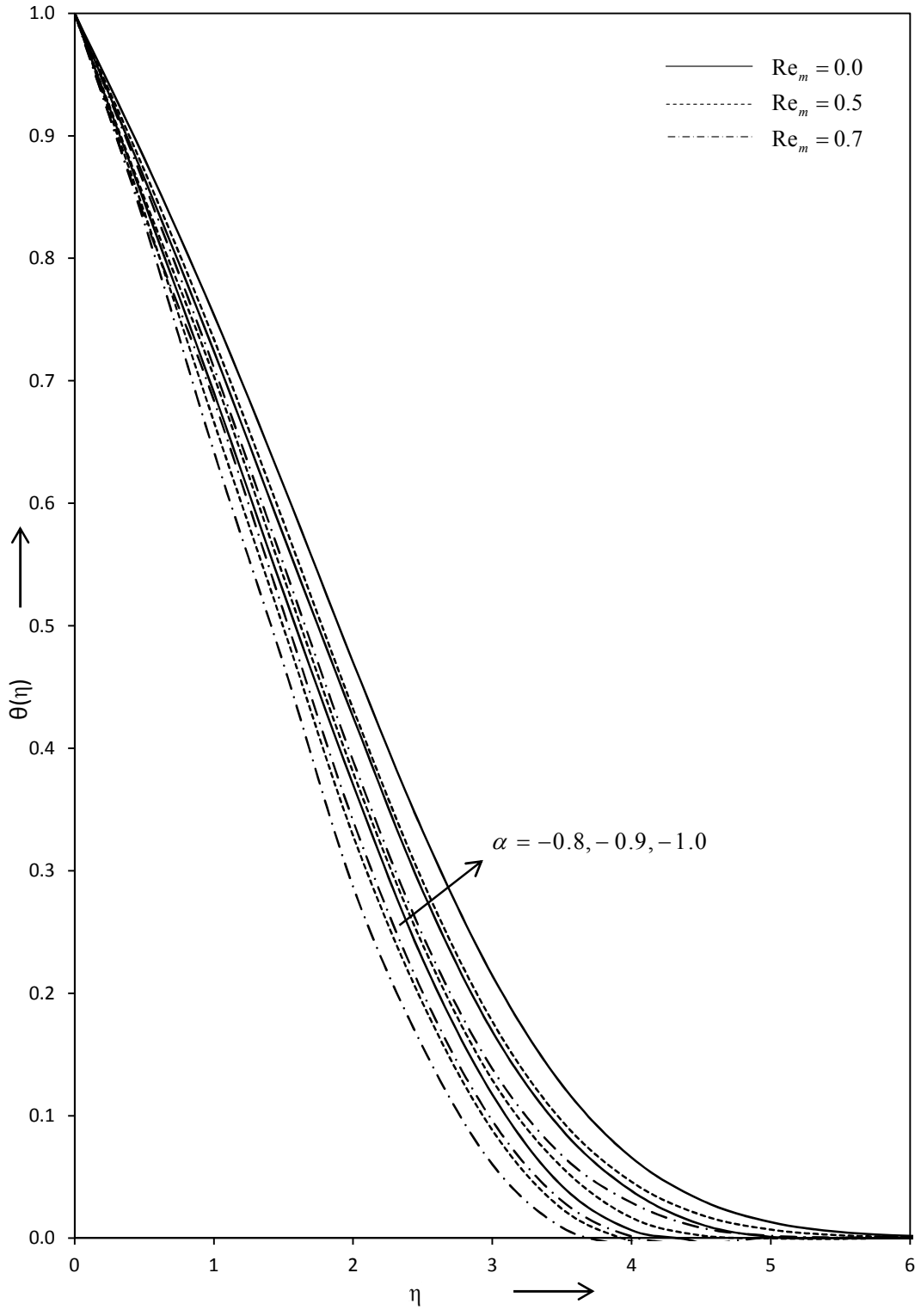

Fig. 7.5 Behavior of temperature distribution against η for various values of α and Re_m with $\beta = 0.1$, $\mathrm{Pr} = 0.5$ and $Ec = 0.000$.

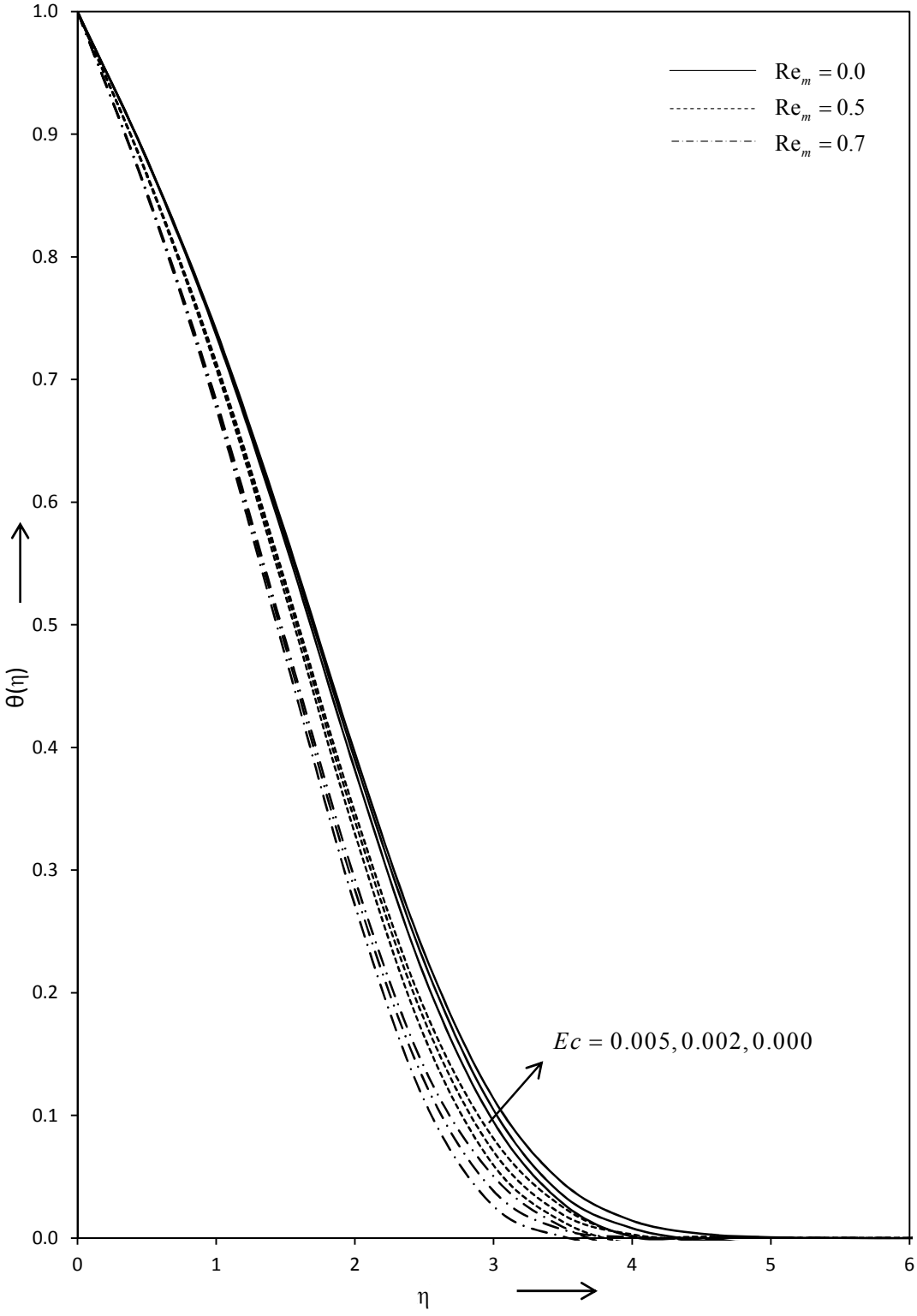

Fig. 7.6 Behavior of temperature distribution against η for various values of Re_m and Ec with $\beta = 0.1$, $\alpha = -1.0$ and $\mathrm{Pr} = 1.0$.

Table 7.1 Computed values of $f''(0)$ for different values of β, α and Re_m.

α	$f''(0)$								
	$\beta = 0.0$			$\beta = 0.1$			$\beta = 0.2$		
	$Re_m = 0.0$	$Re_m = 0.5$	$Re_m = 0.7$	$Re_m = 0.0$	$Re_m = 0.5$	$Re_m = 0.7$	$Re_m = 0.0$	$Re_m = 0.5$	$Re_m = 0.7$
-0.1	1.3288	1.3164	1.3104	1.2041	1.1955	1.1937	1.0623	1.0586	1.0512
-0.8	1.2614	1.2406	1.2251	1.1985	1.1805	1.1801	1.0210	1.0190	1.0070
-0.9	1.2516	1.2303	1.2207	1.1803	1.1795	1.1780	1.0108	1.0099	1.0047
-1.0	1.2305	1.2285	1.2178	1.1776	1.1706	1.1701	1.0098	1.0058	1.0015

Table 7.2 Computed values of $-\theta'(0)$ for different values of β, α, Re_m, Pr and Ec.

$-\theta'(0)$										
α	Pr	$\beta = 0.0$								
		$Ec = 0.000$			$Ec = 0.002$			$Ec = 0.005$		
		$Re_m = 0.0$	$Re_m = 0.5$	$Re_m = 0.7$	$Re_m = 0.0$	$Re_m = 0.5$	$Re_m = 0.7$	$Re_m = 0.0$	$Re_m = 0.5$	$Re_m = 0.7$
-1.0	0.05	0.1493	0.1530	0.1590	0.1493	0.1533	0.1595	0.1493	0.1549	0.1610
	0.50	0.2259	0.2440	0.2646	0.2259	0.2443	0.2653	0.2259	0.2448	0.2663
	1.00	0.2227	0.2450	0.2710	0.2227	0.2455	0.2720	0.2227	0.2462	0.2736
	2.00	0.1815	0.2016	0.2203	0.1815	0.2106	0.2227	0.1815	0.2157	0.2270
-0.9	0.50	0.2571	0.2705	0.2937	0.2571	0.2712	0.2948	0.2571	0.2719	0.2805
-0.8	0.50	0.2813	0.2993	0.3017	0.2813	0.2999	0.3024	0.2813	0.3011	0.3021

Table 7.2 Computed values of $-\theta'(0)$ for different values of β, α, Re_m, Pr and Ec. – Contd. 1

$-\theta'(0)$										
α	Pr	$\beta = 0.1$								
		$Ec = 0.000$			$Ec = 0.002$			$Ec = 0.005$		
		$Re_m = 0.0$	$Re_m = 0.5$	$Re_m = 0.7$	$Re_m = 0.0$	$Re_m = 0.5$	$Re_m = 0.7$	$Re_m = 0.0$	$Re_m = 0.5$	$Re_m = 0.7$
-1.0	0.05	0.1511	0.1562	0.1620	0.1511	0.1563	0.1622	0.1511	0.1563	0.1623
	0.50	0.2330	0.2520	0.2741	0.2330	0.2523	0.2748	0.2330	0.2528	0.2758
	1.00	0.2322	0.2559	0.2842	0.2322	0.2563	0.2852	0.2322	0.2570	0.2866
	2.00	0.1919	0.2194	0.2536	0.1919	0.2201	0.2553	0.1919	0.2213	0.2578
-0.9	0.50	0.2661	0.2842	0.3040	0.2661	0.2845	0.3046	0.2661	0.2849	0.3056
-0.8	0.50	0.2939	0.3102	0.3273	0.2939	0.3105	0.3279	0.2939	0.3109	0.3288

Table 7.2 Computed values of $-\theta'(0)$ for different values of β, α, Re_m, Pr and Ec. – Contd. 2

$-\theta'(0)$										
α	Pr	$\beta = 0.2$								
		$Ec = 0.000$			$Ec = 0.002$			$Ec = 0.005$		
		$Re_m = 0.0$	$Re_m = 0.5$	$Re_m = 0.7$	$Re_m = 0.0$	$Re_m = 0.5$	$Re_m = 0.7$	$Re_m = 0.0$	$Re_m = 0.5$	$Re_m = 0.7$
-1.0	0.05	0.1517	0.1576	0.1623	0.1517	0.1585	0.1637	0.1517	0.1595	0.1643
	0.50	0.2413	0.2623	0.2895	0.2413	0.2653	0.2705	0.2413	0.2693	0.2917
	1.00	0.2385	0.2639	0.2957	0.2385	0.2644	0.2966	0.2385	0.2650	0.2980
	2.00	0.2217	0.2415	0.2713	0.2217	0.2503	0.2802	0.2217	0.2505	0.2817
-0.9	0.50	0.2951	0.3105	0.3317	0.2951	0.3101	0.3320	0.2951	0.3140	0.3303
-0.8	0.50	0.3216	0.3401	0.3625	0.3216	0.3501	0.3703	0.3216	0.3501	0.3701

References

1. Ali, F.M.; Nazar, R.; Arifin, N.M.; Pop, I. 2011 Unsteady flow and heat transfer past an axisymmetric permeable shrinking sheet with radiation effect. Int J Num Meth Fluids, 67: 1310-1320

2. Aly, E.H.; Vajravelu, K. 2014 Exact and numerical solutions of MHD nano boundary layer flows over stretching surfaces in a porous medium. Appl Math Comp, 232: 191-204

3. Andersson, H.I. 2002 Slip flow past a stretching surface. Acta Mechanica, 158: 121-125

4. Ariel, P.D.; Hayat, T.; Asghar, S. 2006 The flow of an elastico-viscous fluid past a stretching sheet with partial slip. Acta Mechanica, 187: 29-35

5. Attia, H.A. 2007 On the effectiveness of porosity on stagnation point flow towards a stretching surface with heat generation. Comp Matl Sci, 38: 741-745

6. Aydin, O.; Kaya, A. 2008 Non-Darcian forced convection flow of viscous dissipating fluid over a flat plate embedded in a porous medium. Trans Porous Media, 73: 173-186

7. Bachok, N.; Ishak, A.; Nazar, R. 2011 Flow and heat transfer over an unsteady stretching sheet in a micropolar fluid. Meccanica, 46: 935-942

8.	Bachok, N.; Ishak, A.; Pop, I.	2012	Boundary layer stagnation-point flow and heat transfer over an exponentially stretching/shrinking sheet in a nanofluid. Int J Heat Mass Transf, 55: 8122-8128
9.	Bansal, J.L.	1979	The ‘similar’ solution of the hydromagnetic free-jet boundary layer equations. Zeit Angew Math Phys, 30: 129-132
10.	Bansal, J.L.	1981	On the hydromagnetic boundary layer flow past a flat plate. Acta Mechanica, 41: 35-40
11.	Bansal, J.L.	1994	Magnetofluiddynamics of viscous fluids. Jaipur Pub House, India
12.	Bansal, J.L.	2004	Viscous fluid dynamics. Oxford & IBH Publishing Co Pvt Ltd, New Delhi, India
13.	Bansal, J.L.; Jat, R.N.	1984	Boundary layer flow of an electrically conducting fluid past a flat plate in the presence of uniform transverse magnetic field. Proc 20th congress ISTAM, 1981: 1-22
14.	Bansal, J.L.; Jat, R.N.	1985	Similarity solutions for two dimensional MGD boundary layer flow in an aligned magnetic field. J Math Phys Sci, 19: 449-460
15.	Bansal, J.L.; Jat, R.N.	1986	Similarity solutions for two-dimensional MGD boundary layer flow in a transverse magnetic field. IL NUOVO CIMENTO, 8D: 635-646

16. Bansal, J.L.; Jat, R.N. 1988 Recovery factor for a MHD laminar boundary layer over a flat plate. Proc Nat Acad Sci India 58(A): 277-281

17. Bansal, J.L.; Kumari, R. ; Jat, R.N. 1987 Unsteady MHD boundary layer flow past a semi-infinite flat plate. IL NUOVO CIMENTO, 100B: 467-483

18. Bansal, J.L.; Kumari, R. ; Jat, R.N. 1989 MHD boundary layer with an exponentially increasing pressure gradient. Proc Nat Acad Sci India, 59(A), I: 117-130

19. Bansal, J.L.; Mishra, J.J.; Jat, R.N. 1988 MHD laminar wall jet over a curved surface in a variable normal magnetic field. Appl Scient Res, 45: 75-94

20. Bear, J. 1972 Dynamics of fluids in porous media. American Elsevier Pub Co, New York

21. Bear, J.; Bachmat, Y. 1990 Introduction to modeling of transport phenomena in porous media. Kluwer Academic Pub Dordrecht Netherland

22. Beavers, G.S.; Joseph, D.D. 1967 Boundary conditions at a naturally permeable wall. J Fluid Mech, 30: 197-207

23. Bejan, A.; Dincer, I.; Lorente, S.; Miguel, A.; Reis, H. 2004 Porous and complex flow structures in modern technologies. Springer-Verlag, New York

24.	Bhattacharyya, K.; Layek, G.C.	2011	Effects of suction/blowing on steady boundary layer stagnation-point flow and heat transfer towards a shrinking sheet with thermal radiation. Int J Heat Mass Transf, 54: 302-307
25.	Bhattacharyya, K.; Mukhopadhyay, S.; Layek, G.C.	2011	Slip effects on boundary layer stagnation-point flow and heat transfer towards a shrinking sheet. Int J Heat Mass Transf, 54: 308-313
26.	Bidin, B.; Nazar, R.	2009	Numerical solution of the boundary layer flow over an exponentially stretching sheet with thermal radiation. Eur J Scient Res, 33: 710-717
27.	Bush, W.B.	1958	Magnetohydrodynamic hypersonic flow past a blunt body. J Aerospace Sci, 25: 685-690
28.	Bush, W.B.	1960	Compressible flat-plate boundary-layer flow with an applied magnetic field. J Aerospace Sci, 27: 49-58
29.	Cabannes, H.	1970	Theoretical magnetofluiddynamics. Academic Press, New York
30.	Cambel, A.B.	1963	Plasma physics and magnetofluidmechanics. McGraw-Hill, New York
31.	Carragher, P.; Crane, L.J.	1982	Heat transfer on a continuous stretching sheet. Zeit Angew Math Mech, 62: 564-565

32.	Cess, R.D.	1961	The effect of radiation upon forced-convection heat transfer. Appl Scient Res, 10: 430-438
33.	Cess, R.D.	1966	The interaction of thermal radiation with free convection heat transfer. Int J Heat Mass Transf, 9: 1269-1277
34.	Chamkha, A.J.; Takhar, H.S.; Soundalgekar, V.M.	2001	Radiation effects on free convection flow past a semi-infinite vertical plate with mass transfer. Chem Eng J, 84: 335-342
35.	Chaudhary, S.; Kumar, P.	2014	MHD forced convection boundary layer flow with a flat plate and porous substrate. Meccanica, 49: 69-77
36.	Chen, C.K.; Char, M.I.	1988	Heat transfer of a continuous, stretching surface with suction or blowing. J Math Anal Appls, 135: 568-580
37.	Chiam, T.C.	1994	Stagnation-point flow towards a stretching plate. J Phys Soc Japan, 63: 2443-2444
38.	Collatz, L.	1966	The numerical treatment of differential equations. Springer-Verlag, New York
39.	Cramer, K.R.; Pai, S.I.	1973	Magnetofluiddynamics for engineers and applied physicists. McGraw-Hill, New York
40.	Crane, L.J.	1970	Flow past a stretching plate. Zeit Angew Math Phys, 21: 645-647

41.	Crolet, J.M.; Hatri, M.E.	1998	Recent advances in problems of flow and transport in porous media. Springer
42.	Darcy, H.P.G.	1856	Les fontaines publiques de la ville de Dijon. Victor Dalmont, Paris
43.	Date, A.W.	2005	Introduction to computational fluid dynamics. Cambridge University Press, New York
44.	Dutta, B.K.; Roy, P.; Gupta, A.S.	1985	Temperature field in flow over a stretching sheet with uniform heat flux. Int Comm Heat Mass Transf, 12: 89-94
45.	Elbashbeshy, E.M.A.	2001	Heat transfer over an exponentially stretching continuous surface with suction. Arch Mech, 53: 643-651
46.	Elbashbeshy, E.M.A.; Bazid, M.A.A.	2003	Heat transfer over a stretching surface with internal heat generation. Can J Phys, 81: 699-703
47.	Elbashbeshy, E.M.A.; Bazid, M.A.A.	2003	Heat transfer over an unsteady stretching surface with internal heat generation. Appl Math Comp, 138: 239-245
48.	Evans, H.L.	1968	Laminar boundary-layer theory. Addison-Wesley Pub Com
49.	Fang, T.; Yao, S.; Zhang, J.; Aziz, A.	2010	Viscous flow over a shrinking sheet with a second order slip flow model. Comm Nonlinear Sci Num Simul, 15: 1831-1842

50.	Faraday, M.	1832	Experimental researches in electricity. Phil Trans R Soc London, 122: 125-162
51.	Ferraro, V.C.A.; Plumpton, C.	1966	An introduction to magnetofluidmechanics. Clarendon Press, Oxford
52.	Ganesan, P.; Loganathan, P.	2002	Radiation and mass transfer effects on flow of an incompressible viscous fluid past a moving vertical cylinder. Int J Heat Mass Transf, 45: 4281-4288
53.	George, F.P.; William, G.G.	2008	Essentials of multiphase flow and transport in porous media. John Wiley
54.	Gerbeau, J.F.; Bris, C.L.; Lelievre, T.	2006	Mathematical methods for the magnetohydrodynamics of liquid metals. Oxford University Press, USA
55.	Ghoshal, S.; Ghoshal, A.	1970	Thermal boundary layer theory near the stagnation point in three-dimensional fluctuating flow. J Fluid Mech, 43: 465-476
56.	Gorla, R.S.R.	1979	Unsteady viscous flow in the vicinity of an axisymmetric stagnation point on a circular cylinder. Int J Eng Sci, 17: 87-93
57.	Gorla, R.S.R.	1981	Unsteady thermal boundary layer flow of a non-newtonian fluid over a flat plate. Int J Eng Sci, 19: 1391-1399
58.	Gorla, R.S.R.; Dakappagari, V.; Pop, I.	1993	Boundary layer flow at a three-dimensional stagnation point in power-law non-newtonian fluids. Int J Heat Fluid Flow, 14: 408-412

59.	Gribben, R.J.	1965	Numerical solution of magnetohydrodynamic stagnation-point flow equations. AIAA J, 3: 972-973
60.	Gribben, R.J.	1967	Heat transfer in magnetohydrodynamic flow near a stagnation point. Appl Scient Res, 17: 270-290
61.	Gribben, R.J.	1967	Magnetohydrodynamic boundary layers with variable properties. Phys Fluids, 10: 1849-1851
62.	Grubka, L.J.; Bobba, K.M.	1985	Heat transfer characteristics of a continuous, stretching surface with variable temperature. J Heat Transf, 107: 248-250
63.	Gupta, P.S.; Gupta, A.S.	1977	Heat and mass transfer on a stretching sheet with suction or blowing. Can J Chem Eng, 55: 744-746
64.	Hartmann, J.	1937	Hg-dynamics I: Theory of the laminar flow of an electrically conductive liquid in a homogeneous magnetic field. Mathematisk-fysiske Meddelelser 15, 6
65.	Hartmann, J.; Lazarus, F.	1937	Hg-dynamics II: Experimental investigations on the flow of mercury in a homogeneous magnetic field. Mathematisk-fysiske Meddelelser 15, 7

66. Hayday, A.A.; Bowlus, D.A. 1967 Integration of coupled nonlinear equations in boundary-layer theory with specific reference to heat transfer near the stagnation point in three-dimensional flow. Int J Heat Mass Transf, 10: 415-426

67. Hiemenz, K. 1911 Die Grenzschicht an einem in den gleichformigen Flussigkeitsstrom eingetauchten geraden Kreiszylinder. Dinglers polytech J, 326: 321-410

68. Hossain, M.A.; Rees, D.A.S.; Pop, I. 1998 Free convection-radiation interaction from an isothermal plate inclined at a small angle to the horizontal. Acta Mechanica, 127: 63-73

69. Hossain, M.A.; Takhar, H.S. 1996 Radiation effect on mixed convection along a vertical plate with uniform surface temperature. Heat Mass Transf, 31: 243-248

70. Howarth, J.A. 1975 Boundary-layer growth at a three-dimensional rear stagnation point. J Fluid Mech, 67: 289-297

71. Huang, P.C.; Vafai, K. 1994 Analysis of flow and heat transfer over an external boundary covered with a porous substrate. J Heat Transf, 116: 768-771

72. Ishak, A.; Nazar, R.; Pop, I. 2006 Mixed convection boundary layers in the stagnation point flow toward a stretching vertical sheet. Meccanica, 41: 509-518

73.	Jat, R.N.; Chaudhary, S.	2007	MHD stagnation flows with slip. IL NUOVO CIMENTO,122B: 823-831
74.	Jat, R.N.; Chaudhary, S.	2008	Magnetohydrodynamic boundary layer flow near the stagnation point of a stretching sheet. IL NUOVO CIMENTO, 123B: 555-566
75.	Jat, R.N.; Chaudhary, S.	2009	Magnetohydrodynamic boundary layer flow past a porous substrate with Beavers-Joseph boundary condition. Indian J Pure & Appl Phys, 47: 624-630
76.	Jat, R.N.; Chaudhary, S.	2009	Unsteady magnetohydrodynamic boundary layer flow over a stretching surface with viscous dissipation and Joule heating. IL NUOVO CIMENTO, 124B: 53-59
77.	Jat, R.N.; Chaudhary, S.	2009	MHD flow and heat transfer over a stretching sheet. Appl Math Sci, 3: 1285-1294
78.	Jat, R.N.; Chaudhary, S.	2010	Radiation effects on the MHD flow near the stagnation point of a stretching sheet. Zeit Angew Math Phys, 61: 1151-1154
79.	Jat, R.N.; Chaudhary, S.	2010	Hydromagnetic flow and heat transfer on a continuously moving surface. Appl Math Sci, 4: 65-78
80.	Jeffrey, A.	1966	Magnetohydrodynamics. Oliver and Boyd, New York

81. Kaviany, M. 1995 Principles of heat transfer in porous media. Springer, New York

82. Kuznetsov, A.V. 1997 Influence of the stress jump condition at the porous-medium/clear-fluid interface on a flow at a porous wall. Int Comm Heat Mass Transf, 24: 401-410

83. Kuznetsov, A.V. 1998 Analytical study of fluid flow and heat transfer during forced convection in a composite channel partly filled with a Brinkman-Forchheimer porous medium. Flow, Turbulence and Combustion, 60: 173-192

84. Kuznetsov, A.V. 2000 Analytical studies of forced convection in partly porous configurations. In: Handbook of porous media (Vafai, K., ed.), Marcel Dekker, New York, 269-312

85. Liao, S.J.; Pop, I. 2004 Explicit analytic solution for similarity boundary layer equations. Int J Heat Mass Transf, 47: 75-85

86. Lykoudis, P.S. 1958 On a class of magnetic laminar boundary layers. Heat Transfer and Fluid Mechanics Institute (Stanford University Press, Stanford, Calif)

87. Magyari, E.; Keller, B. 1999 Heat and mass transfer in the boundary layers on an exponentially stretching continuous surface. J Phys D: Appl Phys 32: 577-585

88.	Magyari, E.; Keller, B.	2000	Exact solutions for self-similar boundary-layer flows induced by permeable stretching walls. Eur J Mech B-Fluids, 19: 109-122
89.	Mahapatra, T.R.; Gupta, A.S.	2002	Heat transfer in stagnation-point flow towards a stretching sheet. Heat Mass Transf, 38: 517-521
90.	Mahapatra, T.R.; Nandy, S.K.	2011	Unsteady stagnation-point flow and heat transfer over an unsteady shrinking sheet. Int J Appl Math Mech, 7: 11-26
91.	Mahapatra, T.R.; Nandy, S.K.	2013	Slip effects on unsteady stagnation-point flow and heat transfer over a shrinking sheet. Meccanica, 48: 1599-1606
92.	Mahapatra,T.R.; Nandy, S.K.	2013	Stability of dual solutions in stagnation-point flow and heat transfer over a porous shrinking sheet with thermal radiation. Meccanica, 48: 23-32
93.	Mahapatra, T.R.; Nandy, S.K.; Gupta, A.S.	2012	Oblique stagnation-point flow and heat transfer towards a shrinking sheet with thermal radiation. Meccanica, 47: 1325-1335
94.	Miklavcic, M.; Wang, C.Y.	2006	Viscous flow due to a shrinking sheet. Quatly Appl Math, 64: 283-290
95.	Molla, M.M.; Hossain, M.A.	2007	Radiation effect on mixed convection laminar flow along a vertical wavy surface. Int J Thermal Sciences, 46: 926-935

96.	Mukhopadhyay, S.; Layek, G.C.	2012	Effects of variable fluid viscosity on flow past a heated stretching sheet embedded in a porous medium in presence of heat source/sink. Meccanica, 47: 863-876
97.	Mukhopadhyay, S.; De, P.R.; Bhattacharyya, K.; Layek, G.C.	2012	Forced convective flow and heat transfer over a porous plate in a Darcy-Forchheimer porous medium in presence of radiation. Meccanica, 47: 153-161
98.	Muskat, M.	1937	The flow of homogeneous fluids through porous media. McGraw-Hill, New York
99.	Nadeem, S.; Hussain, A.; Khan, M.	2010	HAM solutions for boundary layer flow in the region of the stagnation point towards a stretching sheet. Comm Nonlinear Sci Num Simul, 15: 475-481
100.	Nandy, S.K., Sidui, S.; Mahapatra, T.R.	2014	Unsteady MHD boundary layer flow and heat transfer of nanofluid over a permeable shrinking sheet in the presence of thermal radiation. Alexandria Eng J, 53: 929-937
101.	Nath, G.	1971	Compressible axially symmetric laminar boundary layer flow in the stagnation region of a blunt body in the presence of magnetic field. Acta Mechanica, 12: 267-273
102.	Nath, G.	1973	Solution of nonlinear problems in magnetofluiddynamics and non-Newtonian fluid mechanics through parametric differentiation. AIAA J, 11: 1429-1432

103.	Nazar, R.; Amin, N.; Pop, I.	2004	Unsteady mixed convection boundary layer flow near the stagnation point on a vertical surface in a porous medium. Int J Heat Mass Transf, 47: 2681-2688
104.	Nield, D.A.; Bejan, A.	2006	Convection in porous media. 3rd edn, Springer-Verlag, New York
105.	Nield, D.A.; Kuznetsov, A.V.	2003	Boundary-layer analysis of forced convection with a plate and porous substrate. Acta Mechanica, 166: 141-148
106.	Nikaien, K.; Peddieson, J.	1988	Plane two-phase stagnation-point flow above a stretching sheet. Int J Multiphase Flow, 14: 633-643
107.	Ochoa-Tapia, J.A.; Whitaker, S.	1995	Momentum transfer at the boundary between a porous medium and a homogeneous fluid-I. Theoretical development. Int J Heat Mass Transf, 38: 2635-2646
108.	Ochoa-Tapia, J.A.; Whitaker, S.	1995	Momentum transfer at the boundary between a porous medium and a homogeneous fluid-II. Comparison with experiment. Int J Heat Mass Transf, 38: 2647-2655
109.	Oleinik, O.A.; Samokhin, V.N.	1999	Mathematical models in boundary layer theory. Chapman and Hall/CRC, Boca Raton

110.	Pai, S.I.	1956	Viscous flow theory: I, Laminar flow. D. Van Nostrand Company, New York
111.	Pai, S.I.	1962	Magnetogasdynamics and plasma dynamics. Springer-Verlag, New York
112.	Pal, D.; Hiremath P.S.	2010	Computational modeling of heat transfer over an unsteady stretching surface embedded in a porous medium. Meccanica, 45: 415-424
113.	Pop, S.R.; Grosan, T.; Pop, I.	2004	Radiation effects on the flow near the stagnation point of a stretching sheet. Technische Mechanik, Band 25, Heft 2: 100-106
114.	Prandtl, L.	1904	Uber Flussigkeitsbewegung bei sehr kleiner Reibung, in: Verhandlungen des III, Internationalen Mathematiker-Kongresses, Heidelberg, 484-491
115.	Ram, P.; Kumar, A. ; Singh, H.	2013	Effect of porosity on unsteady MHD flow past a semi-infinite moving vertical plate with time dependent suction. Indian J Pure & Appl Phys, 51: 461-470
116.	Ramamoorthy, P.	1965	Heat transfer in hydromagnetics. Quart J Mech Appl Math, 18: 31-40
117.	Ramamoorthy, P.	1968	Karman-Pohlhausen method for MHD boundary layers. AIAA J, 6: 1407-1409
118.	Rehberg R.K.; Kluwick A.; Leipner H.S.	1998	Recent advances in boundary layer theory. Springer

119.	Rosali, H.; Ishak, A.; Pop, I.	2011	Stagnation point flow and heat transfer over a stretching/shrinking sheet in a porous medium. Int Comm Heat Mass Transf, 38: 1029-1032
120.	Rosca, N.C.; Pop, I.	2015	Unsteady boundary layer flow over a permeable curved stretching/shrinking surface. Eur J Mech B-Fluids, 51, 61-67
121.	Rosenhead, L.	1963	Laminar boundary layers. Oxford University Press, London
122.	Rosseland, S.	1936	Theoretical astrophysics. Oxford University Press, London
123.	Rossow, V.J.	1958	Magnetohydrodynamic analysis of heat transfer near a stagnation point. J Aerospace Sci, 25: 334-335
124.	Rossow, V.J.	1958	On flow of electrically conducting fluids over a flat plate in the presence of a transverse magnetic field. NACA Report TN 1358
125.	Sakiadis, B.C.	1961	Boundary-layer behavior on continuous solid surfaces: I. Boundary-layer equations for two-dimensional and axisymmetric flow. AIChE J, 7: 26-28
126.	Sano, T.	1977	Unsteady boundary layer in impulsive stagnation flow. Int J Heat Mass Transf, 20: 1000-1001

127. Scheidegger, A.E. 1974 The physics of flow through porous media. University of Toronto Press, Toronto, Canada

128. Schlichting, H. 1968 Boundary layer theory. McGraw-Hill, New York

129. Singh, K.D.; Pathak, R. 2012 Effect of rotation and hall current on mixed convection MHD flow through a porous medium filled in a vertical channel in presence of thermal radiation. Indian J Pure & Appl Phys, 50: 77-85

130. Smith, C.G.; Slepian, J. 1917 Electromagnetic ship's log. US1249530A, Grant

131. Sobey I.J. 2000 Introduction to interactive boundary layer theory. Oxford University Press, USA

132. Soundalgekar, V.M.; Ramana Murty, T.V. 1980 Heat transfer in flow past a continuous moving plate with variable temperature. Warme-Und Stoffubertragung, 14: 91-93

133. Vafai, K.; Kim, S.J. 1990 Analysis of surface enhancement by a porous substrate. ASME J Heat Transf, 112: 700-706

134. Viskanta, R.; Grosh, R.J. 1962 Boundary layer in thermal radiation absorbing and emitting media. Int J Heat Mass Transf, 5: 795-806

135. Vleggaar, J. 1977 Laminar boundary-layer behaviour on continuous, accelerating surfaces. Chem Eng Sci, 32: 1517-1525

136.	Wang, C.Y.	1990	Liquid film on an unsteady stretching sheet. Quart Appl Math, 48: 601–610
137.	Wang, C.Y.	2008	Stagnation flow towards a shrinking sheet. Int J Nonlinear Mech, 43: 377-382
138.	Wang, C.Y.	2013	Viscous flow in a curved tube filled with a porous medium. Meccanica, 48: 247-251
139.	White, F.M.	2006	Viscous fluid flow. McGraw Hill, New York
140.	Wilcox, M.W.	1962	Magnetohydrodynamics (Ed.). Northwestern University Press, Evanston
141.	Williams, E.J.	1930	The induction of electromotive forces in a moving liquid by a magnetic field, and its application to an investigation of the flow of liquids. Proc Phys Soc (London), 42: 466-478
142.	Zheng, L.; Wang, L.; Zhang, X.	2011	Analytic solutions of unsteady boundary flow and heat transfer on a permeable stretching sheet with non-uniform heat source/sink. Comm Nonlinear Sci Num Simul, 16: 731-740

List of Publications

During the research work, the following papers have been published by the author-

1. MHD forced convection boundary layer flow with a flat plate and porous substrate. *Meccanica* (2014), 49 (1), 69-77, coauthored with S. Chaudhary.
2. Magnetohydrodynamic stagnation point flow past a porous stretching surface with heat generation. *Indian Journal of Pure & Applied Physics* (2015), 53 (5), 291-297, coauthored with S. Chaudhary.
3. Magnetohydrodynamic boundary layer flow over an exponentially stretching sheet with radiation effects. *Applied Mathematical Sciences* (2015), 9 (23), 1097-1106, coauthored with S. Chaudhary.
4. MHD Stagnation Point Flow and Heat Transfer over a Permeable Surface. *Engineering* (2013), 5 (1), 50-55, coauthored with S. Chaudhary.
5. MHD Slip Flow past a Shrinking Sheet. *Applied Mathematics* (2013), 4 (3), 574-581, coauthored with S. Chaudhary.
6. Unsteady magnetohydrodynamic boundary layer flow near the stagnation point towards a shrinking surface. *Journal of Applied Mathematics and Physics* (2015), 3 (7), 921-930, coauthored with S. Chaudhary.

Author's Brief Bio-Data

Full Name : Pradeep Kumar

Education

July, 2009 – Till Date : Research Scholar, Department of Mathematics, Malaviya National Institute of Technology Jaipur, Jaipur

August, 2007 – June, 2008 : Master of Philosophy in Mathematics
Dr. B. R. A. University, Agra, U. P.

July, 2002 – May, 2004 : Master of Science in Mathematics
M. J. P. R. University, Bareilly, U. P.

July, 1999 – May, 2002 : Bachelor of Science in Mathematics
M. J. P. R. University, Bareilly, U. P.

Working Experience

August 2013 – Till Date : Assistant Statistical Officer, Sugarcane Development Department, Government of Uttar Pradesh